THE CONTROL of TEXTURE in RIMMED STEEL STRIP.

Author: Bryan Neville Hellewell.

November, 1971.

Submitted for the degree of Doctor of Philosophy.

THE UNIVERSITY OF ASTON IN BIRMINGHAM

Summary.

Through thickness texture segregation has been observed in cold rolled rimmed steel. The effect of rolling draught and lubrication upon the segregation has been recorded. For a constant cold reduction, the mid-plane texture was always the same and was comprised of two partial fibre textures, $\langle 110\rangle_{RD} + \{111\}_{RP}$. Texture segregation is associated with deviation from this texture through the rest of the strip. Four types of segregation have been observed and categorised according to rolling draught, i.e. .025 mms for Type I textures and greater than .500 mms for Type IV textures.

Type I texture segregation results from variations in $\{111\}_{RP}$ texture intensity through the strip. Type III textures are characterised by segregation in the extreme surface planes only. In this zone there is a general reduction in texture intensity rather than a change in textural components. Type II texture segregation is a composite of Types I and III.

Type IV texture segregation is produced by rolling with heavy draughts and magnesia dusted rolls. The surface texture is described as $\{110\}\langle UVW\rangle$ where $\langle UVW\rangle$ ranges between $\langle 001\rangle$ and $\langle 111\rangle$

Mechanisms are devised to account for texture segregation and, where appropriate, discussed in relation to the literature.

Texture segregation is retained after annealing and therefore influences the R value of finished strip. There is a general reduction in

R value commensurate with the intensity of segregation. Thus, for a constant cold reduction, $R_{IV} < R_I < R_{II} < R_{III}$. Also the cold reduction at which the maximum (Romax) occurs in the plot of R_o value versus percentage reduction is dependent upon texture segregation. Romax is associated with the balancing of $\{111\}_{RP}$ texture with the detrimental $\langle 110 \rangle_{RD}$ texture. This balance is disturbed by texture segregation such that $\langle 110 \rangle_{RD}$ texture predominates at variable cold reductions.

$\bar{R}$ and R_o values of strip can be improved by the presence of intragranular cementite approximately 1μ in size. Textural measurements show that the effect is due to the inhibition of the detrimental reorientation of $\langle 110 \rangle_{RD}$ textures normally observed during tensile strain.

CONTENTS

1. Introduction.

The British Steel Corporation (B.S.C.) produced 24 million tonnes of steel during 1969. Steel is, therefore, the single most important material to be considered in Britain's economy. One of B.S.C.s largest customers is the motor car industry which uses over one million tonnes of rimmed steel each year in the form of sheet approximately 0.75 mm. thick. Furthermore, this tonnage is likely to increase within the forseeable future regardless of the competition from plastics and other metals.

Next to commercial considerations steel owes its popularity as a raw material for pressings, such as inner car door panels, to good formability, where a combination of deep drawing and stretch forming properties are required. Stretchformability is limited by the level of strain at which plastic instability occurs and depends largely upon the strain hardening capacity of the metals. Stretchformability is, therefore, generally regarded as a fundamental metal property(1). Crystal orientation or texture is the material property controlling the deep drawability of rimmed steel strip. Consequently the metallurgical factors influencing the development of texture will be examined and appraised.

As deep drawability can be related to the strain ratio or R value a correlation between texture and R value is indicative of an equivalent correlation between texture and deep drawability. An account will be given of the theoretical basis for the relationship between R value and texture since R value will be used in the present work as the measure of deep drawing performance. R value can be precisely defined but the adequate description of texture is difficult.

Consequently the account will include a description of the methods of representing texture to be used throughout the text.

A variety of properties other than texture also have to be controlled during the production of rimmed steel sheet. A typical process cycle, which includes hot rolling, coiling, cold rolling, batch annealing, and temper rolling, will therefore be outlined to indicate the metallurgically important factors and to emphasise the sections of the process where a compromise is necessary between suitable texture and other properties.

Textures in finished sheet are mainly established during the cold rolling process. The development of b.c.c. iron cold rolling textures have been widely reported upon in the literature [2-5]. It will be shown that there is general agreement with regard to the textures developed but that present rolling theories do not account for all the observations. Through-thickness texture segregation, which has been attributed to the inhomogeniety of strain associated with some cold rolling conditions[6], has received relatively little attention although it is of significance with regard to the drawability of sheet. The literature pertaining to texture segregation and the rolling conditions under which it is developed will be reviewed. Draught and lubrication will be shown, despite the confusion arising in the literature, to be important rolling conditions that influence texture segregation and therefore R value.

The first objective of the present work is to critically examine the effect of these two rolling variables upon texture and texture segregation in rimmed steel. Texture segregation will be re-examined in corresponding annealed strip and the compounded textural data correlated with R values.

Texture intensity increases with increase in total percentage rolling reduction. However, R value, for rimmed steel, does not increase correspondingly, but reaches a maximum at approximately 75% reduction (R max), and thereafter decreases with further increase in rolling reduction[7]. The explanations to account for this phenomenon will be appraised, illustrating how, for some cases, R max can be associated with texture segregation, thereby complicating texture R max analyses. It will be further shown that, since R value is measured in the uniaxial tensile test, a knowledge of the behaviour of textured rimmed steel strip to tensile strain is of fundamental importance, if a satisfactory explanation of R max is to be established. The second objective of this investigation will be to examine this factor experimentally. This will enable a satisfactory explanation to be made of the influence of texture segregation upon R value and R max value.

Single phase metals or alloys develop characteristic preferred orientations when subjected to deformation. However, the presence of second phases have been reported[8] to modify the texture developed.

Therefore the effect of cementite precipitates upon the reaction of textured rimmed steel to tensile strain will be examined and its consequent effect upon measured R value recorded.

2. The Correlation between Drawing Limits, R values, D values and Texture.

Many of the materials used in the sheet metal industry are applied to forming operations that are markedly affected by anisotropy. This is particularly evident in deep drawing operations. The anisotropic properties of metals, as represented by the strain ratio (R value), can be attributed to the anisotropic character of individual grains being imparted, at least to some degree, to the textured polycrystalline sheet.

The correlation between drawing limits, R value or D value and texture will be dealt with in three sections, each being a logical development of the previous one. The measurement of R value will be shown to be a satisfactory laboratory technique of assessing drawing limits. The methods of describing texture suitable for texture-R value analyses will then be ennunciated, and finally the correlation between R value and crystallographic texture established.

2.1. The drawing limits - R value relationship.

Strain ratio or R value is measured in the uniaxial tensile test and is defined by the formula:

$$R = \frac{\ln Wo/W}{\ln To/T} \quad .... \quad 2.1.\ 1$$

where Wo and To are the initial width and thickness of the specimen respectively and W and T are the width and thickness after tensile strain. As thickness strains are very small, a more practical relationship which uses the constancy of volume criterion is :

$$R = \frac{\ln Wo/W}{\ln (L/Lo \cdot W/Wo)} \quad \text{.........} \; 2.1.\ 2$$

where Lo and L are specimen length before and after tensile strain.

R values can be measured in any direction in the plane of the sheet and the difference between the highest and lowest value, ΔR, is a measure of planar anisotropy. High planar anisotropy values lead to 'earing', which is undesirable since an additional expensive machining operation is necessary to remove the feature. The average normal anisotropy ratio is defined by the relationship :

$$\bar{R} = \left(R_0 + R_{90} + 2(R_{45}) \right) 1/4 \text{...} 2.1.\ 3$$

where suffixes 0,45 and 90 refer to the angle, between the sheet rolling direction and tensile axis. An $\bar{R}$ value of one indicates an isotropic metal, whereas a value of zero indicates a metal that accommodates uniaxial extension by reduction in thickness only. An $\bar{R}$ value of infinity is exhibited by metals that accommodate uniaxial extension by reductions in width only.

In the pure deep drawing case, i.e. a flat bottomed cup, there are two regions of special significance[9]:

the flange where the drawing load is determined by the stress required to maintain plane strain, and the cup wall which must support the necessary forces without tearing,also under conditions of plane strain. Therefore, for maximum drawability the wall strength should be as high as possible relative to that of the flange. Fig 2.1. 1 is a schematic representation of a segment of a drawn cup illustrating the relationship between the principal strains.

Although both the flange and wall yield under conditions of plane strain the axis of zero strain is different in each case. Reference to anisotropic yield loci for various loading conditions, Fig.2.1. 2, which are based on Hill's[10] yield criterion and associated flow rules, indicates thatthe wall strength increases with the R value parameter while the flange strength decreases with R value. Hence drawability improves with increasing R value. However, failure usually occurs over the punch nose radius and not in the cup wall, under conditions close to balanced biaxial tension[11]. Strength in biaxial tension also increases with increase in R value, Fig. 2.1. 2. Therefore, drawability is expected to be closely correlateable with R value whether potential failure sites are in the cup wall or over the punch nose radius.

$\bar{R}$ value is the value usually quoted in the literature as being indicative of drawingperformance and is a measure of the resistance of sheet metal to strain in the sheet normal direction when subjected to uniaxial tension.

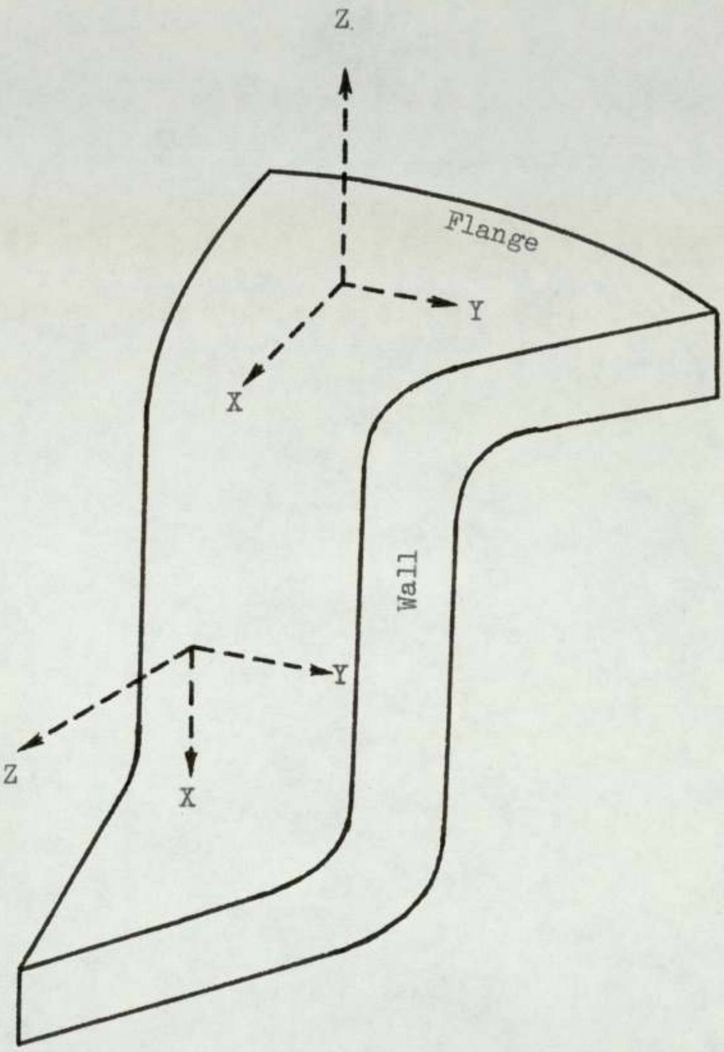

Fig.2.1.1. Section from drawn flat bottomed cup.

Flange and Wall yield under conditions close to plane strain but the axis of zero strain is different in each case. For flange $\delta\varepsilon_Z \simeq 0$ and for wall $\delta\varepsilon_Y = 0$

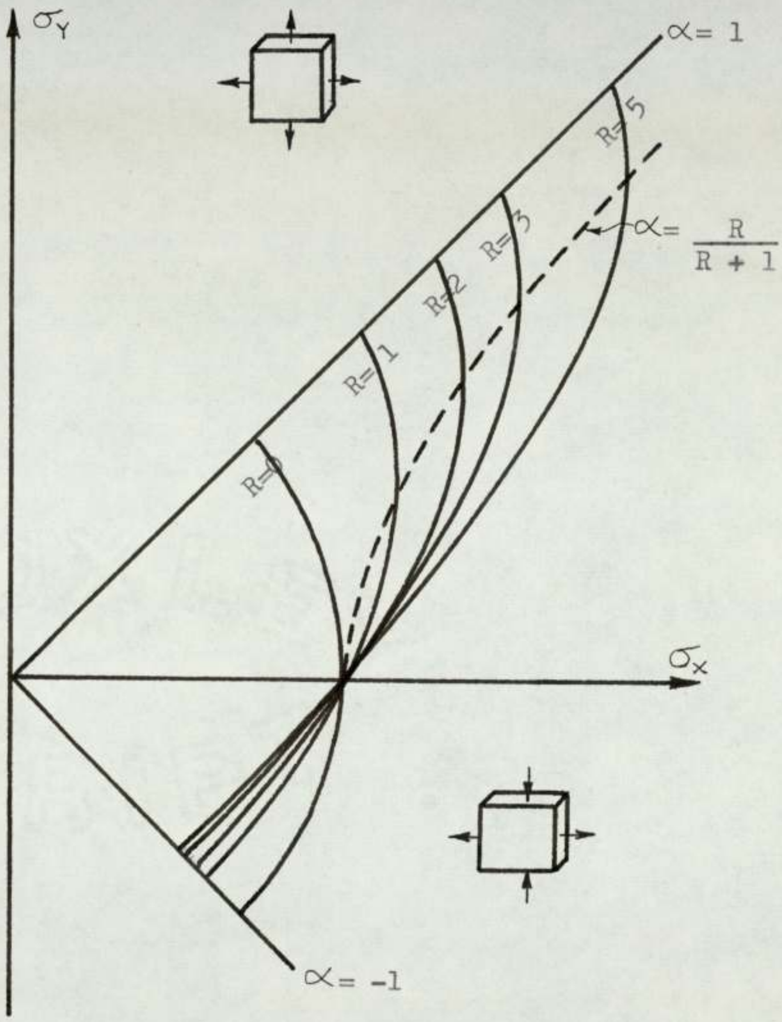

Fig. 2.1. 2. Yield loci for sheets with textures that are rotationally symmetrical about the thickness direction. Applied biaxial stresses are characterised by the ratio $\alpha = \sigma_Y / \sigma_x$. The intersection of the dashed line and any yield locus identifies the stress ratio for a state of plane plastic strain.

2.2. Methods of describing texture.

Before one can equate drawability and R value to texture, a suitable means of describing preferred orientation has to be devised. There are two common methods of describing texture in rolled sheet and two methods by which the magnitude of the textures can be represented.

Sheet textures are conveniently described in terms of ideal textures with certain crystal planes lying parallel to the plane of the sheet, and crystallographic directions that are parallel to the rolling direction e.g. $\{xyz\}\langle uvw\rangle$ where $\{xyz\}$ denotes the rolling plane and $\langle uvw\rangle$ the rolling direction. One graphical representation of texture is known as a pole figure, which is a statistical distribution diagram of a single convenient crystallographic pole relative to suitable reference axes.

A number of X-ray methods for obtaining pole figures are available, and have recently been reviewed(2). The basic principles are described in Standard text books (12, 13). Conventionally, two geometries of specimen arrangement relative to the incident and diffracted beam are used. For the transmission method the counter is arranged to measure the intensity of the diffracted beam transmitted through the sheet specimen, whilst in the reflection method the reflected beam is measured. The X-ray counter arm is set at the 2θ angle of the Bragg reflection of the selected plane and the specimen is rotated to obtain data for an area of the stereographic projection.

Both techniques are necessary to obtain the complete pole figure as absorption in the former case and defocussing in the latter, limit the angle of specimen rotation over which accurate determinations can be made. Cylindrical, spherical and sandwich specimens have been used in an attempt to overcome the above difficulties[2] so that the complete pole figure can be obtained from one specimen. However, for most purposes, sufficient information regarding sheet texture of steel can be obtained by simply using either the transmission or reflection technique.

A second method of texture description uses a pole density parameter 'p' which is usually the density of a rational index pole, parallel to a single reference axis, compared with the density of equivalent poles in a randomly oriented sample. The normal to the plane of the sheet is the usual reference axis for the description of rolling textures i.e. an $\{xyz\}$ texture indicates that $\{xyz\}$ planes are parallel to the plane of the sheet. 'p' values are usually quoted in multiples of random intensity. The 'p' values of all available rational index poles can be graphically plotted in the unit stereographic triangle and is known as the inverse pole figure[14-16].

The inverse pole figure description of texture is only precise for fibre textures that are symmetrical about a single principal axis, but, as rolled steel exhibits a distinctive partial fibre texture, it is often used to assist in the interpretation of the textures represented in direct pole figures.

Furthermore, as one assigns a numerical value to the intensity of a particular texture component, texture analysis is simplified, and very small texture dissimilarities can often be distinguished.

2.3. The R value - texture relationship.

$\overline{R}$ value, in the absence of mechanical fibering and internal stresses, is related to the orientation of individual grains within a polycrystalline aggregate[17]. For good deep drawability 'strong' crystallographic directions are required normal to the sheet. The particular relevance of the inverse pole figure texture description to $\overline{R}$ value analyses can now readily be appreciated. $\overline{R}$ is the mean value of all R values at angles to the $\langle uvw \rangle$ rolling direction in the $\{xyz\}$ rolling plane. Therefore, the definition of the $\langle uvw \rangle$ direction is of no significance when correlating $\overline{R}$ value with texture. However, the rolling direction is required to be known when analysing R_x values and texture unless the texture is rotationally symmetrical about the sheet normal direction when $\overline{R} = R_0 = R_{90} = R_{45}$

Crystallographic[17-20] and macroplasticity[9] theories have been used to predict $\overline{R}$ and R values for textured sheet. All the different analyses generally lead to similar results to each other for predominantly single component textured steel. A texture with $\{111\}$ planes parallel to the plane of the sheet will give high $\overline{R}$ values and also little variation in R value with angle of testing in the plane of the sheet, i.e. low planar anisotropy.

The predominance of this texture will, therefore, not only promote good drawability, but will also limit the incidence of earing. Similarly $\{100\}$ textures give very low $\bar{R}$ values and high ΔR values and $\{110\}$ texture result in very high planar anisotropy.

The crystallographic[19] and macroplasticity theories[9] predict different anisotropic behaviour for multicomponent textured sheet. This can be illustrated by comparing the two basic theories for a sheet containing the orientations $\{111\}$ and $\{100\}$. Since $\bar{R}$ value varies between zero and infinity and an isotropic metal has a value of one, the relative contribution of two orientations to an over all $\bar{R}$ value cannot be obtained simply by averaging. Therefore, crystallographic analyses[18, 19] invoke the $\bar{D}$ value concept where

$$\bar{D} = (\bar{R} - 1)/(\bar{R} + 1) \quad \text{......... 2.3.1.}$$

$\bar{D}$ has a range of values betwen -1 and +1. A $\bar{D}$ value of zero is indicative of an isotropic material. Relating $\bar{D}$ to texture[19],

$$\bar{D} = \sum \bar{D}_{\{hkl\}} \cdot \bar{P}_{\{hkl\}} \quad \text{......... 2.3. 2.}$$

where $\bar{D}_{\{hkl\}}$ is the $\bar{D}$ value for the individual texture components of orientation $\{hkl\}$ and $\bar{P}_{\{hkl\}}$ is the probability of the plane $\{hkl\}$ being parallel to the plane of the sheet. Therefore, in the two component system being considered the $\bar{D}$ value is a function of the $\bar{D}_{\{hkl\}}$ and $\bar{P}_{\{hkl\}}$ values of the individual components.

For a particular orientation $\{hkl\}\langle uvw\rangle$

$$\bar{D}_{\{hkl\}} = \tfrac{1}{4}(D_0 + 2D_{45} + D_{90}) \quad \text{......... 2.3. 3.}$$

where the suffix is the angle from $\langle uvw \rangle$ in the $\{hkl\}$ plane. The calculation of D value for a metal is in two parts. Firstly, using resolved shear stress criteria, the operative slip system has to be deduced for a given tension direction. Secondly, the D value is estimated from the resultant strain in the width and thickness directions after slip on this slip system. The calculation is generally complicated by the need to make the decision as to the number of slip systems operative[20]. Typical $\bar{D}_{\{100\}}$ and $\bar{D}_{\{111\}}$ are -0.5 and 0.4 respectively.[19] $\bar{P}_{\{100\}}$ and $\bar{P}_{\{111\}}$ are proportional to the volume fraction of $\{100\}$ and $\{111\}$ crystals. Therefore five crystals of $\{111\}$ orientation balance the effect upon $\bar{D}$ value of four crystals of $\{100\}$ orientation.

The macroplasticity theory[9] is based on Taylors criterion[21] that slip occurs on five systems in each grain that produce the required shape change, associated with a particular R value, with the least amount of work. The relationship between tensile stress, X, and shear stress, τ, is

$$X/\tau = 1/\cos\theta . \cos\lambda \qquad \ldots\ldots\ldots \; 2.3.\,4.$$

where θ is the angle between the tensile axis and slip plane normal and λ the angle between the tensile axis and slip direction. Tensile strain is related to shear strain by the same orientation factor, m.

$$\text{i.e. } m = 1/\cos\theta . \cos\lambda \qquad \ldots\ldots\ldots \; 2.3.\,5.$$

As slip occurs on five systems simultaneously, in a polycrystalline aggregate, tensile strain is related to shear strain by an average orietation factor M.

M can be plotted against R value, or D value, for a particular crystallographic orientation and a probable real R value corresponds to the minimum in the plot since this is the condition of least work.

For axially symmetrical textures, or for the calculation of $\bar{R}$ and $\bar{D}$ values, a parameter $\bar{M}$ is used which is the weighted average of M obtained at all angular displacements of the texture in the plane of the sheet. $\bar{M}$ is plotted against $\bar{R}$ and $\bar{D}$ in Fig. 2.3. 1. for three crystal textures and a randomly oriented aggregate.

If the two orientations $\{111\}$ and $\{100\}$ are present the minimum in the resultant curve would occur when,

$$f\{100\}\frac{d\bar{M}\{100\}}{d\bar{D}} + f\{111\}\frac{d\bar{M}\{111\}}{d\bar{D}} = 0 \quad \ldots\ldots\ldots 2.3.\ 6.$$

For a $\bar{D}$ value of 0.1. which corresponds to a typical $\bar{R}$ value of 1.2 for steel sheet

$$\frac{d\bar{M}\{100\}}{d\bar{D}} = \cdot 9 \quad \text{and} \quad \frac{d\bar{M}\{111\}}{d\bar{D}} = -\cdot 2$$

Therefore, 18 crystals of $\{111\}$ orientation balance the effect upon $\bar{R}$ or $\bar{D}$ value of 4 crystals of $\{100\}$ orientation. Consequently the macroplasticity theory ascribes far more importance to $\{100\}$ texture relative to $\{111\}$ texture in controlling $\bar{R}$ value than does the crystallographic theory. However, the theories are in agreement that intense $\{111\}$ texture and weak $\{100\}$ texture is beneficial for good deep drawing properties.

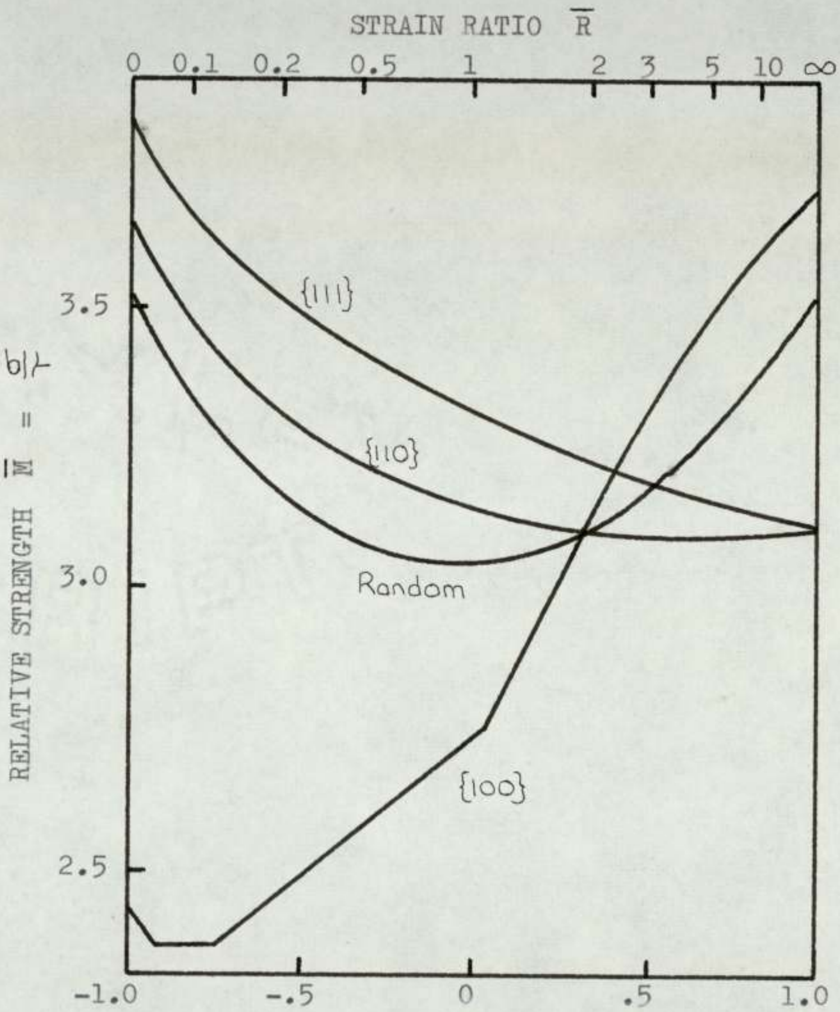

Fig. 2.3.1. Curves relating $\overline{M}$ to $\overline{R}$ and $\overline{D}$ for rotationally symmetric textures.

3. Metallurgical Aspects of Rimmed Steel Sheet Production.

During the production of rimmed steel sheet a variety of properties[22] other than satisfactory texture also have to be controlled. Consequently, the development of a $\{111\}$ texture was not the only consideration when the process was designed. The most important additional properties can be briefly listed as follows :-

(i) a yield strength of 31-37 Kgm per mm^2

(ii) a grain count of approximately 2000 per mm^2

(iii) a tensile elongation of 40-50% on a 50.82 mm. (2 inch) gauge length.

(iv) low quench aging and strain aging susceptibility prior to fabrication.

(v) close dimensional tolerances.

(vi) a surface that is amenable to coating.

The following production cycle results in material exhibiting the above properties.

Refined steel is cast into ingot moulds of rectangular cross section where solidification occurs producing the characteristic 'rim and core' ingot zones. The zones contribute to rimmed steel's unique properties primarily as a consequence of the almost pure iron inclusion free rim zone. The slab ingot is re-heated and hot rolled, usually above the A_3 temperature, firstly in a reversing slab mill and then in a tandem finishing mill. The temperature of the steel during 'soaking' and therefore throughout hot rolling is regulated to optimise properties in the finished sheet. The grain size, which is partly controlled by hot rolling practice, is selected to balance the properties of ductility and resistance to 'orange peeling'.

Too high a hot rolling temperature (i.e. $>975^{\circ}C$) results in an over large grain size and 'orange peeling' in fabricated components, whilst too low hot rolling temperatures (i.e. $<900^{\circ}C$), can lead to poor formability as a result of too small a grain size and unsuitable texture.

The hot band is metallurgically unsuitable for the press shop. Furthermore, it can only be produced to a minimum thickness of approximately 2.5 mms. because of scale losses and severe engineering problems, including gauge control and surface finish. The thickness reduction therefore has to be completed by cold rolling. Hot band at approximately 950°C is therefore water sprayed and subsequently coiled at a temperature between 600°C and 700°C. The coiled hot band is air cooled and then pickled to removed scale. Coiling temperature control is important because cooling rates affect the size and distribution of the precipitated carbides, which may ultimately affect sheet characteristics e.g. ductility and anisotropy. Typically a 3 mill tandem with 500 mm. diameter rolls would be used for cold rolling to produce sheet with a suitable surface finish and to close dimensional tolerances. The sheet is generally cold rolled between 60 and 70%, so that a satisfactory balance between grain size and strain ratio value, is obtained in the finished sheet.

The steel is in a work hardened condition and is not suitable for subsequent fabrication. A heat treatment cycle is necessary to render the sheet ductile.

Controlled atomosphere batch annealing furnaces are at present preferred to continuous annealing furnaces, because more precise control is possible. Very slow cooling allows adequate precipitation of carbon and nitrogen, so that quench and strain aging problems are reduced to a minimum and ductility increased to a maximum. The rate of recrystallisation is increased the higher the annealing temperatures. However, the practical limit is the A_3 temperature, since annealing above this can lead to the formation of coarse intergranular carbides which can be detrimental to formability. Grain growth, at sub-critical temperatures, does not materially affect texture[23].

The sheet is finally temper rolled, which improves surface finish and reduces the likelihood of stretcher-strain formation during subsequent fabrication, provided it is used within its' shelf life.

Pronounced textures are not produced during hot rolling, at least above the A_3 temperature, as dynamic recrystallisation occurs. Furthermore, the material passes through a phase transformation during cooling, which also reduces the intensity of any texture. Cold rolling develops intense texture which increases in intensity with the total percentage reduction. Annealing this textured cold rolled sheet results in recrystallisation, leading to new textures which have an orientation relationship to the deformation texture.

For b.c.c. steel the recrystallisation texture, to a first approximation, is very similar to the rolling texture, although there is a marked reduction in intensity. The coiling process, which can be considered to include water spraying of the sheet, to a pre-determined temperature, as well as the action of coiling, has no direct affect upon texture. Temper rolling also has no measurable affect upon texture.

Textures in finished sheet, which are of most importance to the fabricator, are therefore mainly established during the cold rolling process.

4. <u>Cold Rolling Textures in B.c.c. Steel</u>.

Textures have been the subject of several review articles in recent years[2-5]. The theories proposed to account for rolling textures are derived from a geometrical approach and are based upon observations of deformation in single crystals. Rolling can be considered as a combination of tension and compression as the operative slip direction rotates towards the rolling direction and the slip plane normal rotates towards the strip normal. Therefore, textures that are simultaneously stable in tension and compression are stable textures after rolling.

Tension and compression develop textures of high symmetry and are adequately described by quoting the crystallographic direction parallel to the axis of applied force. $\langle 110 \rangle$ texture with spread towards $\langle 311 \rangle$ is predicted after tension and the compression texture is predicted as a duplex $\{100\}$ + $\{111\}$ texture with the $\{111\}$ component predominating. Therefore, the rolling texture is predicted as containing the major components $\{100\}\langle 110 \rangle$ and $\{111\}\langle 110 \rangle$[24].

When rolling polycrystals, if the aggregate is not to disintegrate, each individual crystal must undergo the same strains as the sheet as a whole. This requires a minimum of five independent slip systems, the selection of which is governed by the principles of least work[21]. This condition imposes constraint from neighbouring grains on the deformation of the individual crystals of the polycrystalline aggregate.

Effective stress axes, which allow for constraint stresses, are displaced from the real applied stress. These can be deduced[24] as ⟨110⟩, ⟨111⟩, and ⟨100⟩ since for each case, multiple slip systems have equal likelihood of becoming operative. Since for all three effective stress axes the slip systems are symmetrically disposed, no rotation of the grains relative to the real applied stress occurs and consequently there should be no development of preferred orientation. It has, however, been stated elsewhere[25] that multi-slip, to produce the accommodating strain, generally only occurs close to the grain boundary. Single or duplex slip in the grain centres is therefore dominant. Rotations during the rolling of polycrystals can hence be equated to that of single crystal behaviour.

Although deformation is known to be macroscopically[26] and microscopically[27] inhomogeneous, it is sufficient for statistical problems such as texture development to assume homogeneous deformation[28]. The strain ellipsoid[29] can, therefore, be used to represent the state of strain at any point in a metal during a small plastic strain. The analysis can also be used to explain texture development during the large strains experienced during rolling.

A small plastic strain in a homogeneous medium changes the shape of a spherical volume element to an ellipsoid. The two dimensional vector diagram representing the state of strain at any point during uniaxial extension is shown in Fig. 4.1.

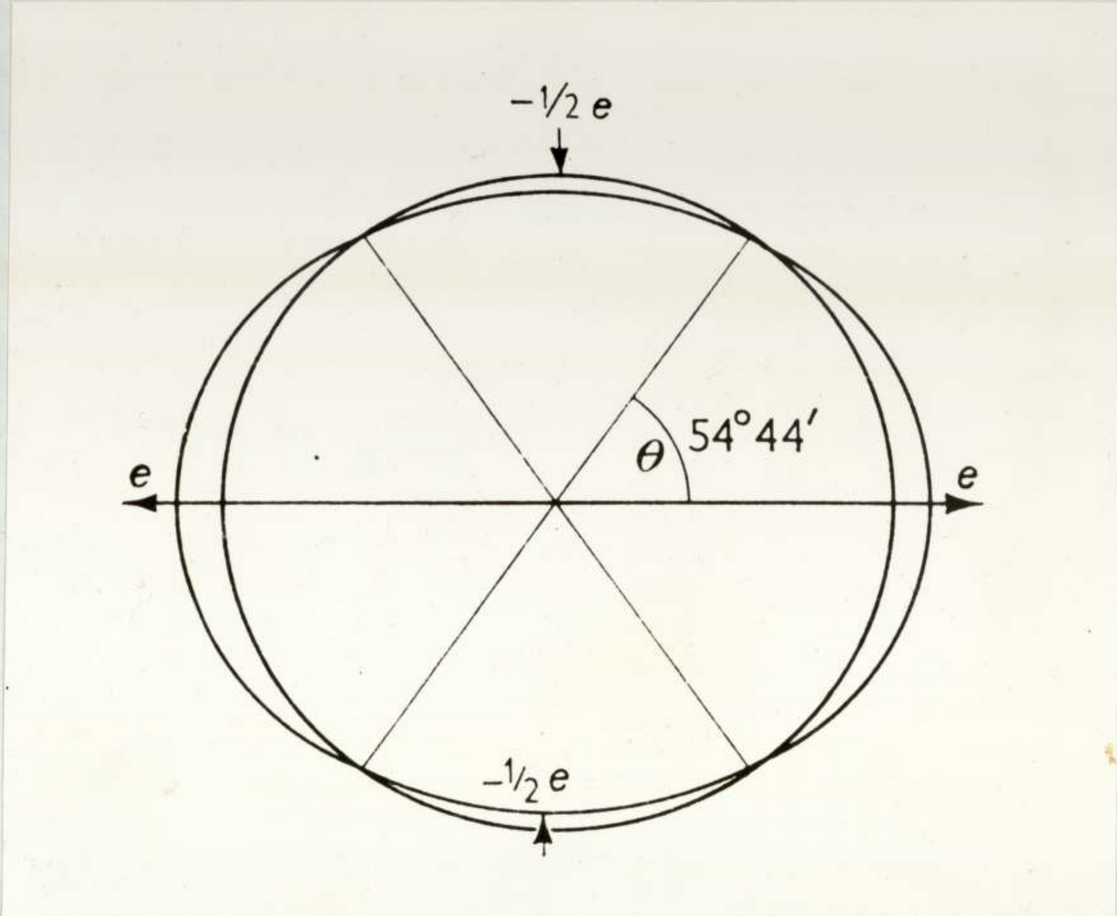

Fig. 4.1. The strain ellipsoid of incremental strain.

As $e \rightarrow 0$ i.e. for very small strains, the surface of the strain ellipsoid intersects the surface of the sphere of zero strain in circles around the extension axis which subtend an angle 2θ at the centre of the sphere where $\theta = 54^{\circ}44'$ (i.e. $\tan^{-1}\sqrt{2}$).

Similarly in uniaxial compression the angle between the compression axis and axis of zero strain is $54^{\circ}44'$. Therefore, for a uniaxial increment of strain during any large strain, the strain can be described by pure shear at $54^{\circ}44'$ from the axis of applied stress.

The strains in rolling are equivalent to a combination of the strains in extension in the rolling direction and compression normal to the sheet plane with zero strain in the transverse direction. In this instance the strain ellipsoid intersects the sphere of zero strain in diametral planes inclined at 45° to the strip surface about the axis transverse to the rolling direction. The geometry of deformation in pure rolling is thus completely defined. The strain ellipsoid analysis of texture has previously been used specifically to account for texture development in f.c.c. metals but the technique has general application. Therefore, the principles outlined by Richards[29] will be used to predict the rolling textures in b.c.c. metals.

The crystallographic rotations involved during rolling strains can be represented stereographically Fig. 4.2. by $54^{\circ}44'$ circles around the strip normal and rolling direction. According to the strain ellipsoid concept the $\langle 111 \rangle$ slip direction rotates towards the rolling direction and is stable on the compression circle $54^{\circ}44'$ from the sheet normal.

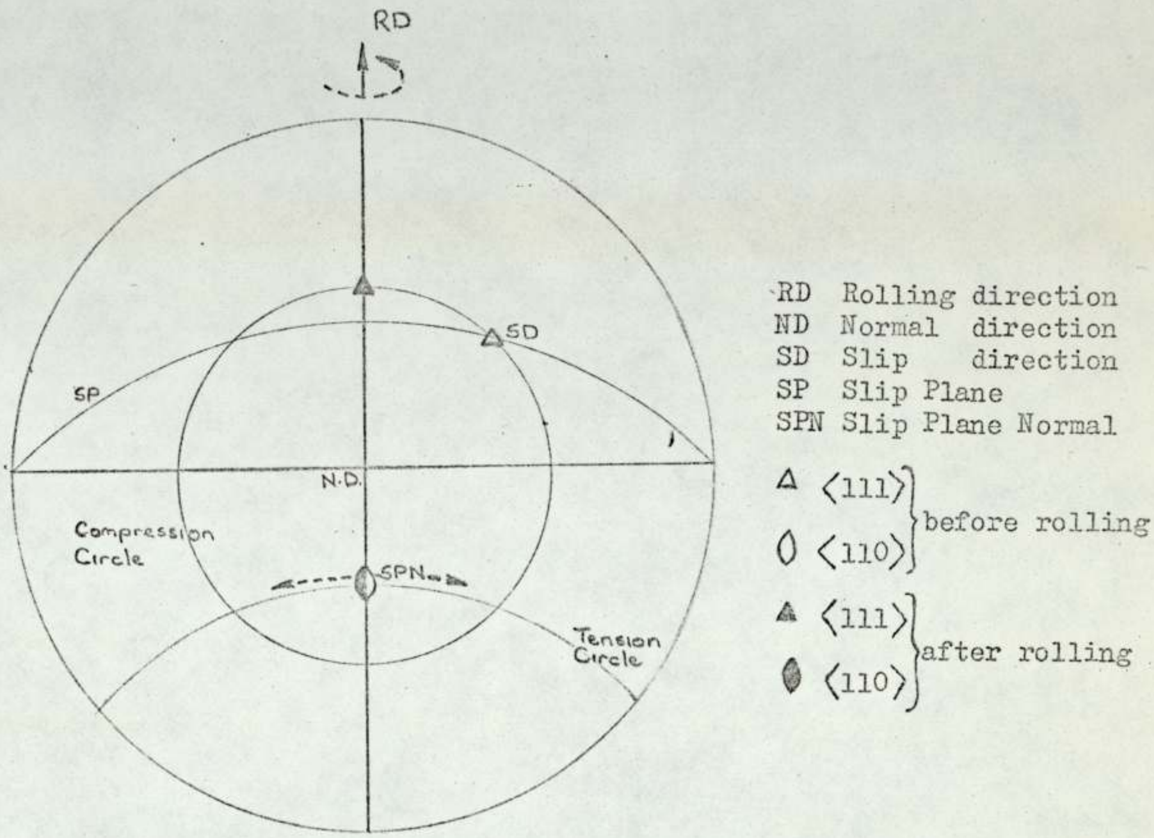

Fig. 4.2. Rolling as combined compression and tension.

The (110) slip plane maintains contact with the compression circle likewise. The slip plane normal is therefore stable on the tension circle $35^{\circ}16'$ from the sheet normal. This geometry results in a texture close to $\{225\}\langle 110\rangle$. However, b.c.c. metals are subject to pencil glide (i.e. there is a distinct $\langle 111\rangle$ slip direction and many alternative slip planes) which is equivalent to rotation of the projection about the rolling direction, and therefore describes a partial fibre texture for b.c.c. metals with $\langle 110\rangle$ directions parallel to the rolling direction. During this rotation the $\langle 111\rangle$ slip direction overshoots the compression circle in an analogous manner to that described[29] during the equivalent analysis of f.c.c. metals.

The rolling textures observed in b.c.c. iron are not affected by small additions of solute elements[30]. Furthermore, small volume fractions of second phase particles have been observed to result in little or no texture modification, particularly if the particles are themselves not plastically deformed during rolling[30]. Deformation textures in rimmed steel are therefore essentially the same as in pure iron.

Richards et al[31] have reviewed the results of several workers regarding the development of rolling texture in iron and have noted minor observational discrepancies. However, a convenient description of the progressive development of texture with increasing rolling reduction based upon the experimental work of Bennewitz[32] is as follows : rolling textures of iron are a combination of two partial fibre textures.

Fibre texture A has a $\langle 110\rangle$ direction parallel to the rolling direction and the prominent texture components are between $\{001\}\langle 110\rangle$ and $\{111\}\langle 110\rangle$. Fibre texture B has a $\langle 110\rangle$ pole inclined 30° from the sheet normal direction, and 60° from the rolling direction. Prominent components of texture B are $\{554\}\langle 225\rangle$ and $\{112\}\langle 110\rangle$. Orientation $\{112\}\langle 110\rangle$ is common to both fibre textures. Fig. 4.3. schematically represents the two fibre textures on one quadrant of a (110) pole figure. The shape of the intensity contours for partial fibre textures A and B are distinctly different, and therefore the presence or absence of either group of orientations can be clearly established.

Texture B develops during rolling to about 60% reduction after which texture A becomes more prominent with further increase in reduction. The texture spread is gradually reduced until, after 95% cold reduction, the common orientation $\{112\}\langle 110\rangle$, is most intense. Subsequent rolling causes rotation to the stable end orientation $\{113\}\langle 110\rangle$.

The components $\{111\}\langle 110\rangle$ and $\{100\}\langle 110\rangle$ of fibre texture A are in agreement with the predictions of Calnan and Clews[24], although fibre texture B is not adequately accounted for. Dillamore and Roberts[25] account for a range of orientations between $\{112\}\langle 110\rangle$ and $\{100\}\langle 110\rangle$ which are components of fibre texture A, but are also unable to explain the presence of components of fibre texture B other than $\{112\}\langle 110\rangle$. The analysis based upon the work of Richards[29] also accounts for fibre texture A but not fibre texture B.

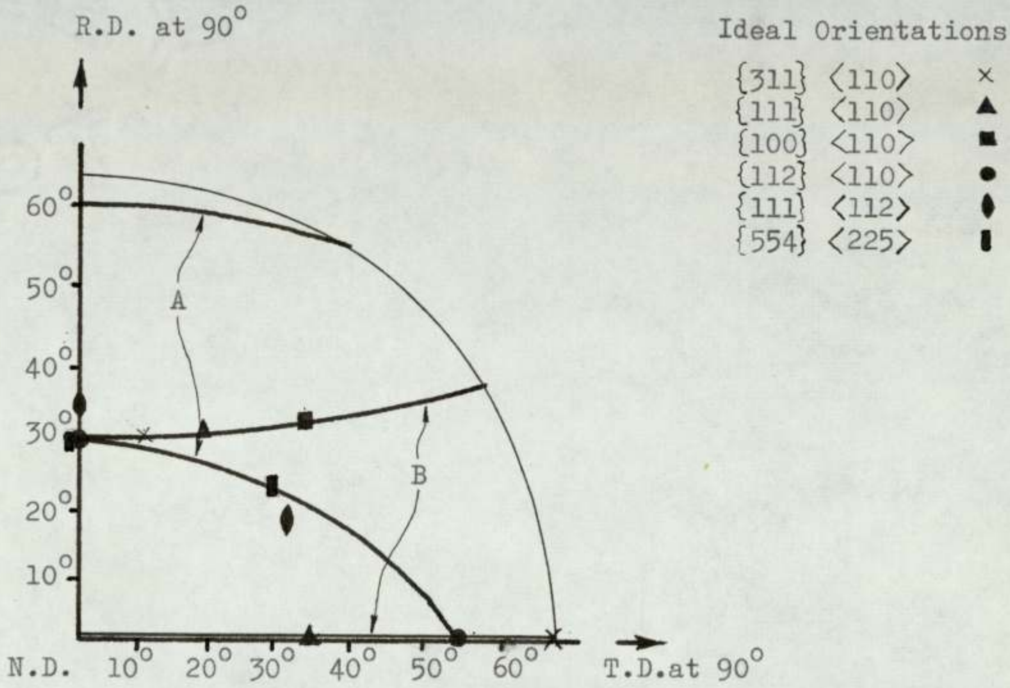

Fig. 4.3. Central 65° of one quadrant of (110) pole figure showing locus of (110) poles for ideal Fibre textures A and B.

Alternative constituent texture components have been proposed to the ones outlined above e.g. $\{111\}\langle 112\rangle$[33]. However, this component is only 6° from the component $\{554\}\langle 225\rangle$ and Takechi et al[34] consider it impossible to distinguish between the two as distinct orientations because of the spread observed in rolling textures. Furthermore, pole density data abstracted from inverse pole figures[19] does not lead to the identical description of rolling textures as the ones outlined above. Fig. 4.4. illustrates the change in density of crystal planes parallel to the plane of the sheet with increasing cold reduction. $\{111\}$ planes increase rapidly with cold reduction, whereas $\{112\}$ planes are constant over the range, and only of approximately 1.5 random intensity. This conflicts with the proposed stable end orientation, at least to 95% reduction, of $\{112\}\langle 110\rangle$ as had previously been deduced from the examination of pole figures[32]. $\{111\}$ texture is far more intense over the complete range of reductions. To overcome this inadequacy, an alternative description of iron rolling textures has been proposed[31]. Fibre texture A is retained, but fibre texture B is replaced by a texture with $\{111\}$ planes parallel to the sheet plane. In this case, orientation $\{111\}\langle 110\rangle$ is common to both textures.

Throughout the present text, the latter description of the typical iron rolling texture will be used. For convenience, fibre texture A will be described as a $\langle 110\rangle_{RD}$ fibre texture and the texture with $\{111\}$ planes parallel to the sheet plane as $\{111\}_{RP}$ fibre texture. The suffixes RD and RP refer to rolling direction and rolling plane respectively.

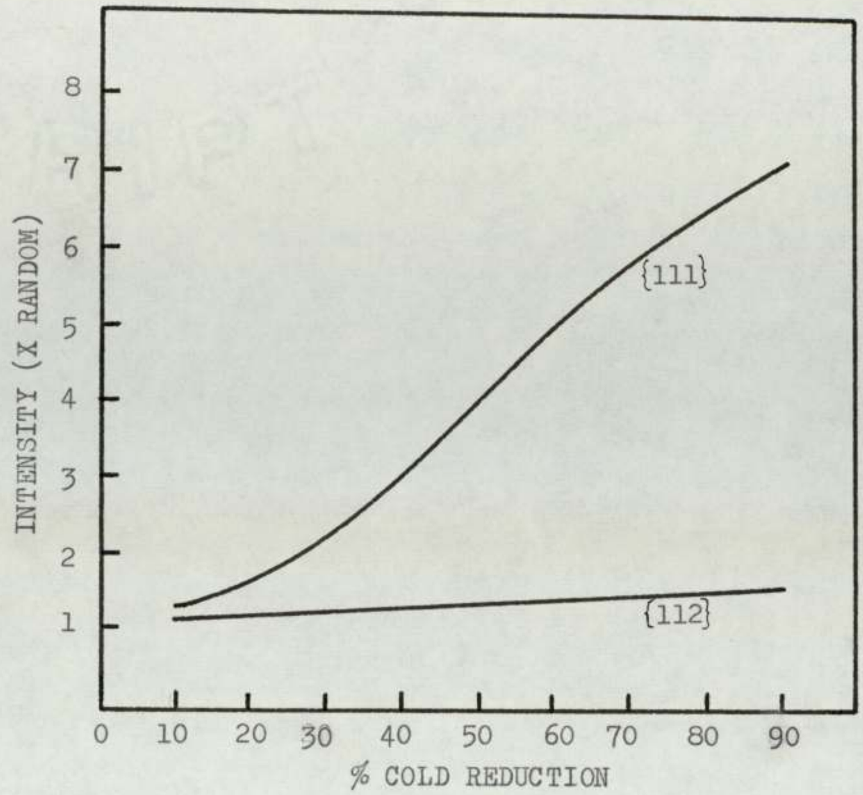

Fig. 4.4. Intensity of {111} and {112} texture as a function of percentage cold reduction.[19]

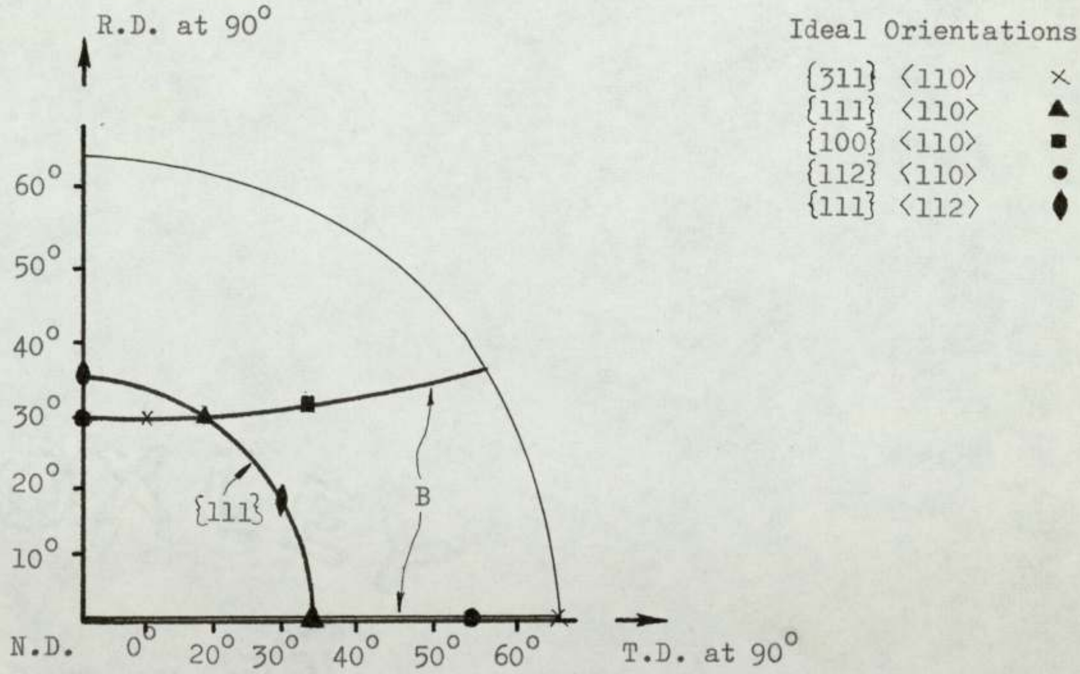

Fig. 4.5. Central 65° of one quadrant of (110) pole figure showing locus of (110) poles for ideal Fibre textures B and texture with {111} planes parallel to sheet plane.

Fig. 4.5. schematically represents the (110) pole figure for the two textures, and the similarity with Fig. 4.3. is readily apparent.

Of far more technological significance than the apparent confusion resulting from different methods of texture measurement and minor observational discrepancies which are really different interpretations of the same thing, is the effect of rolling conditions on the development of texture. Three cold rolling variables will be considered :

(i) draught

(ii) lubrication

(iii) total reduction.

Draught and lubrication will be examined together as their effects upon texture are inter-connected.

5. The Effect of Rolling Draught and Lubrication upon Textures and R value.

Textures quoted in the literature are described by reference to crystallographic axes relative to the plane of the sheet. This presupposes that the texture at the surface plane and mid-plane are the same. In practice, this is generally not the case. The texture changes that occur through the thickness of the sheet are referred to as through-thickness texture segregation.

The plastic strains occurring during rolling have been examined with the aid of grids suitably implanted in sheet[26]. Under certain rolling conditions it was observed that the deformation was not homogeneous i.e. a vertical plane section of the sheet does not remain a vertical plane section after rolling. Obviously differences in strain at different depths in the sheet must result from differing induced stress systems. It is therefore expected that distinct through-thickness texture segregation will occur.

Pronounced surface to centre texture segregation has been observed in rolled 2% Al iron single crystals[35]. The segregation was said to be associated with the shearing action arising from roll friction. There was a predominant $\{001\}\langle110\rangle$ texture at the surface with a gradual transition to a $\{111\}\langle112\rangle$ texture at the centre.

Subsequent investigations with commercial Aluminium killed steel[36] and iron[6] confirmed the general idea of texture segregation in cold rolled polycrystalline ferrous metals.

The results are, however, somewhat confusing.

Held[36] processed steel strip in two different ways. Steel A was rolled with palm oil lubrication and heavy reductions at each pass. Held did not define the magnitude of his reductions at each pass but stated that 75% reduction was achieved in a total of five passes. This represents an average draught of approximately .275 mm. Steel B was rolled without lubrication and 'light' reductions were given at each pass. Inverse pole density data was plotted for different cold reductions and are summarised in Fig. 5.1. Steel A was said to exhibit an homogeneous texture. However, there was a texture irregularity in the extreme surface planes. This has since been attributed to the folding over of surface asperities which was not expected to produce texture as does normal rolling strain[37]. Steel B exhibited pronounced texture segregation. Was the segregation attributable to the small draught or lack of lubrication?

Stickels [6] performed an almost parallel study with iron but lubrication was used in process type B and not A. This time process A gave the composite texture which is therefore evidently the result of rolling under conditions of severe friction, rather than rolling with light draughts. Pole figure analysis revealed that the surface textures were of the type $\{110\}\langle xyz\rangle$ where $\langle xyz\rangle$ ranged between $\langle 001\rangle$ and $\langle 111\rangle$ directions and were therefore similar to shear type textures[38,39] Table 5.1. The surface texture was related to the centre rolling texture by 90° rotations about the transverse axis.

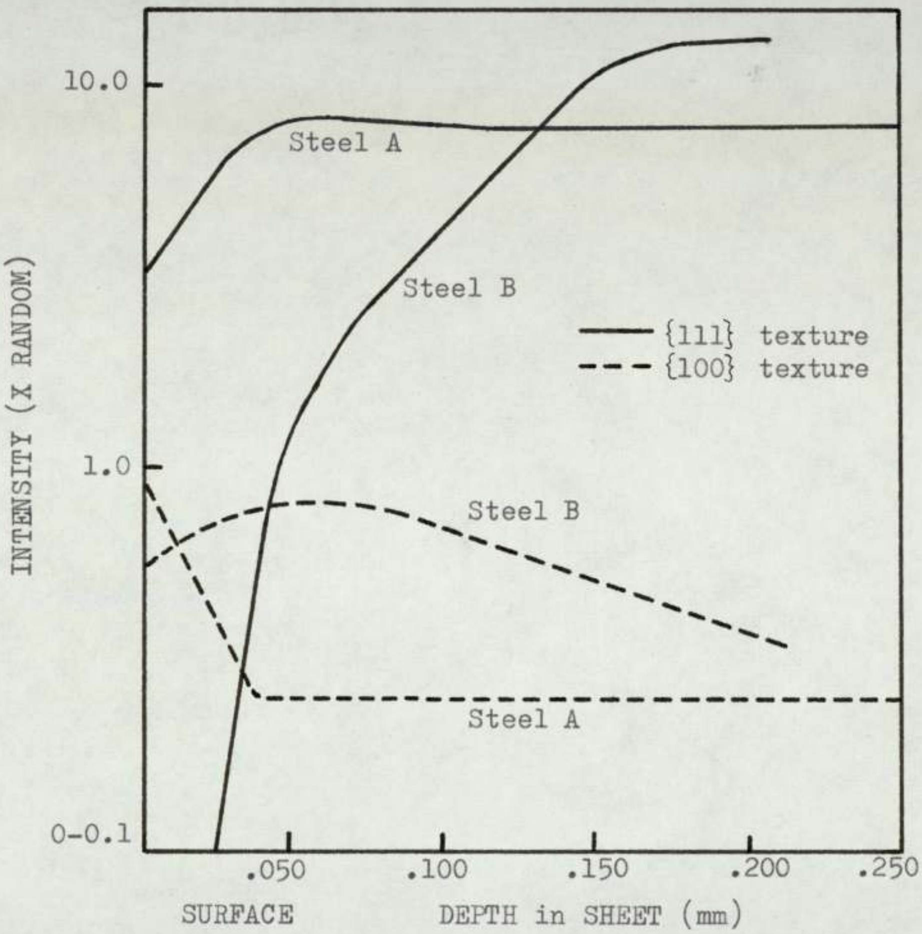

Fig. 5.1. Recrystallisation texture of Steel A and B as a function of depth in the sheet. Steel A was rolled 60% to a thickness of .825 mm., and Steel B was rolled 78% to a thickness of .525 mm. The sheet was originally 2.06mm. thick.

Shear Textures
$\{112\} \langle 111 \rangle$
$\{110\} \langle 001 \rangle$
$\{110\} \langle 112 \rangle$
$\{110\} \langle 111 \rangle$

Table 5.1. Shear texture components observed in b.c.c. metals(38, 39).

In this respect they were similar to surface textures that had previously been observed in f.c.c. metals[40].

Held and Stickels had, by dry rolling creating severe friction conditions, apparently induced shear type strain in the surface elements of their respective metals. Dillamore and Roberts[40] however, showed that rolling draught was also an important parameter as heavy draughts contribute to the increase of friction forces.

Shear type textures have been observed in heavily rolled niobium[37]. Niobium strip 10.0 mms. thick and 18.75 mms. wide was dry rolled with draughts of approximately 0.25 mms. to a total reduction of 95%. The surface texture components were described as strong $\{110\}\langle 113\rangle$ orientations with weaker components of $\{001\}\langle 110\rangle$, $\{001\}\langle 100\rangle$ and $\{112\}\langle 111\rangle$.

The observations of rolled niobium[37] revealed a second type of segregation which developed at moderate reductions up to 70%, Fig. 5.2. The sheet surface plane and mid-plane pole figures were very similar in this case and were typical of b.c.c. metal rolling textures. They were described as consisting of fibre textures A and B, but could also equally have been described as fibre textures $\langle 110\rangle_{RD}$ and $\{111\}_{RP}$. Mid way between the surface and mid-planes however, was an area where the textures were significantly different, Fig. 5.3. Fibre texture B was said to be absent, and the texture remaining was described as consisting primarily of $\{001\}\langle 110\rangle$ ideal orientations.

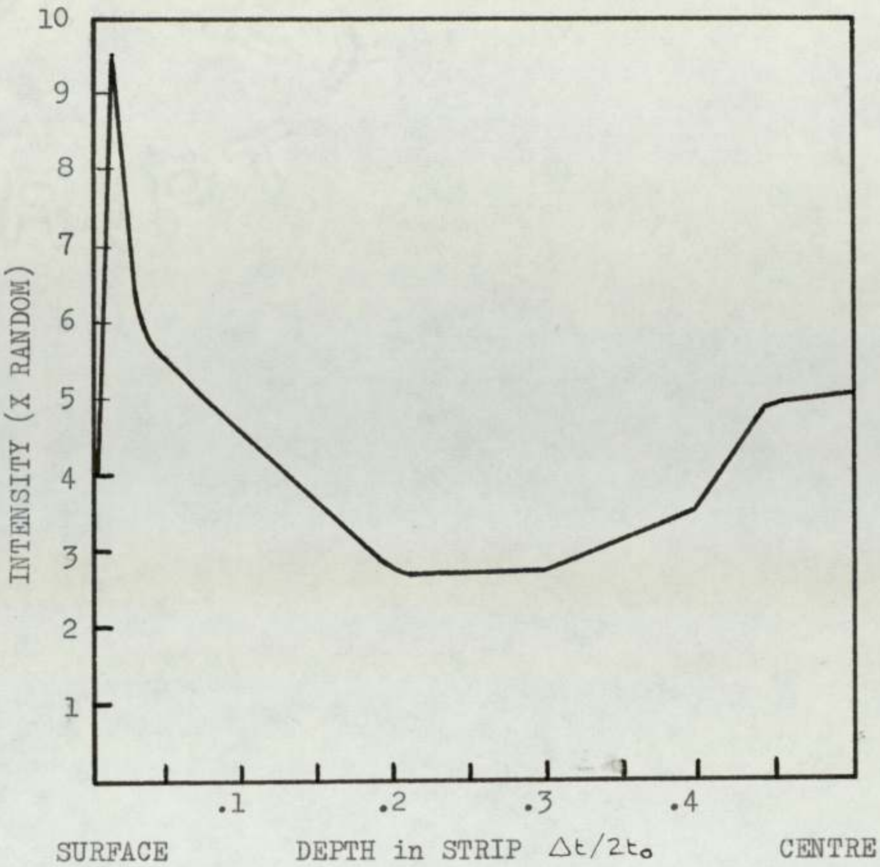

Fig. 5.2. X-ray intensity at angle ϕ, the angle from the rolling plane normal along the N.D. to R.D. radius of (110) pole figure, (See Fig.5.3.) versus strip depth for a niobium specimen cold rolled 70%. Strip depth is plotted as a function of half the original thickness, i.e. $\Delta t/2t_o$

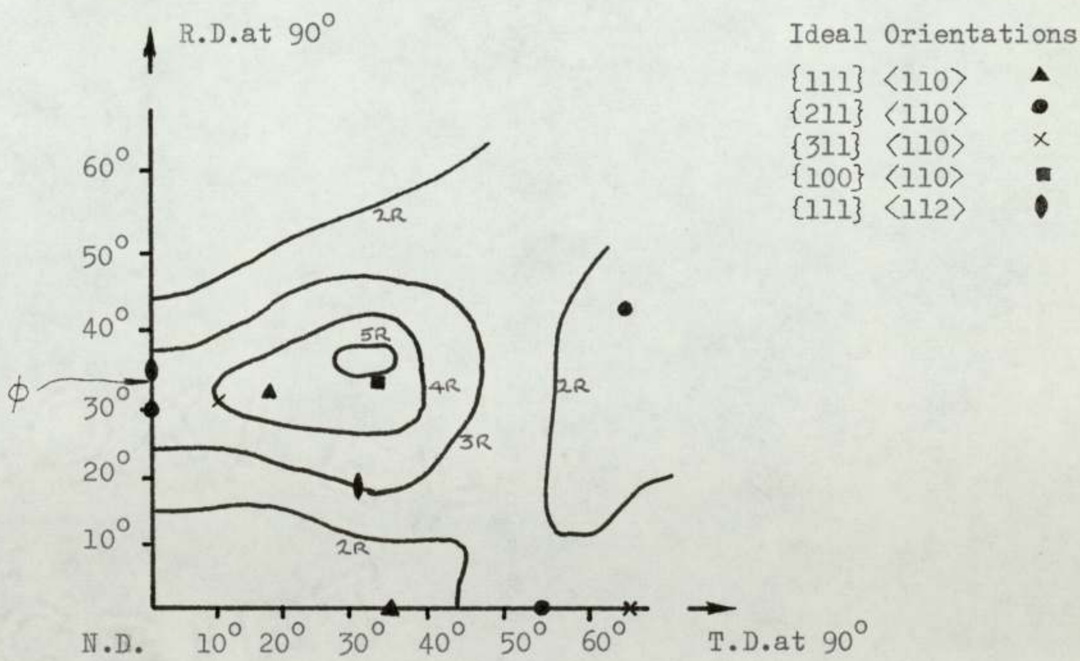

Fig.5.3. (110) pole figure obtained at a sheet depth, $\Delta t/2t_o$, of .3, in niobium cold rolled to 65% reduction in thickness.

This texture was tentatively described as being attributable to the inhomogeniety of rolling strain and developed under conditions of 'high body' rolling :

$$\text{i.e. } l/tm = R^{\frac{1}{2}} \frac{(ta - tb)^{\frac{1}{2}}}{(ta + tb)/2} = < 1.0 \quad \ldots\ldots\ldots \quad 5.1$$

$$\text{and } w/tm = < 8.0$$

where l is the length in the rolling direction of the geometrical zone of deformation, tm is the average thickness of that zone, R is the radius of the work rolls, and ta and tb are the entry and exit thicknesses of the strip respectively, and W is the width of the geometrical zone of deformation.

The existence of deformation twinning was found in some cases to be depth dependent in an analogous way to textures. However, the differences in texture were not attributed to twinning deformation, but since twins were only present in certain areas of the sheet, this was taken as evidence of the inhomogeniety of stress through the sheet.

Crane and Alexander(41) noted that it would be desirable to examine the influence of deformation zone geometry upon the development of rolling textures. Dillamore and Roberts(40) concur, at least for conditions close to sticking friction, as they expected that it would influence the development of texture segregation. The subject has, however, received little attention in the literature. Texture segregation in rolled niobium(37) was explained by reference to the geometry of deformation as defined by l/tm, where l is the length of the geometrical zone and tm is the average thickness of the zone.

However, no attempt was made to use a constant value of 1/tm as the criterion for designing rolling schedules.

Textures have been observed in rolled single crystals of b.c.c. molybdenum[42] that were not the same as those observed in rolled iron single crystals[43]. The crystals of each metal had an initial orientation close to $\{001\}\langle 100\rangle$. After 92% reduction, the iron crystal attained a texture similar to the polycrystalline iron rolling texture, whereas molybdenum after 96% reduction maintained the $\{001\}\langle 100\rangle$ orientation but there was spread about the sheet normal. The stable crystal orientation for molybdenum was similar to the Calnan and Clews[21] predictions for uniaxial compressive strain. It is significant that the rolling draughts used for molybdenum were of the order of .0025 mm. which represents a very different rolling geometry than is normally encountered in rolling experiments. The iron crystal was reduced in 20-40 passes, corresponding to draughts of between .2 and .4 mm.

Table 5.2. summarises the observations of workers mentioned in the preceding section with regard to the development of rolling textures other than $\langle 110\rangle_{RD}$ and $\{111\}_{RP}$ orientations, which are the normal polycrystalline iron rolling textures.

Only Held[36] measured R values for strip rolled under different conditions. Generally, after annealing, strip exhibiting homogeneous textures had higher R values than inhomogeneously textured strip.

Reference		Cold Rolling conditions		Observed texture		Comments
		Draught mm.	Lubrication	Surface Plane SP	Mid-Plane MP	
Held[36]		'light'	degreased rolls	low $\{111\}$ intensity high $\{100\}$ and $\{110\}$ intensity.	high $\{111\}$ intensity low $\{100\}$ and $\{110\}$ intensity.	Textures were variable depending upon total rolling reduction.
Stickels[6]		.750	degreased rolls	$\{110\}\langle xyz\rangle$	$\langle 110\rangle_{RD}+\{111\}\langle 112\rangle$	$\langle xyz\rangle$ ranges between $\langle 001\rangle$ and $\langle 111\rangle$
Vandermeer and Ogles[37]	a	$>.250$	"	$\{110\}\langle xyz\rangle+\{112\}\langle 111\rangle$	"	"
	b	1/tm < 8.0	lubricated rolls	$\{100\}\langle 110\rangle$	"	The SP texture is present between $\Delta t/t_o$ of .04 and .8
Chen and Maddin[42]		.0025	"	-	$\langle 100\rangle$ partial fibre texture	

Table 5.2 Summary of the observations of four previous workers on through thickness texture segregation in cold rolled b.c.c. metals.

6. The Effect of Total Rolling Reductions upon Texture and R value.

Textures are developed during cold rolling and increase in intensity with progressive increments in rolling reduction. The intensity of subsequent annealing textures is similarly related to the prior rolling strain. Whiteley and Wise[7] examined the effect of cold rolling reduction upon the $\bar{R}$ values of finished strip, Fig. 6.1. The strain ratio increased with rolling reduction to a maximum, $\bar{R}_{max}$, and thereafter decreased with further increase in rolling reduction. Recrystallisation textures were also measured over a range of rolling strains which revealed the coincidence of a minimum in $\{200\}$ orientations with $\bar{R}_{max}$, Fig. 6.2. Atkinson et al[44] were unable to confirm any systematic correlation between total cold reduction and $\{200\}$ texture intensity. Their pole density plots comparable to those of Whiteley and Wise[7] showed no $\{200\}$ texture minimum although $\bar{R}_{max}$ was also observed at about 70% cold reduction. They furthermore indicated that the intensity of $\{200\}$ poles was somewhat below that for a random aggregate and therefore questioned whether the $\{200\}$ texture could be capable of reducing $\bar{R}$ below unity. The macroplasticity analysis of R value and texture[9] indicates that a $\{200\}$ texture decreases $\bar{R}$ value 4.5 times as much as $\{111\}$ texture increases it. This relative contribution to $\bar{R}$ value would be necessary to explain the Whiteley and Wise relationship.

Fukuda[20] considered it necessary to examine more than the two orientations $\{200\}$ and $\{222\}$ to establish a correlation between $\bar{R}$ value and texture and therefore

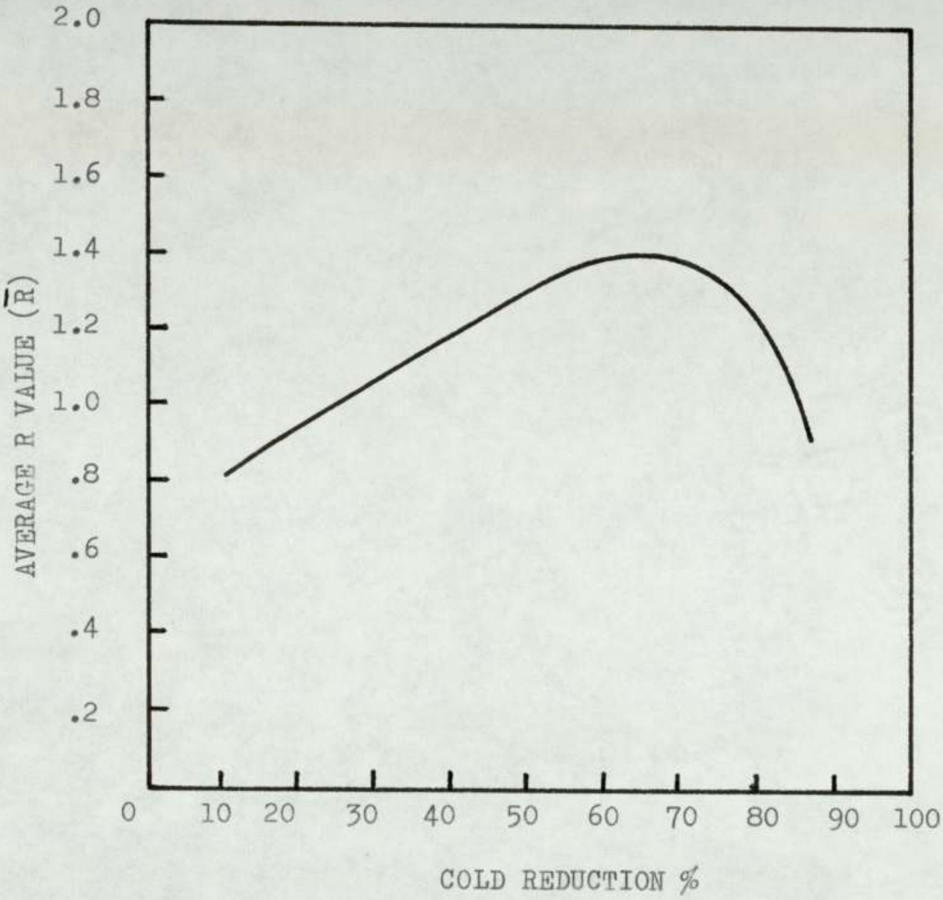

Fig. 6.1. Influence of percentage cold reduction, prior to an annealing treatment, upon the $\overline{R}$ value of aluminium killed steel.

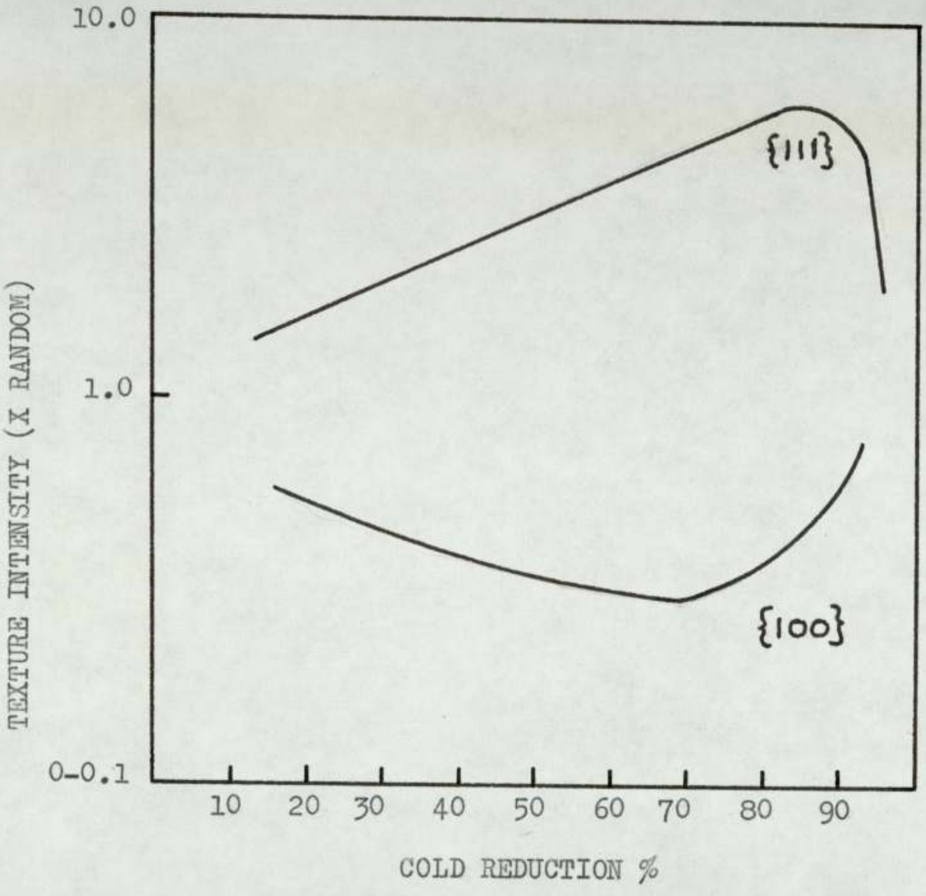

Fig. 6.2. {111} and {100} texture of annealed strip as a function of cold reduction prior to the annealing treatment.

described a new texture parameter 'P' defined by :

$$P = \frac{I\{111\} + I\{233\}}{I\{100\} + I\{311\}} \quad \ldots\ldots\ldots \quad 6.\ 1$$

where I is the intensity of an X-ray reflection relative to a randomly oriented sample and the suffix is the reflecting plane. $\{233\}$ and $\{311\}$ orientations were included because of their relative preponderance in the recrystallisation texture of steel. $\{233\}$ texture was said to contribute to high R values whereas $\{311\}$ crystals are detrimental because of their rotation to $\{100\}$ orientations early during tensile strain with subsequent behaviour as crystals of $\{100\}$ texture. $\{311\}$ texture increased in intensity at high percentage cold reductions and was therefore a contributory cause of the reduction in R value after R_{max}. Furthermore, the summation of $\{100\}$ and $\{311\}$ textures establishes a texture component of more than random intensity and therefore invalidates the arguments of Atkinson[44] regarding the significance of the intensity of $\{100\}$ texture.

The existence of $\{311\}$ and $\{411\}$ textures and their subsequent rotation to $\{100\}$ texture during tensile strain with consequent detriment to R value has been observed by other workers[19]. The crystal rotations were described as follows :

Normal Direction $(311) \rightarrow (411) \rightarrow (611) \rightarrow (100)$

Rolling Direction $[\bar{1}\bar{3}6] \gtrsim [0\bar{1}1] \pm 25^{\circ} \rightarrow [0\bar{1}1]$

This description of crystal rotation can be represented in the stereographic projection, Fig. 6.3.

The incidence of intense $\{311\}$ texture in heavily rolled and annealed material was attributed to the high

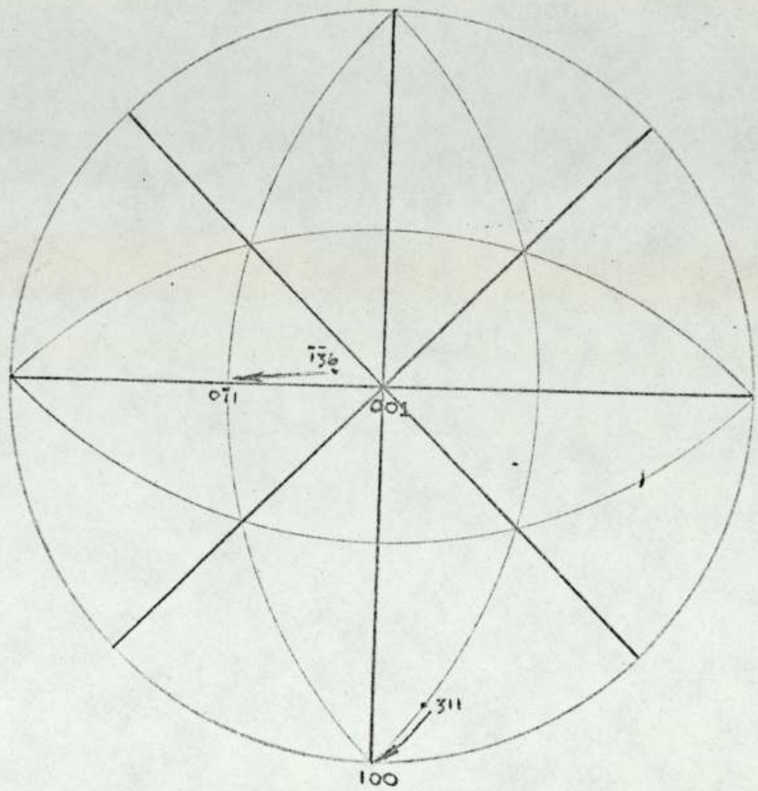

Fig. 6.3. Standard (001) projection representing the rotation of (311) to (100) and [$\bar{1}\bar{3}6$] to [$0\bar{1}1$] during tensile strain.

stored energy of {311} grains[34,45] rather than the predominance of {311} texture in the cold worked state. Therefore relatively intense {311} texture is only evident after the annealing cycle and not after rolling. Consequently care has to be exercised when attempting to correlate rolling textures with R values.

Held[36] was able to change the cold reduction at which $\bar{R}_{max}$ occurred by altering cold rolling conditions, so as to produce texture segregation. A 'skin-zone texture', developed at moderate rolling reductions and had a very high {100} /{111} ratio. This texture ratio was intensified and increased in relative thickness to the central zone with increased cold reduction until at the reduction coincident with $\bar{R}_{max}$ i.e. 40% in this case, the skin zones dominate and result in the subsequent reduction in $\bar{R}$ value. Furthermore, steel processed to give a homogeneous texture did not exhibit a distinctive $\bar{R}_{max}$ up to 88% cold reduction.

Roberts[46], using results obtained from work on stainless steel i.e. 13% Cr 0.5% Ni, has suggested an explanation for discrepancies in previous experimental work. Hot rolling in the $(\alpha + \gamma)$ phase region developed preferred orientations in the α crystals which were retained at room temperature. The texture component, {554}<225>, which developed during hot rolling, was intensified with subsequent cold rolling and retained after annealing. Roberts suggests that the relative proportion of this orientation in the recrystallisation texture controls the R value.

He therefore concludes that X-ray measurements from low order index planes e.g. $\{200\}$ and $\{222\}$, as is usual with pole density determinations, will not consistently support an R value - texture relationship.

The development of texture during cold rolling has been examined by Richards[47] and is of interest with regard to the observations of Roberts[46]. To monitor the development of complex orientations, e.g. $\{554\}\langle 225\rangle$, the North-south and east-west axes of (110) pole figures after progressive increments of cold reduction were examined. The results are illustrated in Fig. 6.4. and the main features can be outlined as follows :

$\{100\}$ textures develop progressively during cold reduction and the component $\{554\}\langle 225\rangle$ reaches a peak at only 20% reduction. The latter component subsequently reduces by rotation towards $\{111\}\langle 112\rangle$ after heavier reductions. Since $\{554\}\langle 225\rangle$ texture reaches a peak at only 20% reduction whereas R_{max} occurs at approximately 70% reduction, it is apparent that the two factors are not related.

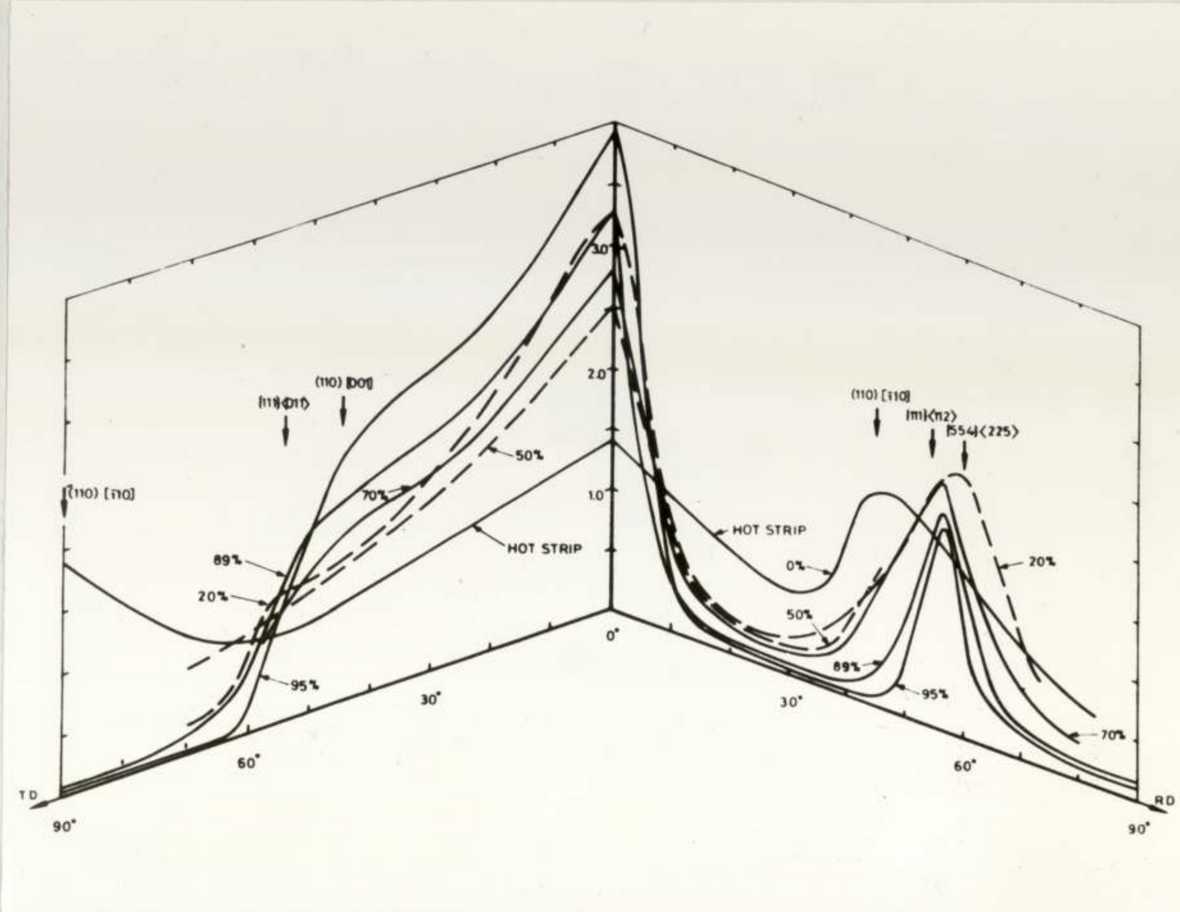

Fig. 6.4. North-south and east-west radial scans of (110) pole figures for low carbon steel after successive increments of cold reduction (47).

7. Scope of the Present Work.

The present investigation is designed primarily to add to the understanding of the metallurgical aspects of the cold rolling section of rimmed steel sheet production with a view to improving forming properties in the finished material. Cold rolling is chosen specifically for examination since crystallographic textures, which are known to control deep drawability, are mainly established during cold rolling. The experimental work will be performed on industrially processed rimmed steel hot band, so that results obtained in the laboratory, are as characteristic as possible of the commercial alloy industrially processed.

The investigation can be subdivided into four sections :-

(i) An examination will be made of the initial hot rolled stock. The presence of any texture segregation or texture will be ascertained and its possible influence upon the textures developed during cold rolling examined.

(ii) The effect of a range of cold rolling draughts and lubrication conditions upon textures and texture segregation will be appraised. Attention will also be given to the change in texture, if any, between the edge and centre line of strip. Material processed in each cold rolling condition will be subjected to a standard annealing treatment. R values will then be measured to establish a correlation between the cold rolling texture and drawability of finished strip.

(iii) Texture measurements will be made on the tensile test pieces used for R value determination to monitor the modification of rimmed steel recrystallisation textures by tensile strain. Three specimens that have included cold rolling to reductions coincident with R_{max}, less than R_{max}, and greater than R_{max} during processing, will be examined in detail to clarify the relationship between R value and texture and account for the R_{max} phenomena.

(iv) Finally a textural study will be made of the effect of intragranular cementite precipitates upon the crystal reorientation associated with tensile strain previously examined in Section (iii). Any coincident effect upon R value will be reported. A range of carbide dispersions will be produced by a series of overaging heat treatment.

Sections (ii), (iii) and (iv) of the investigation, in addition to their common purpose of increasing the knowledge of texture development and associated R value, were devised to overcome specific inadequacies in the literature. These can be outlined as follows :-

An examination of texture segregation has recently been made on niobium[37] which revealed two types of texture segregation. One type resulting from shear strain has also been observed in aluminium killed steel[36] and iron[6]. It is significant that the niobium examined was strip only 18.75 mms. wide and originally 10 mms. thick. Strain at the edges of strip deviate from the condition of plane strain and is the principal reason for lateral spread. The strip in this region is subject to a condition nearer to plane stress and the distance from the edge of strip that this condition applies, is related to its thickness. Low w/tm values would therefore be expected to result in textures significantly different from those produced during rolling with high w/tm values. High w/tm values are used in the commercial cold rolling of steel sheet and relatively high values will be used in the strip rolled in the present investigation.

Section (ii) will therefore yield information concerning texture segregation that is of more relevance to the rolling of b.c.c. metal sheet than was the work on niobium strip.

Section (iii) of the investigation, involving the determination of texture after tensile strain, is designed specifically to explain the decrease in R value of steel after a critical cold reduction. Previous R value texture analyses have generally involved the measurement of strain ratios during a uniaxial tensile test followed by comparison with textures measured in the unstrained parent sheet[7, 18, 19, 44]. An assumption is made that no significant crystal reorientation occurs during the 15-20% tensile strain.

However, considerable significant crystal reorientation has been observed in steel that originally had a strong $\{113\}\langle 110\rangle$ texture[19]. Textured titanium[48] is also subject to crystal reorientation during tensile strain.

Precipitates are reported to inhibit the development of texture during plastic deformation by creating turbulent metal flow[8]. Results from extruded copper wires containing alumina dispersions[49] confirm this observation for particle sizes of 10 - 25μ and volume fractions of 5 - 10%. The effect becomes less pronounced the smaller the volume fraction and particle size. Section (iv) of the investigation is a study of the influence of iron carbide dispersions upon R value. Textures will be determined after tensile strain as any precipitate effect will be attributable to the behaviour of the material to uniaxial extension.

8. Experimental Procedure.

8.1. Processing of material.

Hot band rimmed steel sheet was used as the starting material in the present work and was supplied by the Division of B.S.C. formerly known as the Steel Company of Wales. It was cut from the middle of full length coils. By sulphur printing, it was possible to establish that the 'rim' occupied approximately .15 of the cross-section on each side of the sheet. However, at the extreme edges of the sheet the 'rim' zone was present through the complete section, Fig. 8.1. 1. The 75 mms. of material adjacent to the edge was therefore not used in subsequent experiments.

Cold rolling was performed unidirectionally, on a two high 150 mm. (6 inch) diameter mill, using a roll speed of 20 r.p.m. A wide variety of rolling conditions were used and are summarised in Table 8.1. 1. The width of hot band cut from the parent sheet for cold rolling, was varied between 75 mms. and 150 mms. and the hot band rolling direction was maintained. All annealing was carried out isothermally at 700°C for 30 minutes followed by furnace cooling at an average rate of approximately 150°C per hour. This annealing treatment is not identical to industrial practice which is more typically :

(i) a heating up period of about 24 hours.

(ii) a soaking period of from a few hours to as much as thirty hours.

(iii) a cooling period of approximately twice the duration of the heating period to a final temperature of about 130°C.

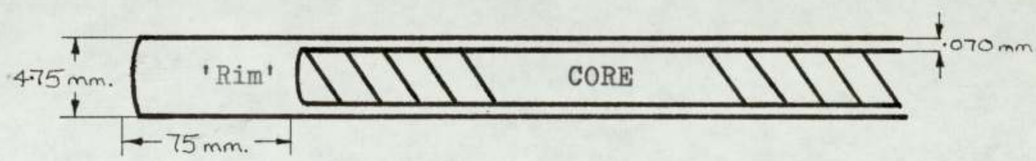

Fig. 8.1.1. Sectioned end elevation of rimmed steel hot rolled stock used in the present investigation. (The diagram is not drawn to scale).

Draught mm.	<.025	.125	.500	>.500*
Rolls lubricated with mineral oil	✓	✓	✓	✓
Rolls degreased	✓	✓	✓	✓
Rolls dusted with MgO			✓	✓

Table 8.1.1. Rolling draughts and lubrication conditions examined in the present work.
* Because of rolling mill limitations, the rolling draught was decreased progressively from 1.3 mm. at the first pass to .25 mm. at the final pass.

There will be a different response to recovery and dissimilar grain growth characteristics for industrially and laboratory heat treated strip. However, the difference in texture, for the two cases, will be small[23,50]. Consequently, even though absolute values of results obtained from material heat treated to each schedule may be marginally different, the relative effect of any prior or subsequent processing variable will be the same. Data obtained for the laboratory processed strip will, therefore, be indicative of what could be achieved with industrially processed strip.

Mechanical tests were performed within 24 hours of heat treatment to avoid any possible complications arising from nitrogen induced 'quench' aging.

As an addition to the standard heat treatment cycle, three overaging treatments were designed, each giving successively finer intragranular carbides and smaller inter particle spacing. The heat treatment schedules are illustrated in Table 8.1.2 As the cementite precipitates were only just resolveable with the optical microscope the stereoscan electron-microscope was used to obtain precipitate sizes and inter particle spacings.

Annealing Temperature, °C.	Time, hrs.	Cooling Conditions
300°C	1	Furnace cool
200°C	5	"
150°C	25	"

Table 8.1.2. Three overaging heat treatment schedules designed to result in the precipitation of a range of cementite particle sizes and interparticle spacings. The prior annealing treatment consisted of 30 minutes at 700°C., followed by air cooling.

8.2. X-ray techniques of texture determination.

(110) direct pole figures were determined using a Shultz X-ray reflection technique and cobalt $K\alpha$ radiation. A Siemens X-ray set was employed incorporating a texture goniometer, proportional counter, and electronic pulse height discrimination.

Molybdenum $K\alpha$ radiation was used for the inverse pole density determinations. Measurements for the first twelve reflections were made using the Siemens wide angle goniometer and scintillation counter. A zirconium counter aperture filter and pulse height discrimination were also used to filter out white radiation and incoherently scattered rays. Specimens were rotated about the sheet normal axis, during irradiation, so that similar areas were examined for all Bragg angles, Fig. 8.2. 1. and to effectively present a perfect fibre textured specimen to the X-ray beam.

Random intensities were obtained from a steel specimen that had been thermally cycled through the α-γ phase transformation several times. This sample was confirmed as being randomly oriented, by comparison of the measured intensities with calculated relative integrated intensities of the first 16 reflections(12), Table 8.2. 1. Intensities were measured using a 'step scanning' and counter technique. The stepping increment was $.05^{\circ}$ and counting time .1 minutes.

Specimens for X-ray examination were cut from hot band, cold rolled strip, heat treated strip and tensile test pieces. The hot band samples were cut from an area adjacent to the centre line of the sheet.

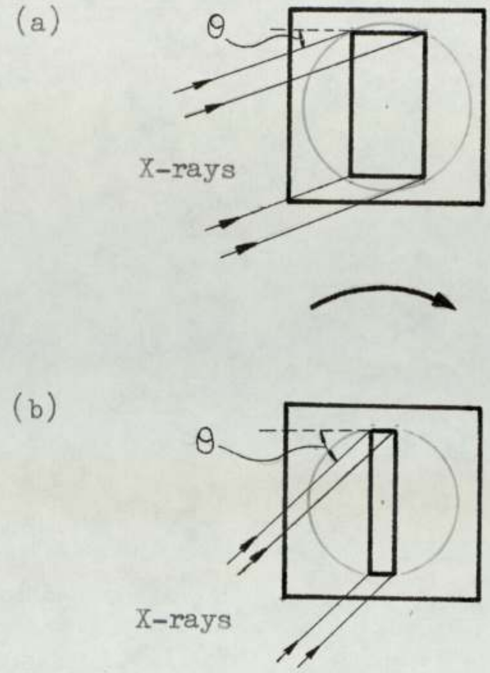

Fig. 8.2.1. Two steel specimens irradi~~c~~ated from the same X-ray source but positioned at different angles to the beam. The areas texturally examined are similar when the specimen is rotated about the strip normal; (a) small Bragg angles and (b) large Bragg angles.

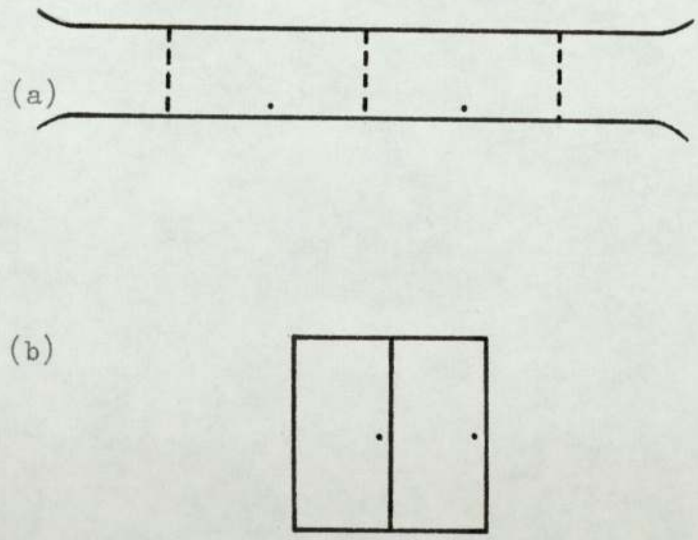

Fig. 8.2.2. Section from s tandard strip tensile specimen showin, (a) areas selected and (b) construction of specimen, for X-ray examination.

Reflecting Planes	Calculated Relative Integrated intensity	Measured intensity Kilocounts/6 seconds
110	100	98.2
200	20	21.1
211	30	30.0
220	9.2	9.5
310	11.3	11.8
222	2.5	2.3
321	10.9	10.2
400	1.0	1.1
411,330	4.3	4.4
420	2.3	2.3
332	1.8	1.7
422	1.45	1.5
510,431	3.4	3.3
521	1.6	1.4
440	.34	-
433,530	1.2	1.2

Table 8.2.1. Measured integrated intensities for the first 16 Bragg reflections for a rimmed steel 'random sample' and compared with calculated relative integrated intensities.

Calculated Relative Intensity $I = |F|^2 p((1+\cos^2 2\theta)/(\sin^2\theta.\cos\theta))e^{-2M}$

where $|F|^2$ is the structure factor

p is the multiplicity factor

$((1+ \cos^2 2\theta)/ \sin^2\theta \cos\theta))$ is the Lorentz polarisation factor and e^{-2M} is the temperature factor(12).

Standard 150 mm (6 inch) strip tensile test pieces were, after straining, sectioned as shown in Fig.8.2. 2. and mounted in a cold setting plastic to produce specimens suitable for X-ray examination. Specimens were thinned, to obtain texture data at various depths in the strip, by chemically etching or surface grinding followed by chemical etching. One face of the specimen was 'blocked' off with Lacomit or diakon and was then thinned with a solution of one part nitric acid in two parts water.

Inverse pole density data was obtained from material in the annealed condition and again after 5% tensile extension to test if primary extinction effects[13] would lead to erroneous results. The results are shown in Fig. 8.2. 3. It will be shown later that the small variation in the two sets of pole density data is associated with crystal rotation accompanying tensile strain. It was therefore concluded that measured diffracted X-ray intensities would not be subject to variation as a result of primary extinction.

When plotting pole density data versus depth within the steel strip the abscissa used was $\Delta t / t_o$ where Δt was the thickness of steel chemically removed and t_o was half the original strip thickness. Pole density data obtained from a plane Δt below the strip's original surface is in fact the average from crystals of a finite thickness element below the quoted position. This thickness, x, was calculated for different $\{xyz\}$ planes using the formula[12]:

$$x = 1.15 \sin\theta / \mu \qquad \text{.........} \; 8.2.\ 1.$$

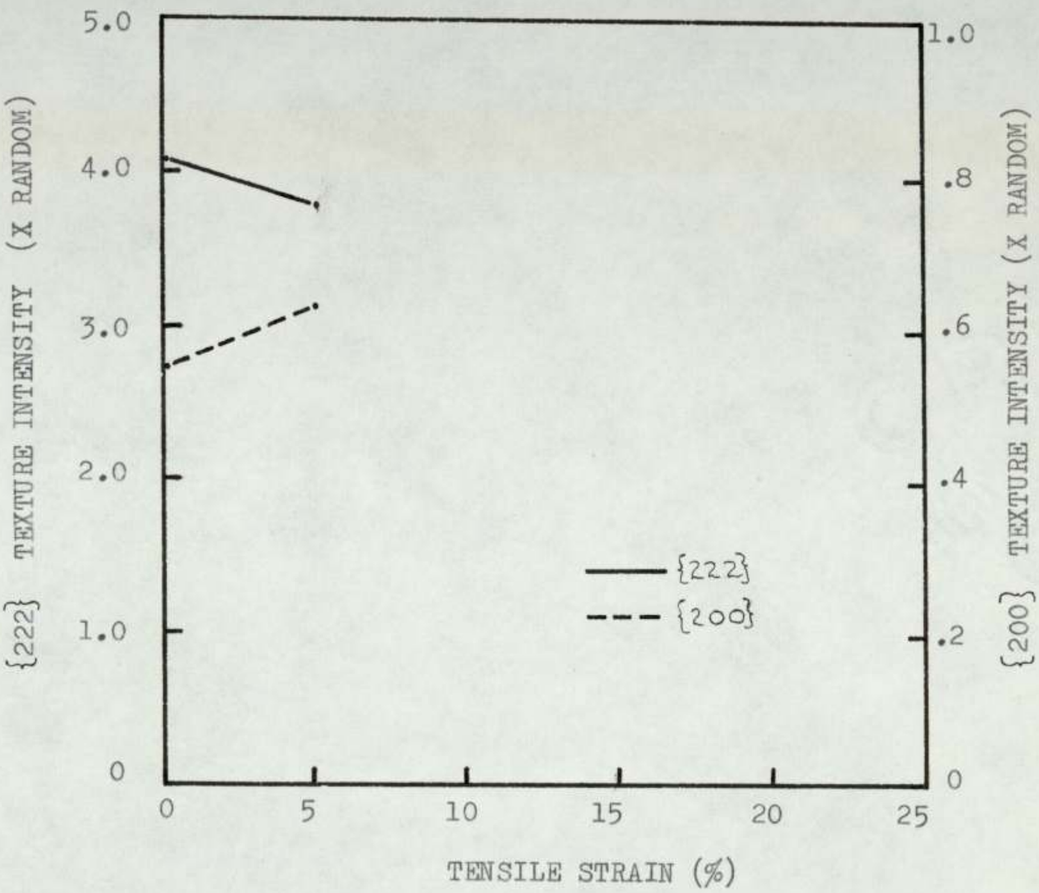

Fig. 8.2.3. Change in texture intensity of annealed rimmed steel strip as a function of tensile strain.

where x is a thickness element when the ratio of the X-ray intensity diffracted from the back face to that from the front face is 1 to 10 and μ is the linear absorption coefficient of iron.

$$x \text{ for } \begin{array}{ll} \alpha \text{ Fe}_{\{100\}} & = 0.0175 \text{ mm.} \\ \alpha \text{ Fe}_{\{111\}} & = 0.0300 \text{ mm.} \end{array}$$

The appropriate x value was added to Δt whereafter points on the graph of pole density venus $\Delta t/t_o$ represents the average pole density of the previous thickness element x/t_o. Results from steel strip of differing thicknesses are then directly comparable.

8.3. R value determinations.

Tensile tests were performed on a Hounsfield tensometer apparatus, at strain rates of 4×10^{-4} per second. R values were measured on standard 150 mm (6 inch) sheet tensile test pieces employing techniques quoted in the literature[51] and using equation 2.1.2.

$$\text{i.e. } R = \frac{\ln W_o/W}{\ln (L/L_o \cdot W/W_o)}$$

The gauge lengths were measured using a cathetometer and the widths using a micrometer.

Most results were obtained for test pieces cut parallel to the rolling direction but the trends obtained from these results were identical to the trends displayed by $\bar{R}$ results. R values were initially measured at successive increments of tensile strain to obtain a strain versus R value graph, Fig. 8.3. 1. All subsequent quoted R values were measured at 20% strain as R values were found to be constant over the range 18 - 24% tensile extension.

The extreme edges of rolled strip were not used for R value measurements.

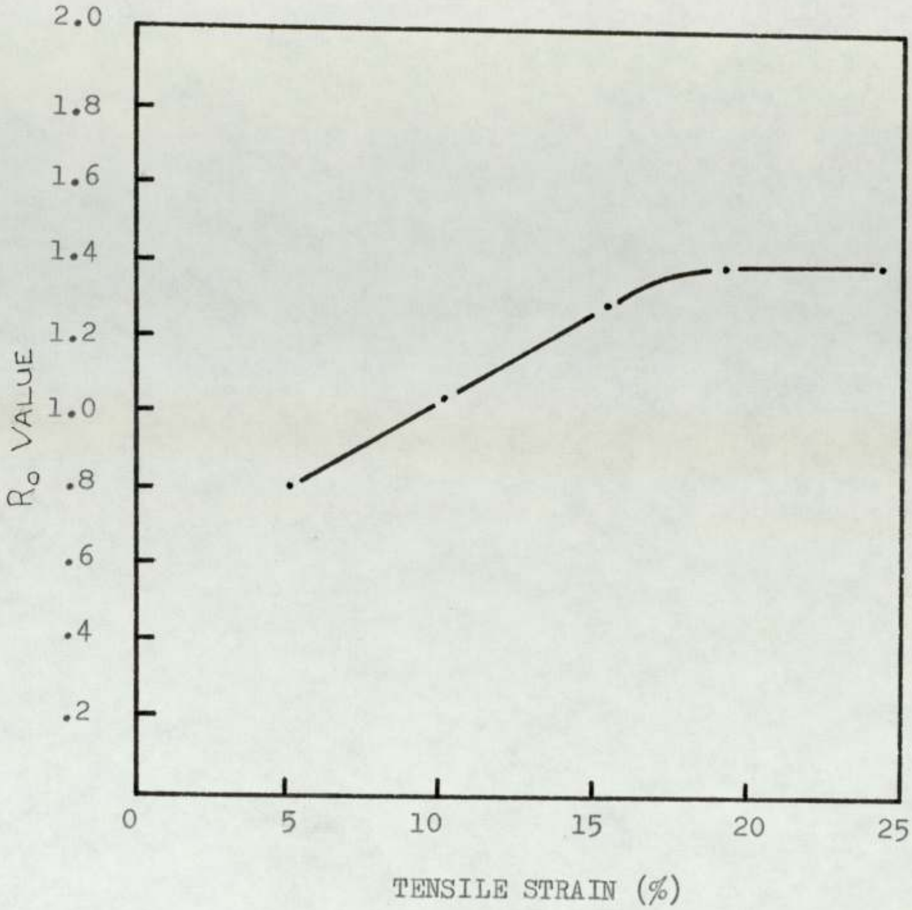

Fig. 8.3.1. R_o value, of rimmed steel cold rolled 75% and annealed, measured after successive increments of tensile strain. The indicated trend is characteristic of material having undergone any of the complete process conditions examined.

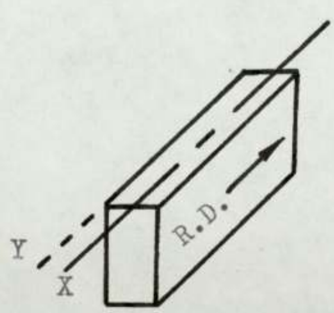

Fig. 8.4.1. Specimen of steel strip with edge plane uppermost. Microhardness measurements were made across the edge plane from Y to X, i.e. from surface plane to mid-plane.

8.4. Micro-hardness measurements.

A series of micro-hardness values of cold rolled strip were obtained on a Leitz Miniload micro-hardness tester. The indenting load was 100 grams and the indentation size about 30μ. Specimens were mounted in diakon with the edge plane uppermost, Fig. 8.4. 1, and consequently hardness values were obtained through the strip thickness.

9. Results.

9.1. Preliminary data pertaining to hot rolled stock.

The rimmed steel hot band 5.0 mm. thick had been hot rolled to a finishing temperature of 965°C and coiled at 683°C. The chemical composition and grain size are given in Table 9.1. 1. Fig. 9.1. 1. is a photomicrograph showing the small equiaxed grains and fine carbide dispersions of the material. Comparison of the microstructure, Fig. 9.1. 1., with typical microstructures of low carbon steel processed with varying hot rolling and coiling temperatures recorded by Ascough[52] show that the microstructural observations are consistent with the reported finishing and coiling temperature.

The through-thickness inverse pole density data for the hot rolled stock is shown in Fig. 9.1. 2. {110} texture is of relatively high intensity at the surface plane and reduces to .6 random intensity at the mid plane. Conversely, {100}, {112} and {111} texture are of relatively low intensity at the surface plane and increase in intensity to the mid plane. {111} texture is, however, less than random intensity at all depths in the sheet.

The textures are of such low intensity that no useful information could be obtained from (110) pole figures.

9.2. The effect of cold rolling draught and lubrication upon textures and R values.

Four types of through-thickness texture segregation have been observed in cold rolled rimmed steel. The textures can be classified according to the draughts used during rolling, i.e. ranging from Type I textures

Element	C	Si	S	P	Mn	Ni	Cu	Al	Sn	N
Weight %	.04	.01	.023	.011	.32	.003	.035	.01	.01	.0024

Grain Size 25 - 30μ

Table 9.1.1. Chemical composition and grain size of rimmed steel hot band used in the present investigation.

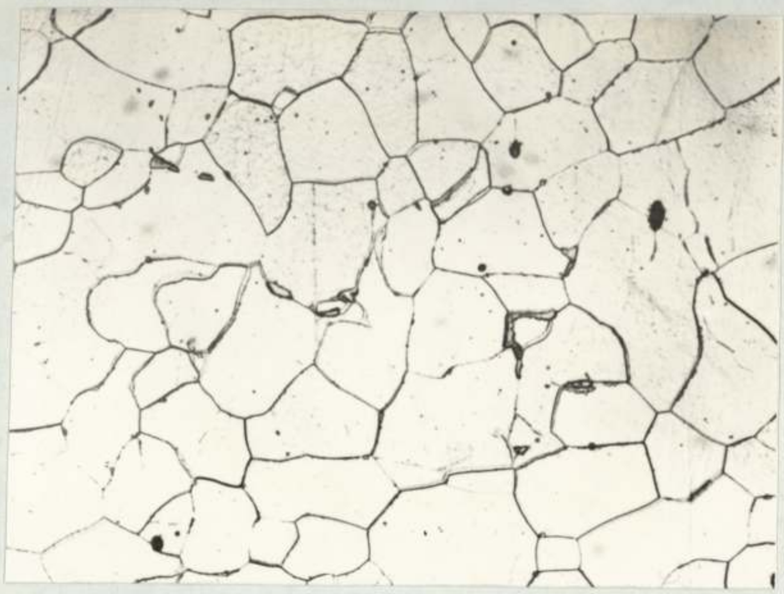

Fig. 9.1.1. Photomicrograph of hot rolled stock; rolling temperature 965°C, coiling temperature 683°C.
Magnification X 500

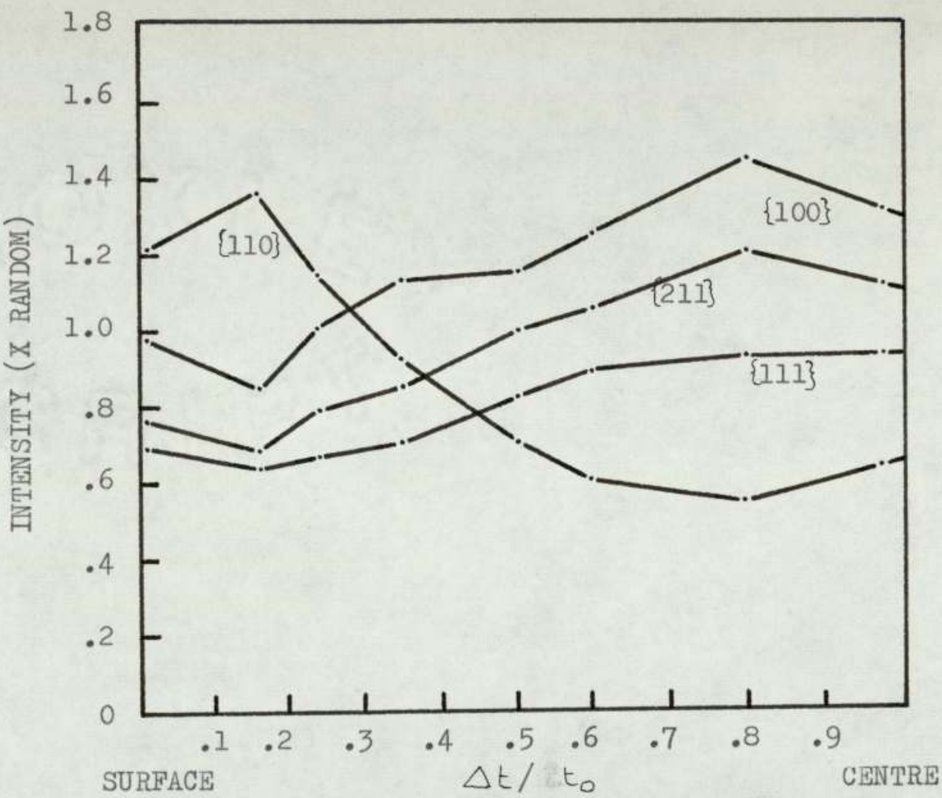

Fig.9.1.2 {110}, {100}, {211} and {111} pole densities as a function of sheet depth for hot rolled stock; finishing temperature 965°C, coiling temperature 683°C.

developed with the lightest draughts to Type IV textures developed with the heaviest draughts. Textures of all four types were found to be symmetrical about the sheet mid-plane and therefore, texture measurements from only one surface plane to the mid-plane were graphically plotted.

Generally, only graphs of $\{111\}$ and $\{100\}$ pole density as a function of $\Delta t / t_o$ are plotted for illustration purposes because of the importance of these textures in controlling R value, but more specifically because these two orientations are most intense in rolling textures and were also generally found to be the components most segregated. (110) pole figures for various depths in the strip are also used for illustrative purposes. Only one quadrant of the pole figures are shown, as the four quadrants of the complete pole figure are symmetrical.

Most of the texture data to be presented is for material cold rolled 80% since this corresponds to the maximum cold reduction normally encountered in industrial practice. However, where total reductions between 60% and 90% significantly influence texture segregation, the effect is noted.

9.2. 1. <u>Texture segregation Type I</u>.

Texture segregation Type I is illustrated in Fig. 9.2.1. 1. and was developed by using rolling draughts of less than 0.025 mms. No significant difference was observed in texture when rolling with either dry rolls or copiously lubricated rolls. Type I texture is developed over a range of cold reductions, i.e. 60% - 85%. The through-thickness texture profile for material cold rolled 80% is illustrated, in Fig. 9.2.1.1., as typical of the range.

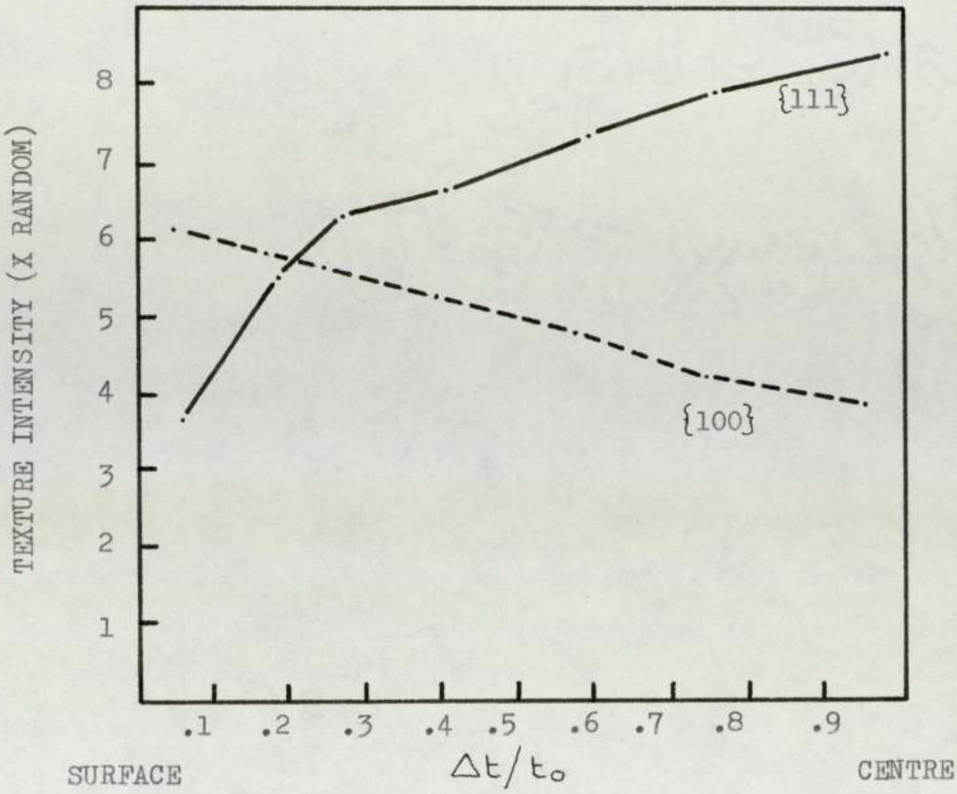

Fig. 9.2.1.1. The variation of {111} and {100} texture intensity with strip depth; steel cold rolled 80% with draughts of .025 mm. and oil lubrication. The texture profile is indicative of Type I texture segregation.

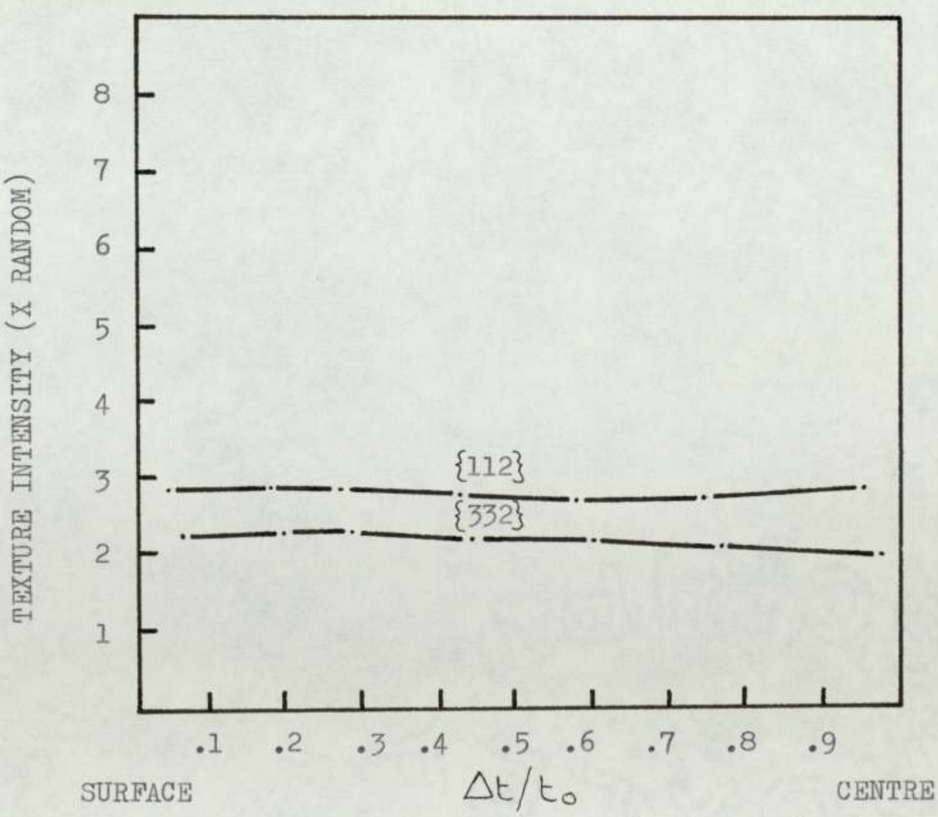

Fig. 9.2.1. 2. The variation of {112} and {332} texture intensity with strip depth; steel cold rolled 80% with draughts of .025 mm. and oil lubrication.

The intensity of $\{111\}$ texture increases progressively from approximately 4.0 random to 8.0 random between sheet surface plane and mid-plane. $\{100\}$ texture decreases correspondingly from 6.5 random to 4.0 random. The intensity of other orientations is approximately uniform through the sheet thickness. Fig. 9.2.1. 2. shows $\{112\}$ and $\{332\}$ texture contours as an example.

(110) pole figures were plotted for sheet mid-plane and sheet surface plane, Fig. 9.2.1. 3. The sheet mid-plane exhibits a typical b.c.c. iron texture which can be dèscribed as consisting of the two partial fibre textures $\langle 110\rangle_{RD}$ and $\{111\}_{RP}$ previously outlined. The texture at the surface plane displays distinct dissimilarities to the mid-plane texture, although there is also a peak intensity at approximately the same angle, ϕ, 30° from the sheet normal along the sheet normal-rolling direction radius of the pole figure quadrant. The peak area, at the mid-plane, is wider spread on the pole figure ranging from angles of 27° to 37°, whereas for the surface plane it is sharper and at angles between 28° and 32°.

The presence of the peak is attributed to two subsidiary peaks associated with $\{111\}\langle 112\rangle$ texture at ϕ equals 35° and $\{112\}\langle 110\rangle$ texture at ϕ equals 30° i.e. components of fibre textures $\{111\}_{RP}$ and $\langle 110\rangle_{RD}$ respectively. Consequently, when both components are present there is a tendency for the peak to be spread over a range of ϕ values and conversely, if either is absent, then the peak is restricted to the appropriate ϕ angle.

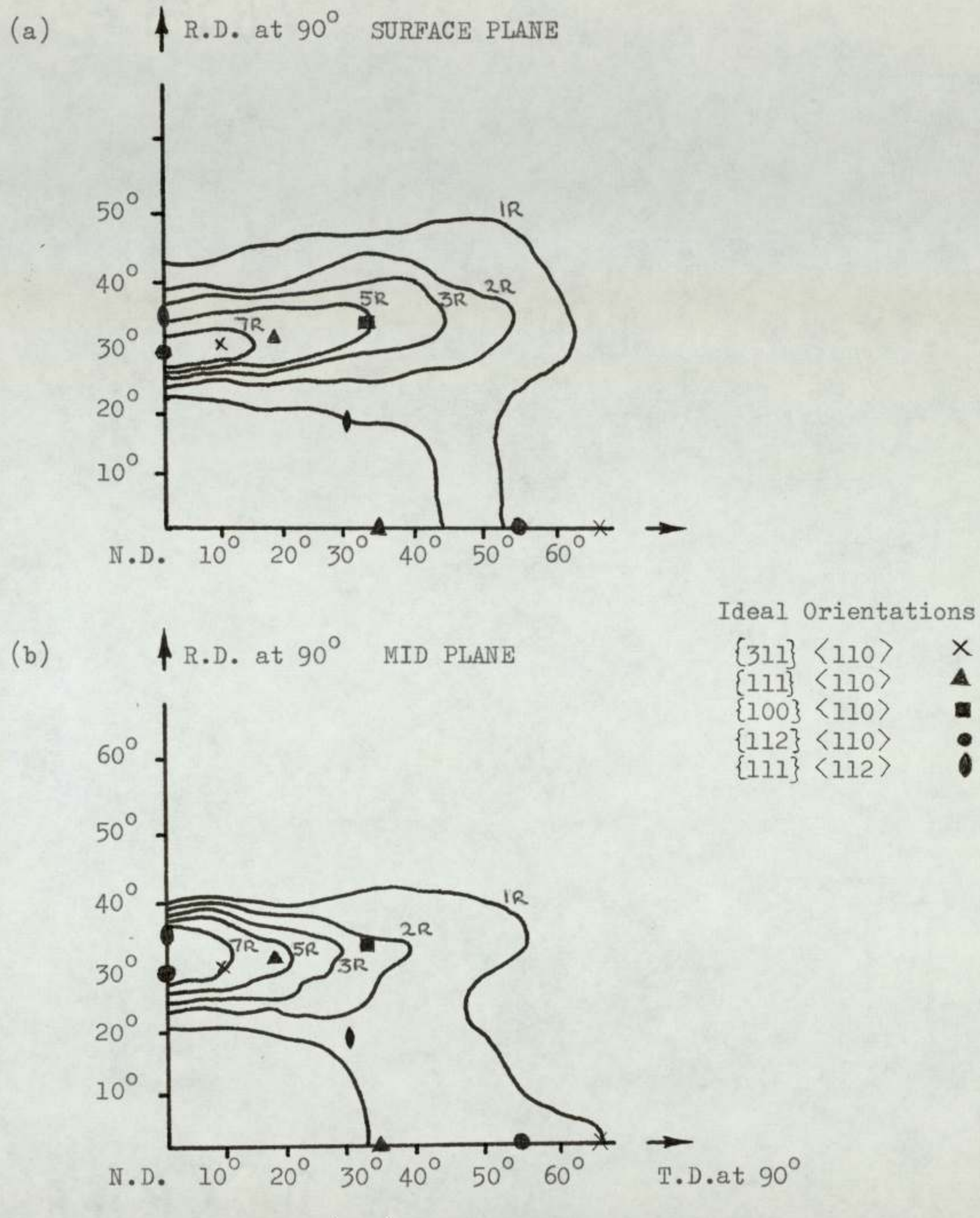

Fig. 9.2.1. 3. (110) pole figures at surface plane and centre plane for steel cold rolled 80% with oil lubrication and draughts of .025 mm. The rolled strip exhibits Type I texture segregation.

The spread of the peak for the mid-plane therefore suggests both components are present, whereas the 30° peak for the surface plane suggests the relative absence of $\{111\}\langle 112\rangle$ texture, i.e. this component of fibre texture $\{111\}_{RP}$ is diminished. This conclusion is also confirmed by the difference in shape of the one random intensity curve for the two cases, (compare the two pole figures in Fig. 9.2.1. 3a and 9.2.1. 3b, with the ideal (110) pole figure for $\langle 110\rangle_{RD}$ and $\{111\}_{RP}$ fibre textures in Fig. 4.5). Thus orientations of the $\{111\}_{RP}$ partial fibre texture other than $\{111\}\langle 110\rangle$, which is a component of the $\langle 110\rangle_{RD}$ partial fibre texture, are absent at the strip surface plane.

Pole density data shows that $\{111\}$ texture is less intense at the sheet surface plane than at the mid-plane, and therefore corroborates the idea of low intensity $\{111\}_{RP}$ partial fibre texture at the surface.

The texture segregation illustrated in Fig.9.2.1. 1., is therefore not simply a result of differences in texture intensity with depth in the sheet, but rather distinct changes in texture components present. A (110) pole figre for the sheet plane midway between surface and mid-planes confirmed the pole density data with regard to the gradual change from one texture to the other.

9.2.2. <u>Texture segregation Type II</u>.

Type II texture segregation is illustrated in Fig. 9.2.2. 1. The intensity of $\{111\}$ texture is low at the sheet surface plane but increases progressively to $\Delta t/t_o$ of approximately .25

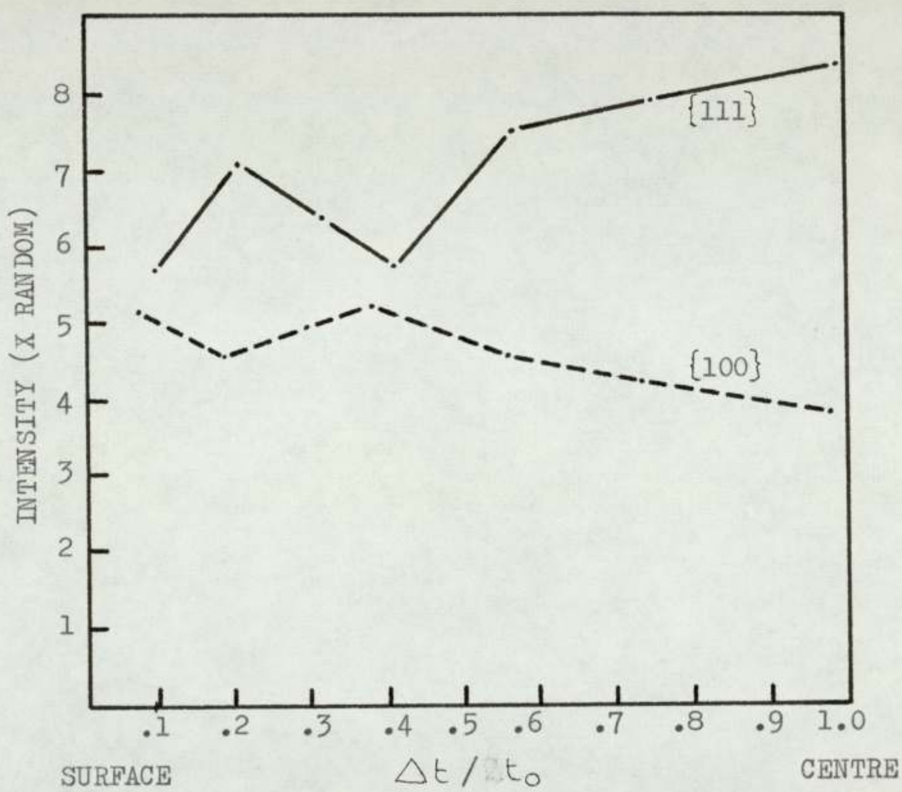

Fig. 9.2.2. 1. {111} and {100} pole density as a function of depth in the strip; strip cold rolled 80% with draughts of .125 mms. and oil lubrication. The texture profile is indicative of Type II texture segregation.

$\{111\}$ texture then decreases in intensity to a value approximately equal to the surface plane intensity at $\Delta t/t_0$ of .4 and finally increases to a maximum at the sheet mid-plane. Like Type I texture segregation the plot of $\{100\}$ texture versus sheet depth follows the reverse trend to the plot of $\{111\}$ texture.

The (110) pole figures for different sheet planes, also reveal dissimilarities in texture components. The differences are only slight and therefore one cannot analyse the textures with any certainty simply by examination of the (110) pole figures. However, by considering the equivalent pole density data and the observations already outlined of Type I textures in conjunction with these pole figures, some legitimate conclusions can be made. The mid-plane pole figure, Fig. 9.2.2. 2c, is very similar to the Type I mid-plane pole figure Fig. 9.2.1. 3b, and therefore, can also be described as consisting of fibre textures $\{111\}_{RP}$ and $\langle 110\rangle_{RD}$. The surface plane pole figure Fig. 9.2.2. 2a, can be similarly described, but with a reduction in texture density. This is manifest as a reduction in the area of the pole figure contained by the one random intensity content, as compared to the mid-plane pole figure.

The pole figure to correspond to the minimum in the $\{111\}$ pole density plot, i.e. at $\Delta t/t_0$ equals .4 reveals a small change in the peak intensity and intensity contour shape and can be considered equivalent to the surface texture described in Type I segregation. The texture change between $\Delta t/t_0$ equals .4, and the mid-plane can therefore probably also be described as resulting specifically from a segregation of $\{111\}_{RP}$ partial fibre texture, with a corresponding increase in intensity of $\{100\}$

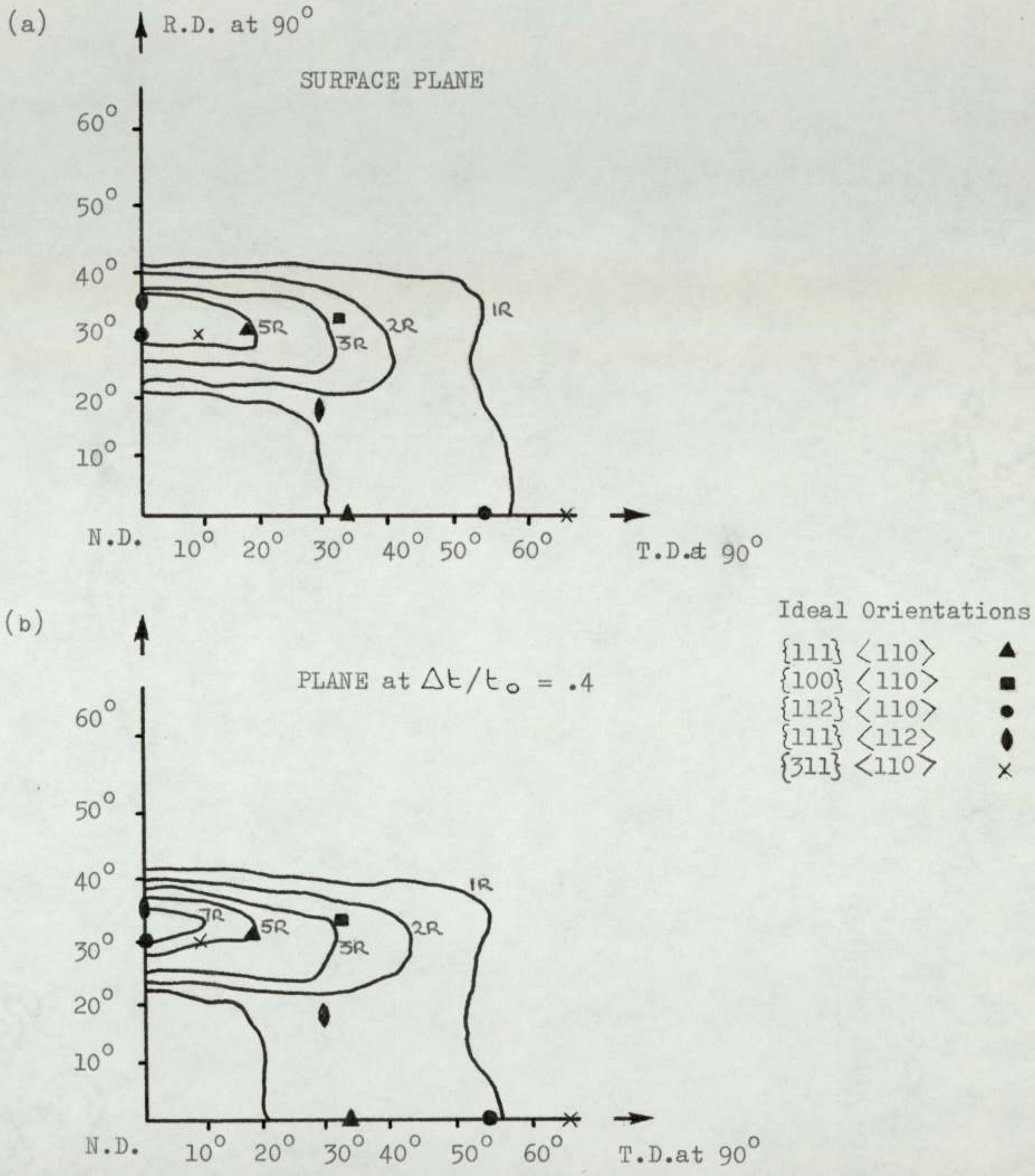

Fig. 9.2.2. 2. Continued overleaf

(c)

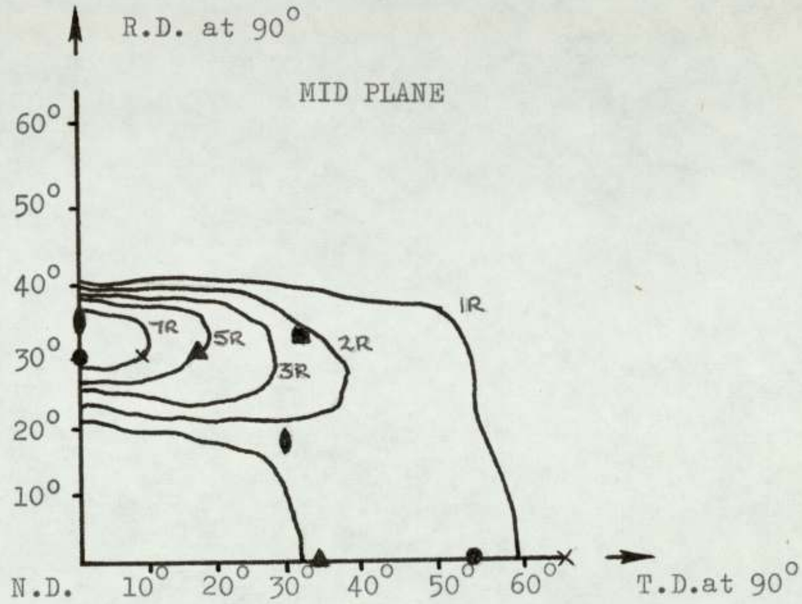

Fig. 9.2.2. 2. (110) pole figures of strip cold rolled 80% to exhibit Type II through thickness texture segregation; rolling draughts .125 mm. and oil lubrication. The rolled strip exhibits Type II texture segregation.

orientations of $\langle 110 \rangle_{RD}$ partial fibre texture.

Type II texture segregation is developed by using rolling draught of .125 mms. and oil lubrication. By dry rolling there is a tendency to lose the first maximum in $\{111\}$ pole density versus sheet depth plot, Fig. 9.2.2. 3, such that the segregation is more like that of Type I.

Pole density data was compared fromthe edge, E, and centre line, C, of rolled 150 mms. wide strip. Fig. 9.2.2. 4 illustrates the method by which suitable samples were selected and constructed for X-ray examination and Fig. 9.2.2. 5 shows the $\{111\}$ and $\{100\}$ through thickness texture profiles for each case. The material was cold rolled 80% to exhibit Type II texture segregation but the sample selected from the edge of the strip exhibited a marked reduction in the severity of segregation relative to the centre line specimen. Samples constructed from areas adjacent to E yielded results similar to those of area C.

9.2.3. Texture segregation Type III.

Texture segregation Type III is illustrated in Fig. 9.2.3. 1. The intensity of $\{111\}$ poles is very low at the sheet surface plane i.e. approximately 4.0 random. The intensity rises rapidly to a maximum of 8.0 random at $\Delta t/t_o$ equals .15 and thereafter remains constant to the sheet mid-plane. The intensity of $\{100\}$ poles increases linearly from 3.0 random at the sheet surface plane to 4.5 random at the sheet mid-plane. The intensity of all other orientations was approximately uniform through the sheet thickness.

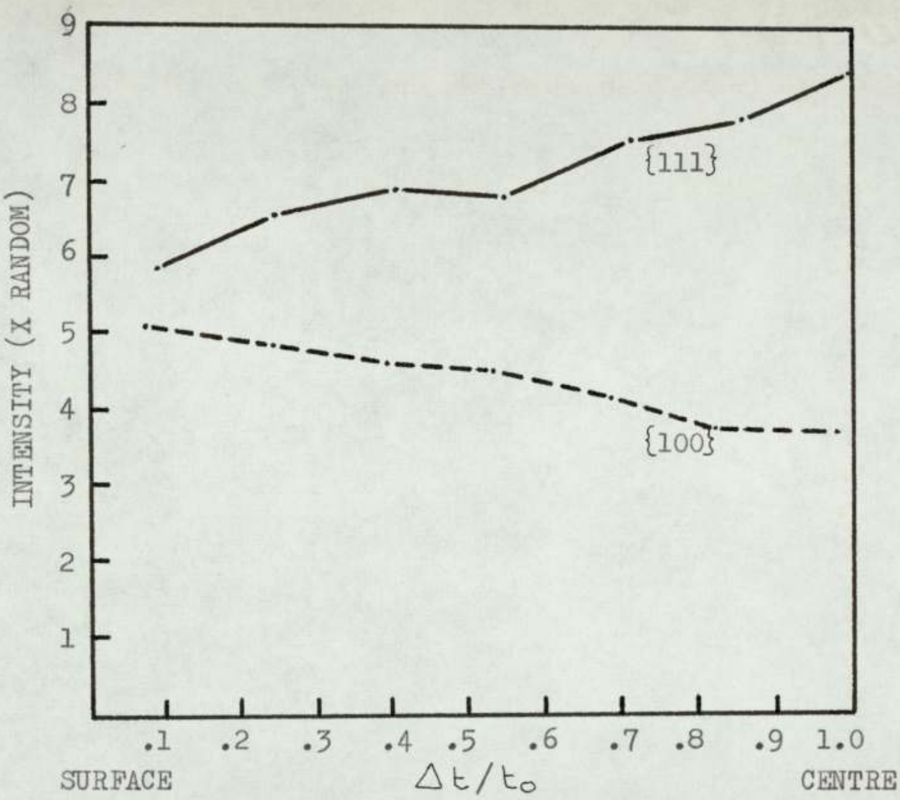

Fig.9.2.2. 3. {111} and {100} pole density as a function of depth in the strip; strip cold rolled 80% with draught of .125 mm. and rolls degreased.

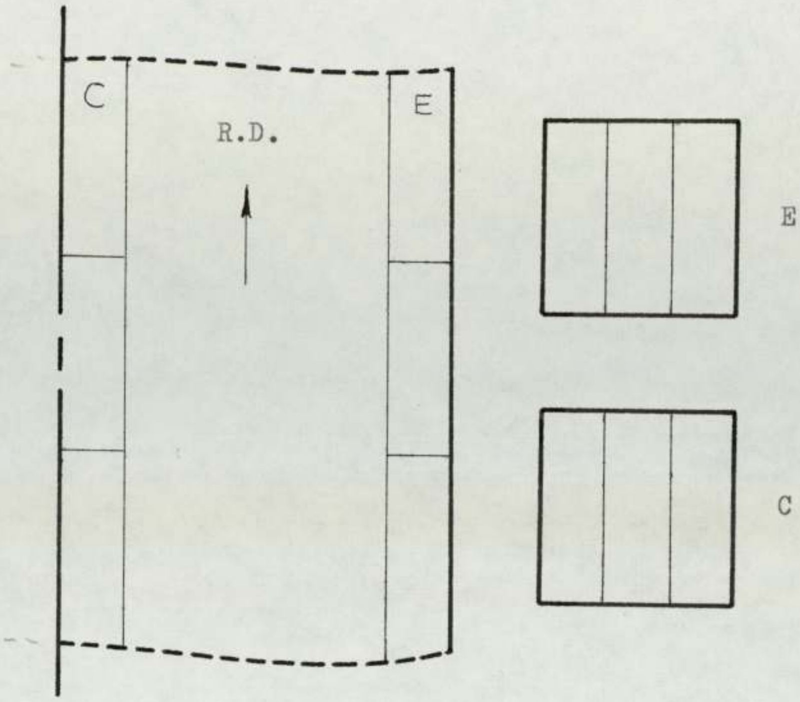

Fig. 9.2.2. 4. Selection and construction of samples representative of strip edge, E, and centreline, C, for through thickness texture determination.

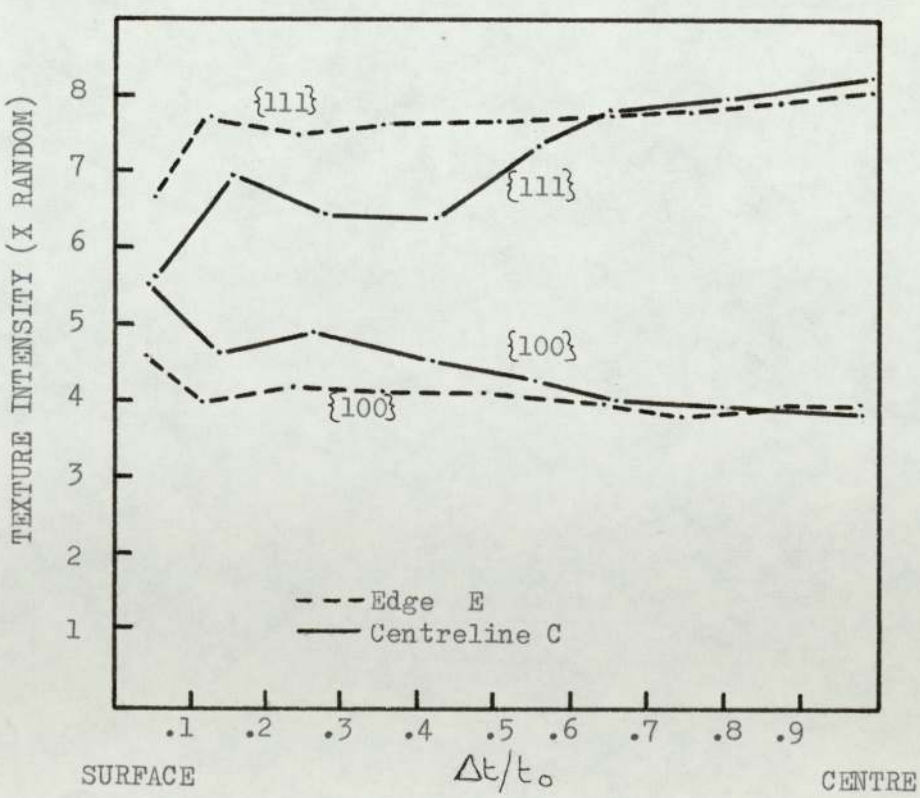

Fig. 9.2.2. 5. Through thickness {111} and {100} texture intensity for samples from strip edge, E, and centreline, C, (see Fig. 9.2.2.4.); strip cold rolled 80% with draughts of .125 mm.

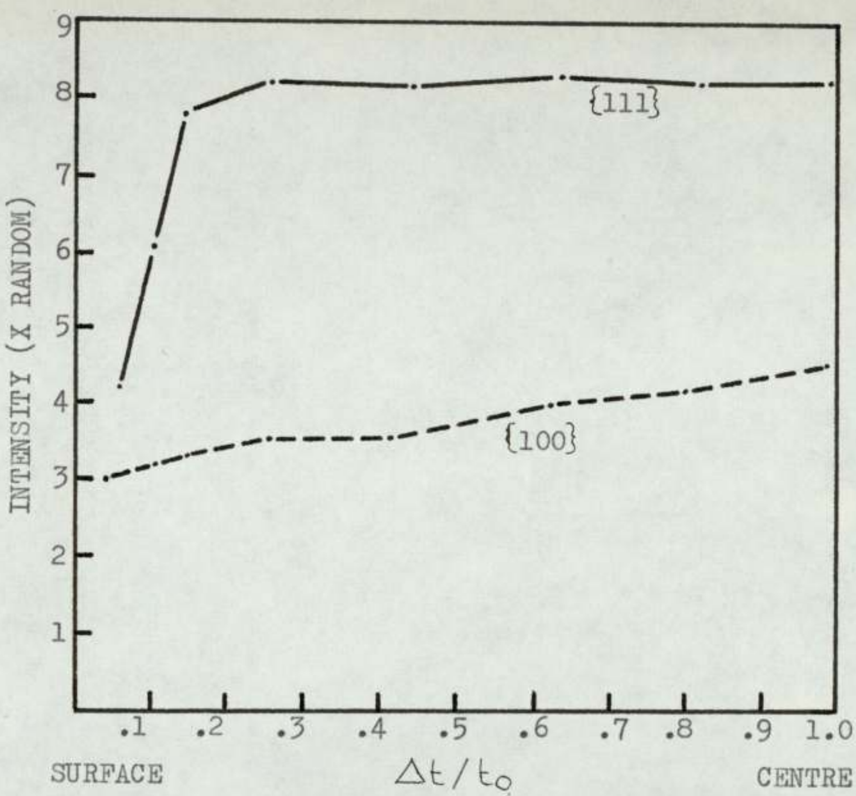

Fig. 9.2.3. 1. {111} and {100} pole density as a function of depth in the strip; strip cold rolled 80% with draught of .500 mm. and oil lubrication. The texture profile is indicative of Type III texture segregation.

The (110) pole figures, Fig. 9.2.3. 2., reveal dissimilarities between surface plane and mid-plane, although there is no gradual change from one to the other as has been previously described for Type I texture segregation. The mid-plane texture Fig. 9.2.3. 2b, is again very similar to Type I mid-plane texture Fig. 9.2.1. 3b, and therefore also consists of fibre textures $\{111\}_{RP}$ and $\langle 110\rangle_{RD}$. However, the near horizontal displacement of the one random contour suggests that fibre texture $\langle 110\rangle_{RD}$ predominates in this case, even at the mid-plane. The surface texture also consists primarily of fibre texture $\langle 110\rangle_{RD}$ but the area covered by the one random contour is reduced in an analagous, but more pronounced way to that of the surface pole figure of Type II segregation, Fig. 9.2.2. 2a. Consequently, the change in texture at the surface plane can be considered not as a result of changes in texture orientations as for Type I texture, but rather as simply to a reduction in all texture components at the surface. This is confirmed by the inverse pole density data since there is a reduction in intensity of almost all texture components at the surface plane rather than the reduction of one orientation being accounted for by the increase in some other orientation.

Texture Type III is developed during rolling with draughts of .125 mm when using oil lubrication. Dry rolling has a significant effect upon Type III texture as illustrated in Fig. 9.2.3. 3. The gradient of the $\{111\}$ texture intensity through the surface elements is considerably reduced whilst the $\{100\}$ pole plot is nearly uniform throughout the sheet thickness. Degreasing the rolls therefore increases the homogeniety of texture Type III.

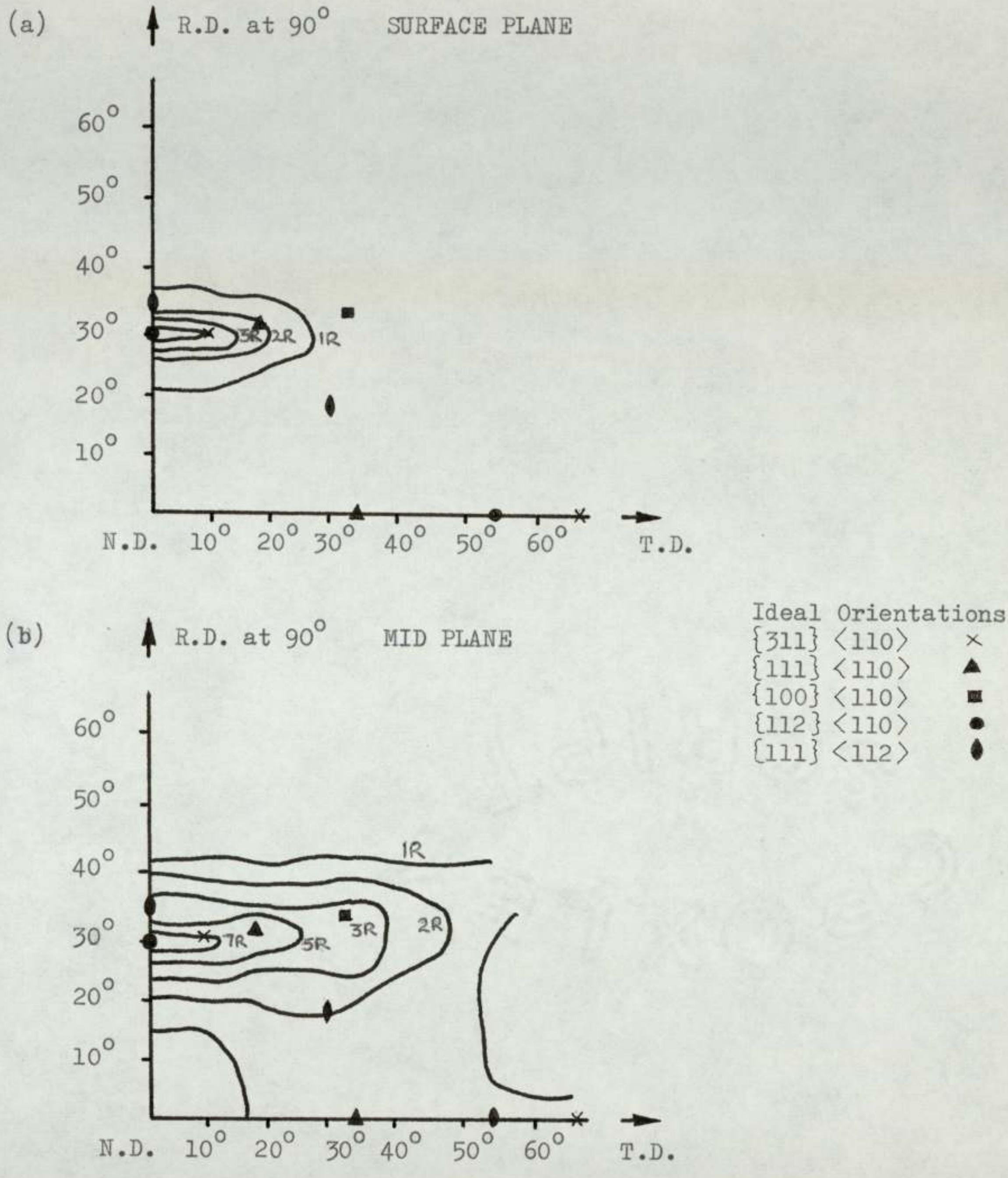

Fig. 9.2.3. 2. (110) pole figures at surface plane and centre plane for steel cold rolled 80% with oil lubrication and draughts of .500 mm. The rolled strip exhibits Type III texture segregation.

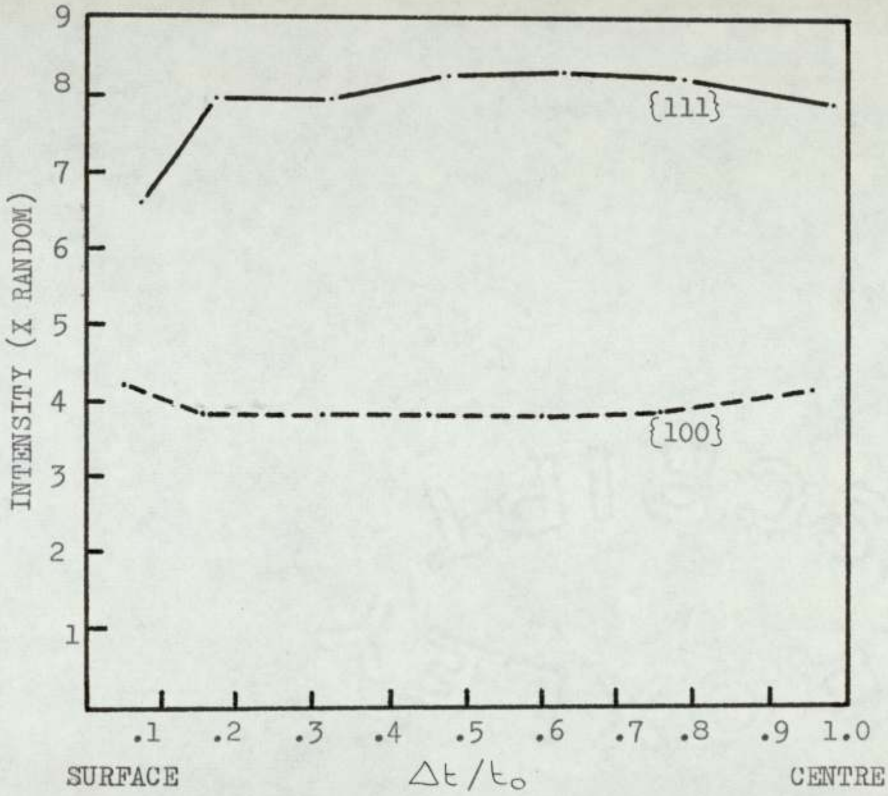

Fig. 9.2.3. 3. {111} and {100} pole density as a function of depth in the strip; strip cold rolled 80% with draughts of .500 mm. and rolls degreased.

9.2.4. Texture segregation Type IV.

Texture segregation Type IV is illustrated in Fig. 9.2.4. 1. $\{111\}$ planes have close to random intensity at the sheet surface, after which there is a linear increase in intensity to approximately 8.0 random at $\Delta t/t_o$ equals 1.0. The intensity of $\{100\}$ texture is not simply related to $\{111\}$ texture intensity, as is the case with textures Type I and II. However, the intensity of $\{100\}$ texture varies with $\Delta t/t_o$ in this case also. $\{110\}$ texture intensity is relatively high at the sheet surface plane i.e. 2.5. random, but decreases rapidly to zero intensity at $\Delta t/t_o$ equals .55.

(110) pole figures reveal that the centre texture is the typical iron rolling texture, Fig. 9.2.4. 2b, and is similar to the mid-plane textures for the rolling conditions that developed Type III texture i.e. $\langle 110\rangle_{RD}$ and $\{111\}_{RP}$ textures with $\langle 110\rangle_{RD}$ texture predominating, (see Fig. 9.2.3. 3b). The surface plane (110) pole figure, Fig. 9.2.4. 2a, is distinctly different to the centre plane pole figure, Fig. 9.2.4. 2b, the peak in (110) poles being at the centre of the pole figure rather than at the angle ϕ from the sheet normal direction. The surface texture is of relatively low intensity, but can be tentatively described as $\{110\}\langle uvw\rangle$ where $\langle uvw\rangle$ represents directions between $\langle 001\rangle$ and $\langle 111\rangle$. The surface texture is therefore related to the centre texture, which is predominantly $\langle 110\rangle_{RD}$ partial fibre texture, by 90 degree rotations about the transverse axis.

It was not possible to produce Type IV texture even when rolling to the limits of the mill if oil lubrication was used.

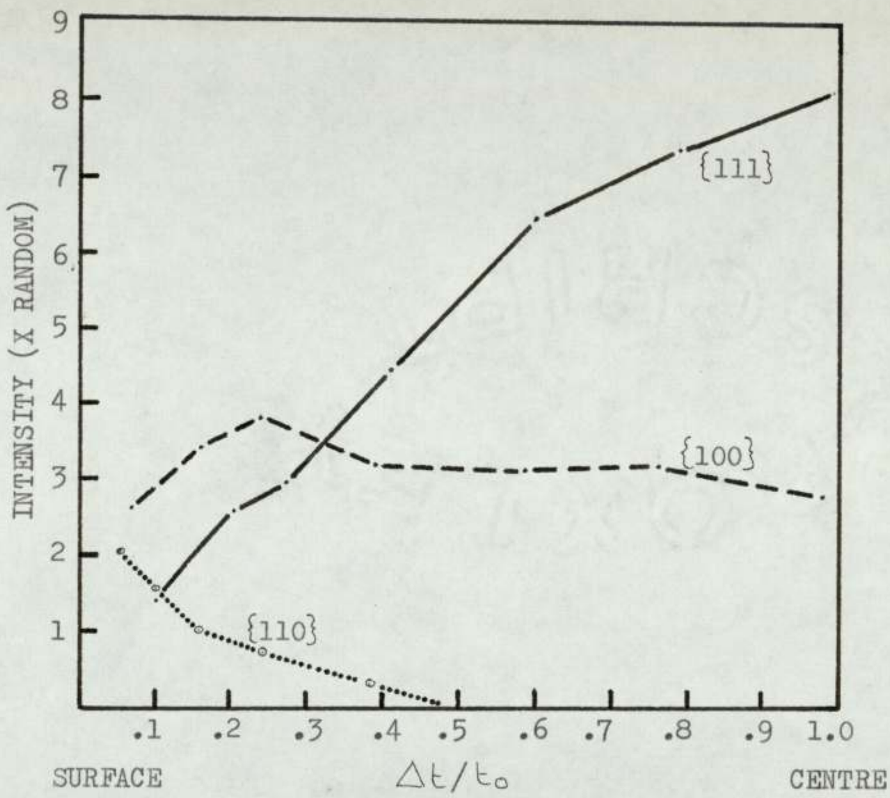

Fig. 9.2.4. 1. {111}{110}and{100} pole density as a function of depth in the strip; strip cold rolled 88% with draughts of greater than .500 mm. and rolls dusted with magnesia. The texture profile is indicative of Type IV texture segregation.

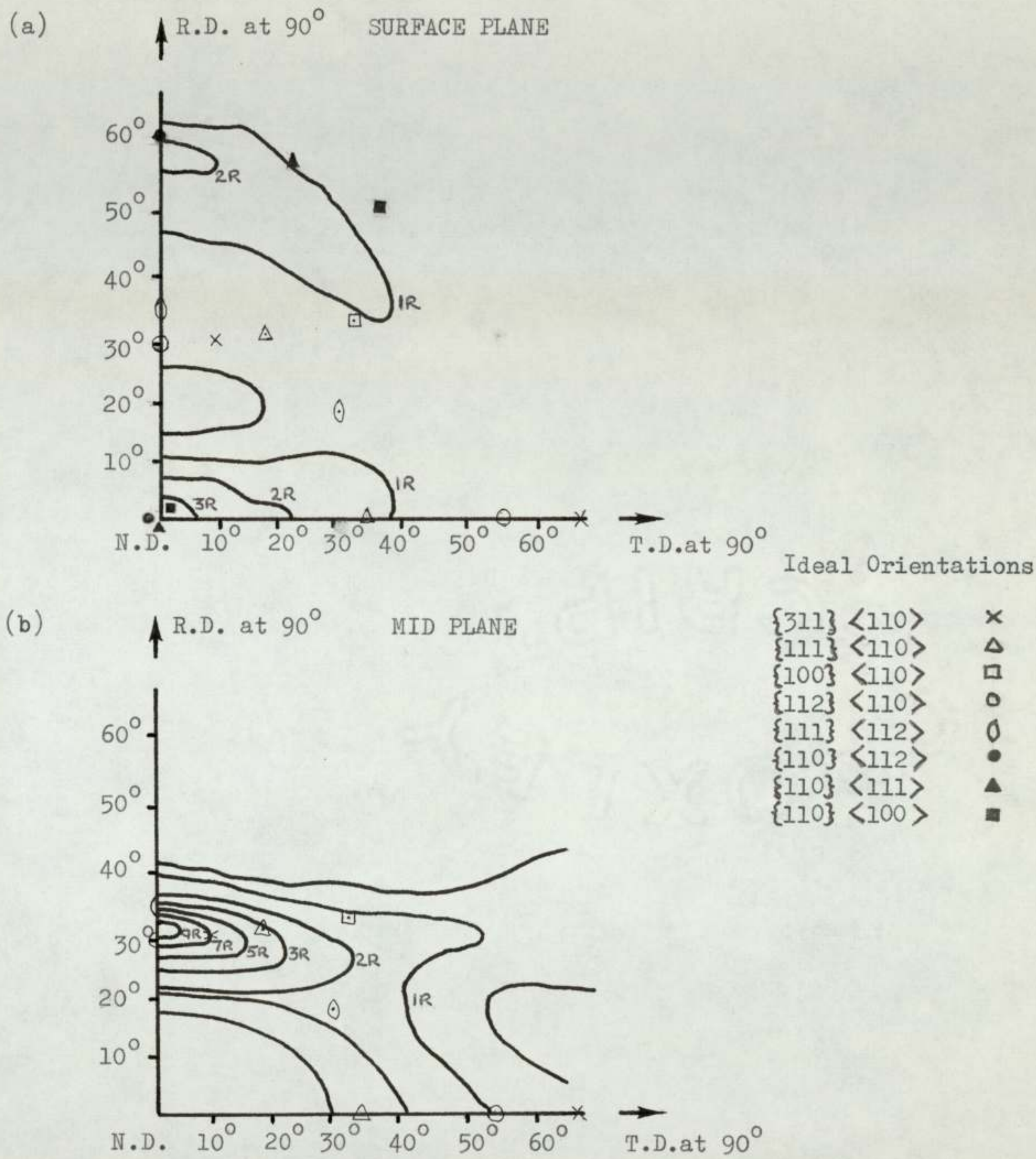

Fig. 9.2.4. 2. (110) pole figures at surface plane and centre plane for steel cold rolled 88% with magnesia dusted rolls and draughts of .500 mm. The rolled strip exhibits Type IV texture segregation.

Furthermore, degreasing the rolls had no effect either for draughts between 1.0 mm and 0.25 mm. It was necessary to sprinkle magnesia powder on the rolls and attain total reductions of greater than 80% before there was any evidence of Type IV segregation at all. Consequently, high friction conditions and heavy rolling reductions are required before Type IV texture develops in cold rolled rimmed steel.

The rolling draughts, % reduction per pass and total rolling reduction, along with an estimate of the intensity of the {110} <uvw> surface texture produced, are listed in Table 9.2.4. 1.

9.2.5. General observations of Types I, II, III and IV texture segregations and their effect upon R values.

Through thickness pole density plots were obtained for cold rolled and annealed material to ascertain if recrystallisation markedly affected texture segregation that had been developed during cold rolling. Fig.9.2.5. 1. and Fig. 9.2.5. 2. show results for Type II and III textures which are typical of the four cases with regard to the similarity between rolling and recrystallisation texture. The {111} and {100} plots for annealed material closely resemble the contours for the cold rolled material. There is, nevertheless, a reduction in texture intensity which is particularly marked in the {100} texture. However, not all components of the recrystallisation texture are reduced in intensity e.g. in the rolled material {411} texture is 1.5 random intensity at the surface plane and .6 random intensity at the mid-plane. After recrystallisation {411} texture intensity of the corresponding planes of the sheet are 1.4 random and .7 random respectively.

Strip thickness. mm.	Draught. mm.	Reduction per pass. %	Total rolling reduction	Estimate of {110}⟨xyz⟩. relative
4.75	0	0	0	1
3.42	1.33	28	28	.8
2.18	1.24	43	46	.5
1.20	.98	44	75	.8
.82	.38	46	83	.9
.57	.25	43	88	2.0

Table 9.2.4.1. Details of rolling sequence to develop Type IV texture segregation in rimmed steel.

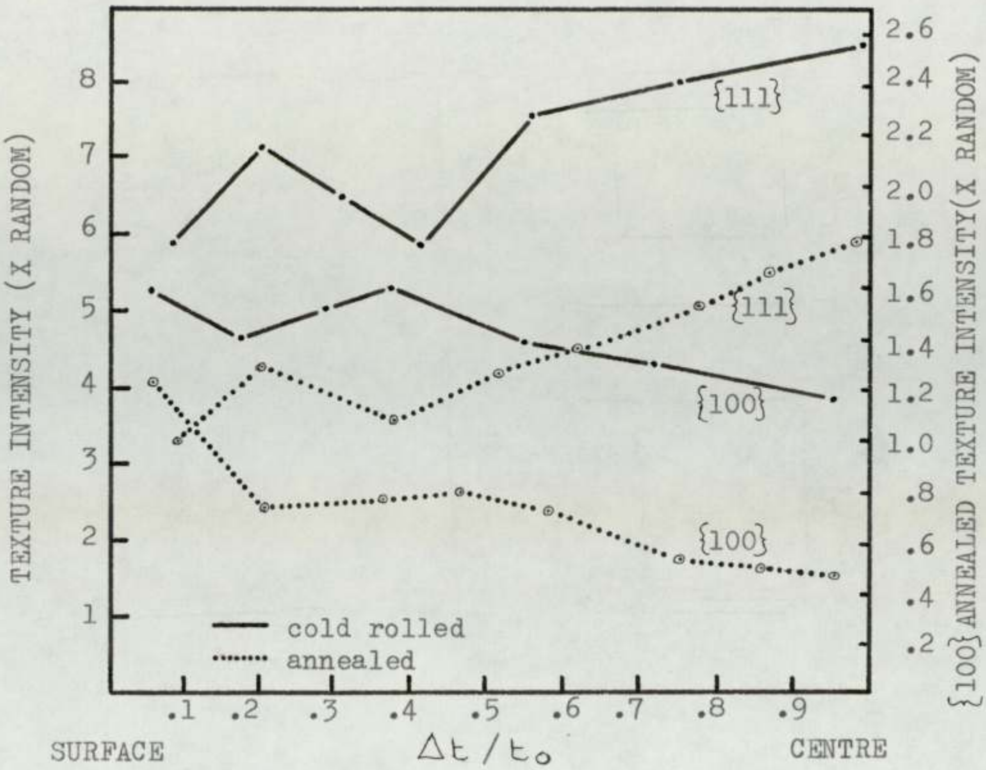

Fig. 9.2.5. 1a. Type II through thickness {111} and {100} texture intensity for 80% cold rolled and 80% cold rolled and annealed strip. (Note the different scale for {100} annealed texture intensity).

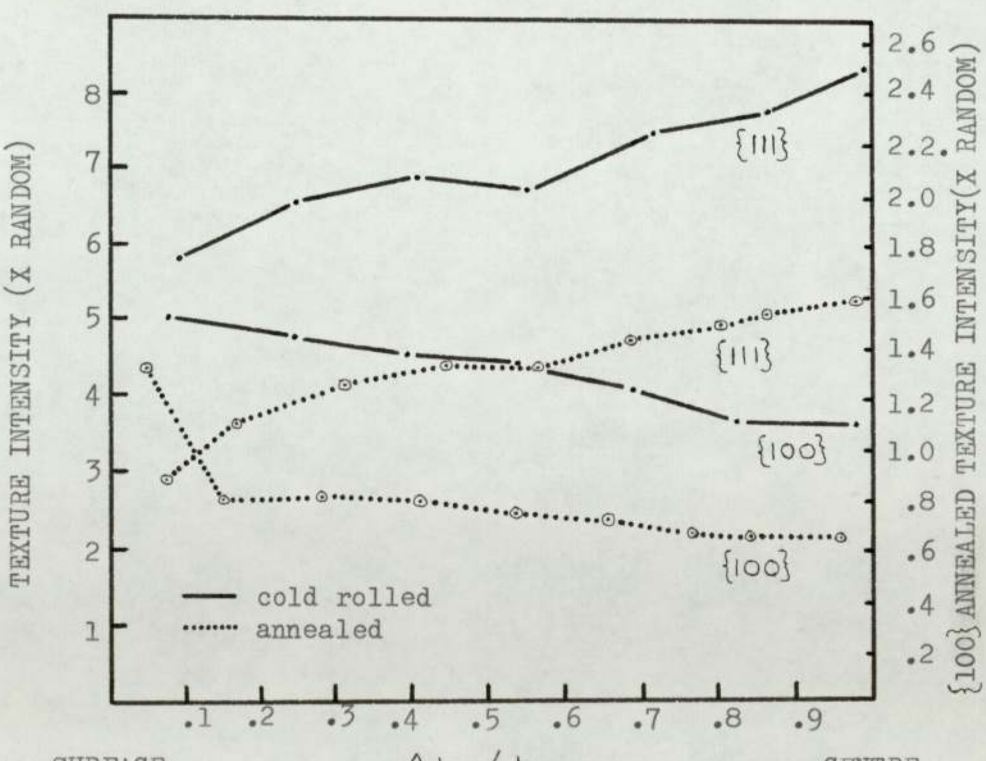

Fig. 9.2.5. 1b. {111} and {100} through thickness texture intensity for 80% cold rolled and 80% cold rolled and annealed strip; strip dry rolled with draughts of .125 mm. (Note the different scale for {100} annealed texture intensity).

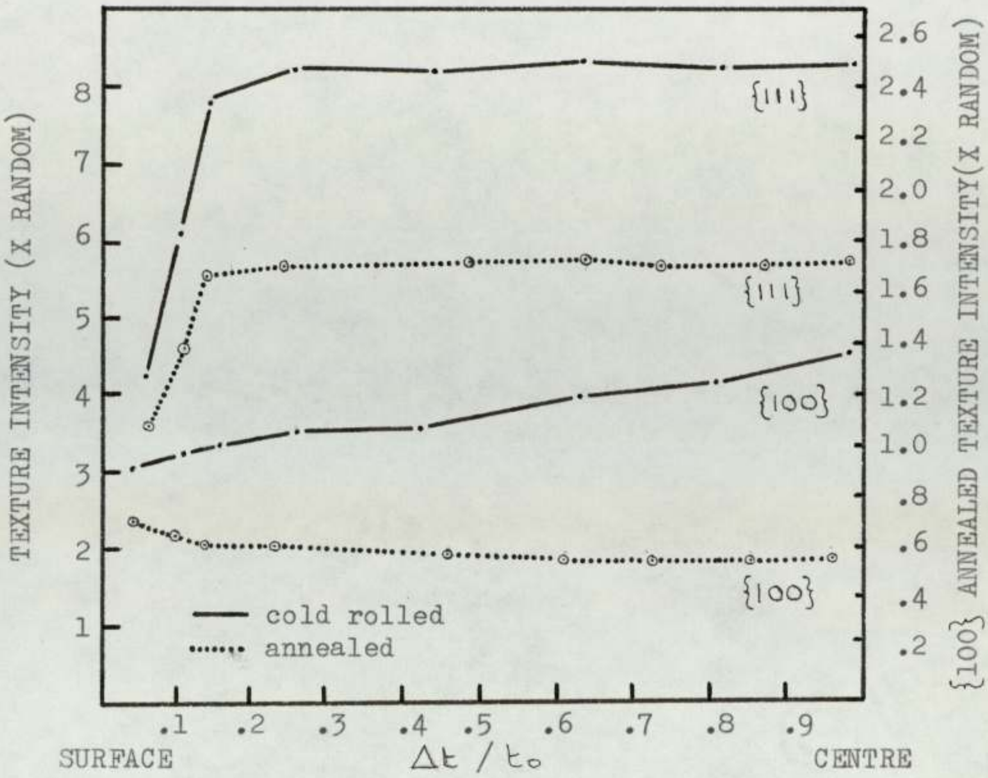

Fig. 9.2.5. 2a. Type III through thickness {111} and {100} texture intensity for 80% cold rolled and 80% cold rolled and annealed strip. (Note the different scale for {100} annealed texture intensity).

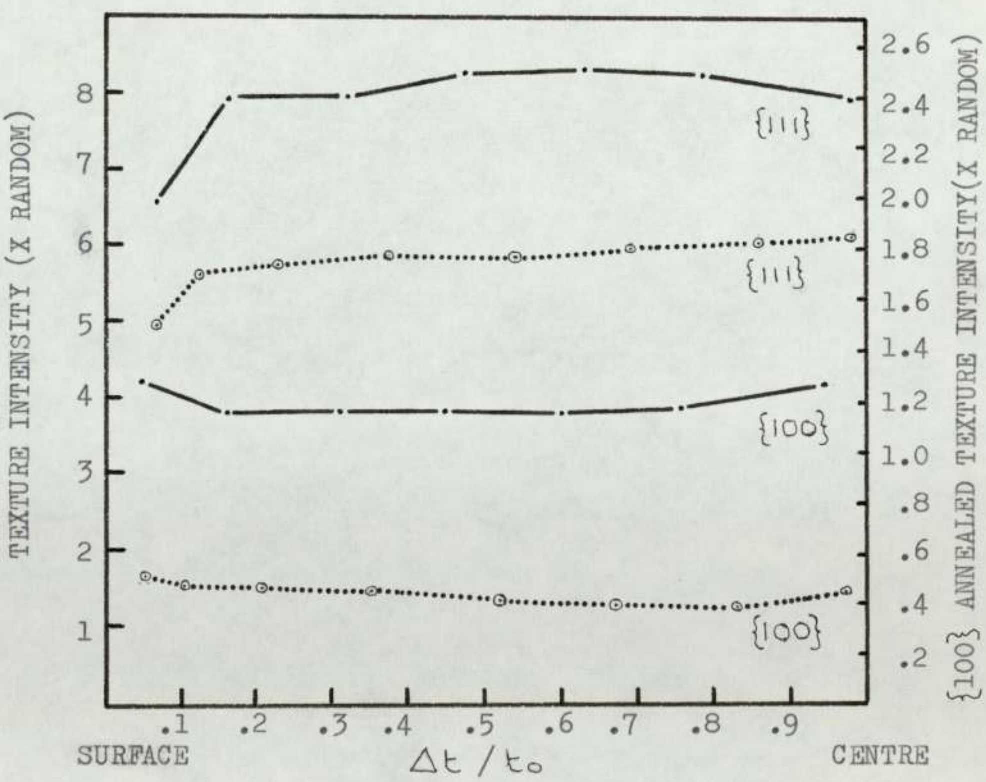

Fig. 9.2.5. 2b. {111} and {100} through thickness texture intensity for 80% cold rolled and 80% cold rolled and annealed strip; strip dry rolled with draughts of .500 mm. (Note the different scale for {100} annealed texture intensity)

Therefore recrystallisation does not significantly change the intensity of $\{411\}$ texture. It can therefore be concluded that texture segregation observed in annealed steel strip is developed entirely as a result of cold rolling. Texture intensity is, however, modified by recrystallisation.

The dependence of the severity of texture segregation Type II upon total rolling reduction can be illustrated by reference to the through thickness pole density plots for annealed specimens that had previously been subjected to a range of rolling reductions, Fig. 9.2.5. 3. This is possible because texture segregation in annealed material is indicative of equivalent texture segregation in the original cold rolled material.

The severity of texture segregation may be quantitatively described by use of a parameter S where

$$S = \text{standard deviation about } \{111\}_{\text{average}} \quad \ldots\ldots\ldots\ldots\ldots \quad 9.2.5.\ 1.$$

and $\{111\}_{\text{average}}$ is the average $\{111\}$ texture intensity through the sheet. Values of S of zero would indicate a material that does not exhibit texture segregation whereas values greater than zero indicate the presence of texture segregation. The larger the value of S the more intense and significant the segregation.

Values of S as a function of total rolling reduction prior to the final anneal were calculated from Fig. 9.2.5. 3. and are plotted in Fig. 9.2.5. 4. After 60% rolling reduction there is little evidence of texture segregation.

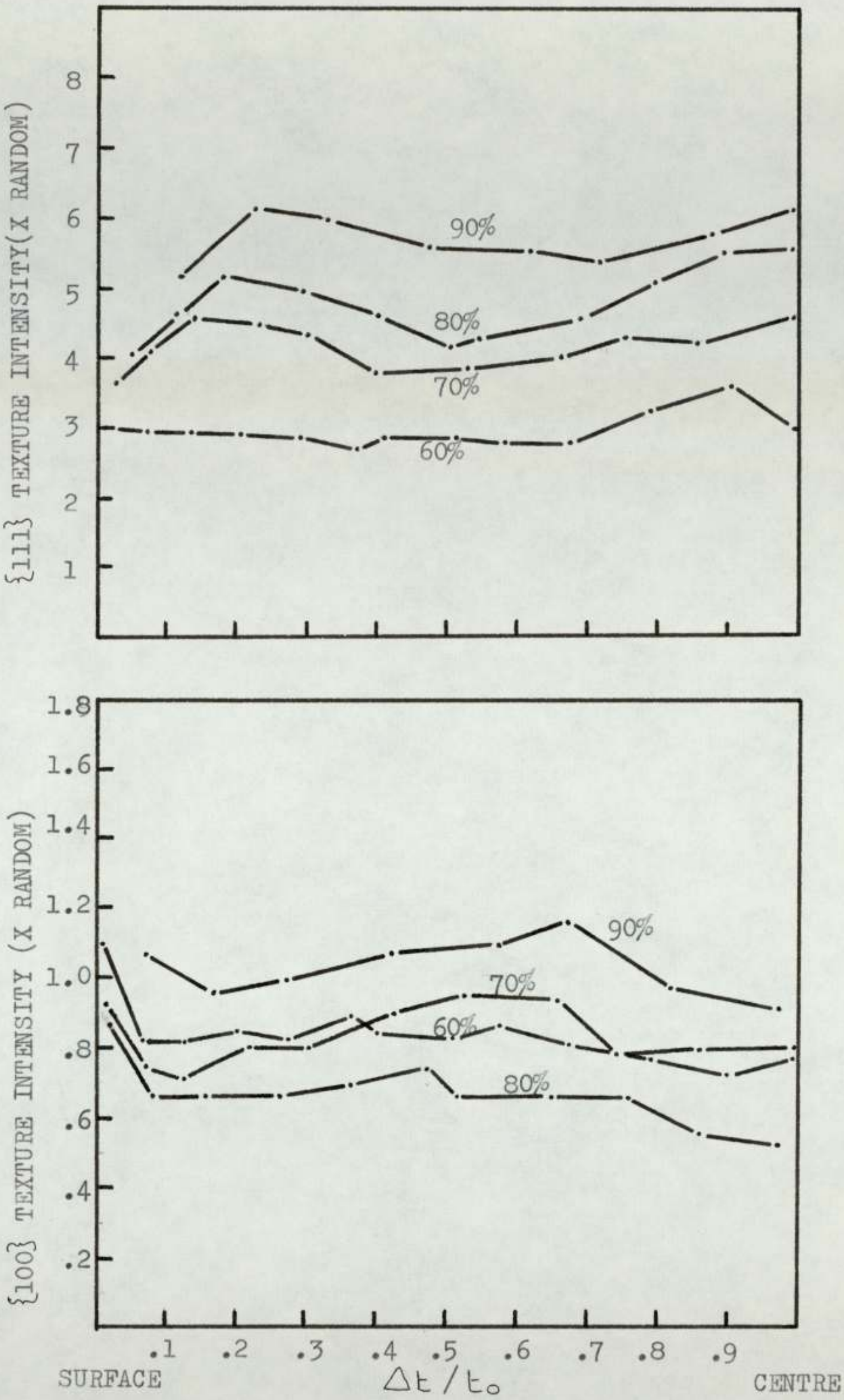

Fig. 9.2.5. 3. {111} and {100} texture intensities as a function of depth for strip samples cold rolled 60%, 70%, 80%, 90% with draughts of .125 mm., and thereafter subjected to a standard annealing treatment.

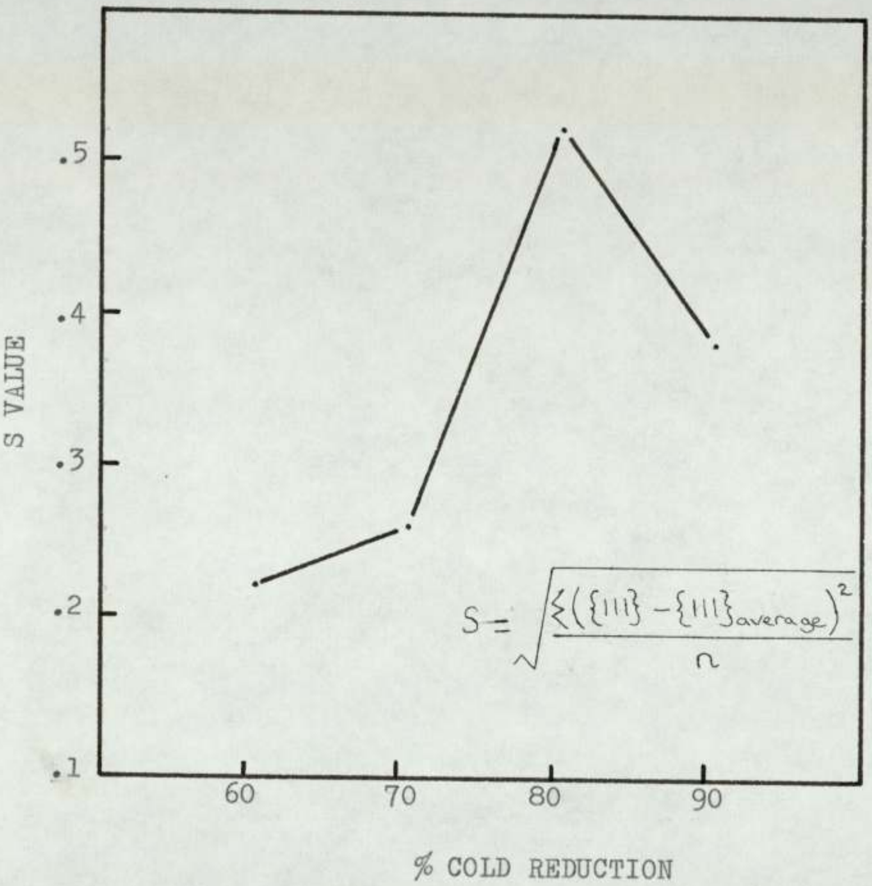

Fig. 9.2.5. 4. Standard deviation, S, of {111} texture intensity through the thickness of strip, plotted as a function of cold reduction prior to a standard anneal.

The magnitude of the segregation thereafter increases to a maximum at 80% cold reduction and then decreases to 90% reduction. This dependence upon total rolling reduction implies that a specific range of rolling geometries rather than rolling draughts, is conducive to the development of Type II texture segregation.

Through thickness pole density plots after approximately 80% cold reduction for texture Types I, II and III and after 88% reduction for Type IV are superimposed in Fig. 9.2.5. 5. If, for convenience, the texture - R value correlation coefficient is defined as :

$$T = \frac{\{111\}_{average}}{\{100\}_{average}} \quad \text{.........} \quad 9.2.5.\ 2.$$

where $\{111\}_{average}$ and $\{100\}_{average}$ are the average $\{111\}$ and $\{100\}$ texture intensities through the sheet, then clearly $R_{IV} < R_{I} < R_{II} < R_{III}$ where R is the predicted R value for steel exhibiting texture segregation of the type defined by the suffix. R values determined for annealed material which corresponds to the cold rolled material used for texture determinations, Fig. 9.2.5. 5. are listed in Table 9.2.5. 1. These measured results comply with the predicted R values. Therefore, if material is rolled with lubricated rolls, R value increases with increase in draught over the range .025 mm. to .500 mm. The improvement in R value is associated with the changes in texture segregation resulting from increasing draughts. Increasing roll friction, by dry rolling with draughts greater than .500 mm. to promote the development of Type IV texture segregation, results in very low R values in the finished material.

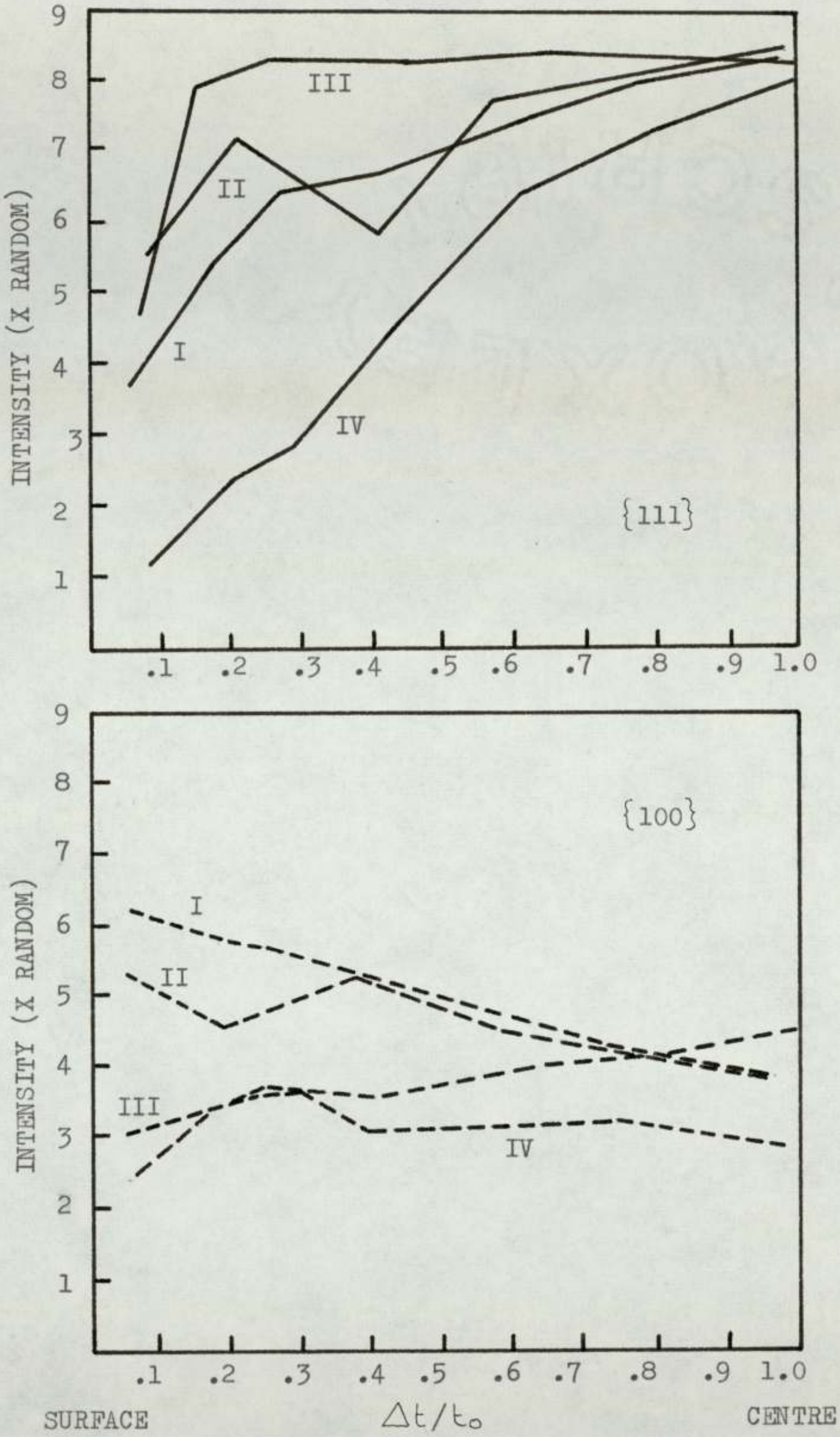

Fig.9.2.5. 5. {111} and {100} pole densities as a function of depth in the strip for steel exhibiting Types I, II, III and IV segregation. All samples cold rolled 80% except sample IV which was cold rolled 88%.

Texture Type	Draught mm.	Lubrication Conditions	R_o value
I	.025	Oil	.87
II	.125	Oil	1.33
III	.500	Oil	1.67
IV	1.3—.250	MgO	.65

Table 9.2.5.1. R_o values for annealed strip displaying Types I, II, III and IV texture segregation; I, II and III cold rolled 80% and IV 88%.

9.2.6. Summary of Types I, II, III and IV texture segregation.

The observations pertaining to texture segregation Type I, II, III and IV are summarised in Table 9.2.6. 1. Textures are described at three sheet planes, if necessary, using data from (110) pole figures, and inverse pole densities. The adjectives 'high' and 'low' are used to assign relative magnitude to texture components within one texture category and not from one category to another, i.e. 'high {xyz}' in category I is not necessarily a higher intensity texture than 'low {xyz} ' in category II.

9.2.7. Micro hardness measurements.

A series of micro hardness plots were obtained on a Leitz micro hardness tester. The main objective of this part of the investigation was to measure the precise thickness of the 'rim' zone of the strip so that any texture segregation effects associated with the rim could be established.

Specimens exhibiting Types I, II and III texture segregation were mounted in diakon with the edge plane uppermost, Fig. 8.4. 1. The grain size of the original hot band was approximately 25 μ . Consequently, since the strips had been cold rolled 80% the thickness of the deformed original crystals would be about 6 μ . However, the effective grain thickness would be even less than this since a crystal heavily deformed fragments into many crystals. The size of the micro hardness indentations were of the order of 30 μ and therefore many grains would contribute to the hardness value measured.

Texture Seg. Type		Cold rolling conditions: Draught mm.	Cold rolling conditions: Lubrication	Description of Texture: Surface Plane S.P.	Description of Texture: Intermediate Plane I.P.	Description of Texture: Mid-Plane M.P.	Comments
I		<.025	Dry rolling and lubricated rolling	$\langle 110\rangle_{RD}$ low $\{\bar{1}11\}$ intensity high $\{100\}$ intensity	-	$\langle 110\rangle_{RD}+\{111\}_{RP}$ high $\{\bar{1}11\}$ intensity low $\{100\}$ intensity	There is a gradual transition from surface plane texture to mid-plane texture
II	a	.125	Lubricated	low intensity $\langle 110\rangle_{RD}+\{111\}_{RP}$ low $\{\bar{1}11\}$ intensity high $\{100\}$ intensity	$\langle 110\rangle_{RD}$ low $\{\bar{1}11\}$ high $\{100\}$	$\langle 110\rangle_{RD}+\{111\}_{RP}$ high $\{\bar{1}11\}$ intensity low $\{100\}$ intensity	The differences in (110) pole figures at SP, IP and MP are not very pronounced. Therefore the texture description has been deduced from examination of pole figures and pole density data.
	b	.125	Dry rolled	$\langle 110\rangle_{RD}$ low $\{\bar{1}11\}$ intensity high $\{100\}$ intensity	-	"	
III	a	.500	Lubricated	low intensity $\langle 110\rangle_{RD}+\{111\}_{RP}$ low $\{\bar{1}11\}$ intensity high $\{100\}$ intensity	As MP.	$\langle 110\rangle_{RD}+\{111\}_{RP}$ with $\langle\bar{1}10\rangle_{RD}$ predominating. high $\{111\}$ intensity low $\{100\}$ intensity	SP texture is restricted to the extreme surface planes.
	b	.500	Dry rolled	as MP	as MP.	"	
IV			MgO dusted rolls	$\{110\}\langle uvw\rangle$ where $\langle uvw\rangle$ ranges between $\langle 001\rangle$ and $\langle 111\rangle$. v.low $\{111\}$ intensity high $\{110\}$ intensity	-	$\langle 110\rangle_{RD}+\{111\}_{RP}$ with $\langle\bar{1}10\rangle_{RD}$ predominating. high $\{111\}$ intensity v.low $\{110\}$ intensity	There is a gradual transition from SP texture to MP texture.

Table 9.2.6. 1. Summary of Types I, II, III and IV through thickness texture segregation.

Therefore the hardness values are not dependent upon the orientation of individual crystals but are a true reflection of the constitutional inhomogeniety of the metal.

Results of the micro hardness survey are shown in Fig.9.2.7. 1. The low hardness values obtained for the surface elements are attributable to the 'rim' zone. The thickness of the 'rim' either side of the sheet is .15 of the total sheet thickness. Types II and III texture display a surface texture irregularity, Fig. 9.2.2. 1. and 9.2.3. 1. The $\Delta t/t_o$ values to which the surface texture irregularity is present in Type II textures is variable and may be greater than the thickness of the rim depending upon the rolling conditions used, Fig. 9.2.5. 3. It can, therefore, be concluded that texture segregation in the surface elements of rimmed steel strip is not directly attributable to the presence of the 'rim' zone.

9.3. <u>The effect of total rolling reduction upon annealing texture and R value.</u>

Material was processed to exhibit Type I, II and III texture segregation for a range of cold reductions. Measurements of R_o value as a function of cold reduction prior to a final standard anneal are shown in Fig.9.3.1. for each of the three cases. R_o max occurs at successively higher percentage reductions in the sequence Type I, II and III texture. It was not possible to investigate Type IV segregation in a similar way as the texture could not be developed over an equivalent range of reductions. However, the cold reduction at which Type IV segregation becomes dominant, i.e. 88%, was found to be coincident with a large reduction in R_o value. The effect of Type IV texture segregation upon R_o value can be represented schematically as in Fig. 9.3. 2., where R_o value is plotted

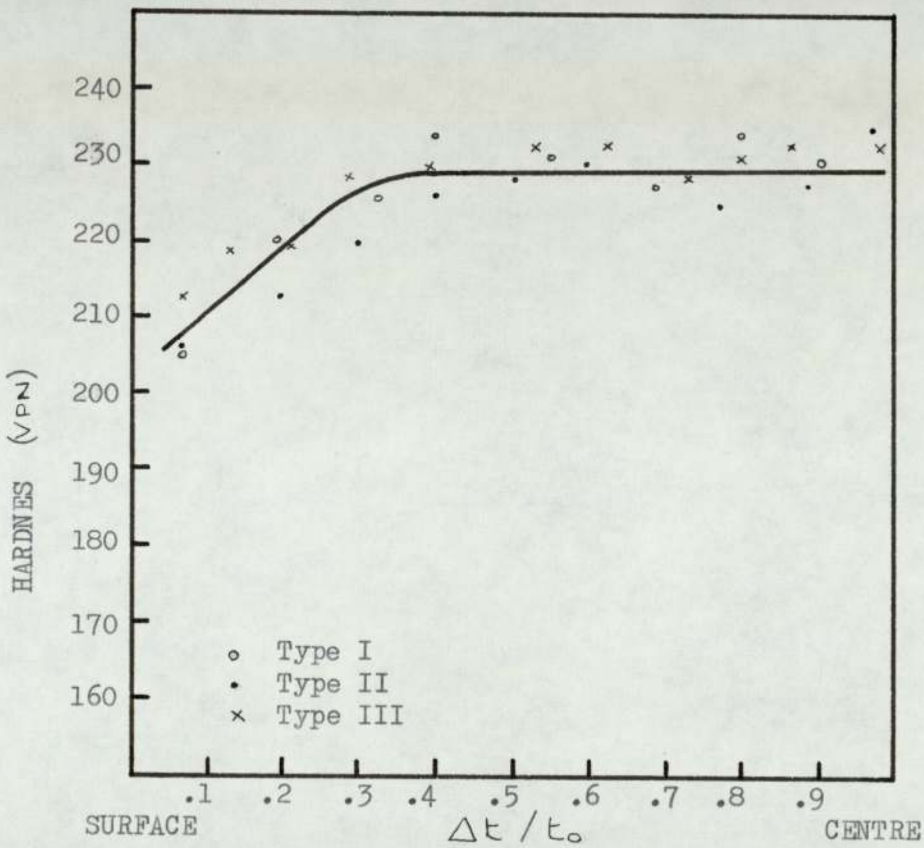

Fig. 9.2.7. 1. Microhardness values as a function of depth in 80% cold rolled rimmed steel strip (see Fig.8.4.1.) exhibiting Types I, II and III texture segregation. Each plotted point is the average of four measurements.

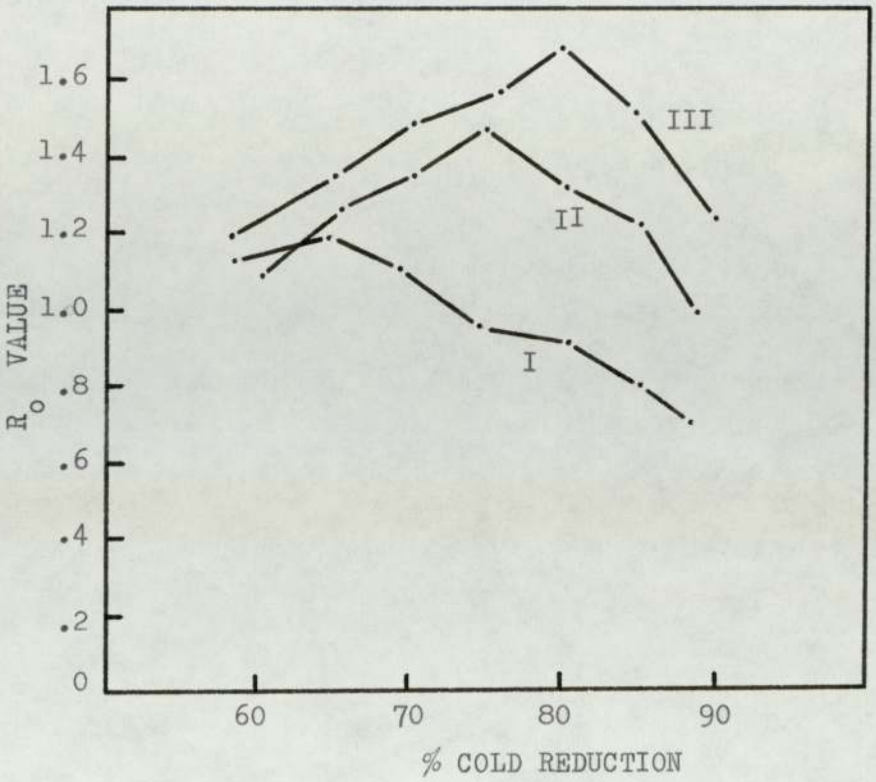

Fig. 9.3.1. R_o value as a function of cold reduction prior to a standard anneal; strip rolled to exhibit Types I, II and III texture segregation.

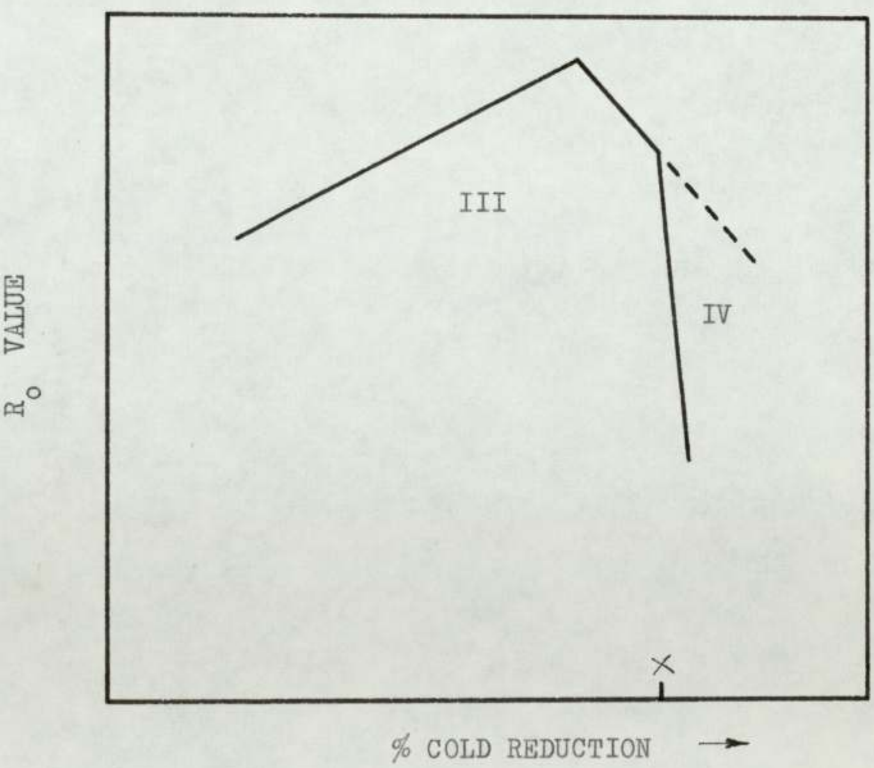

Fig. 9.3.2. Schematic representation of the effect of cold reduction, prior to a standard anneal, upon R_o value; strip dry rolled to exhibit Type III textures until X% when Type IV texture segregation is developed.

for a range of cold reductions. Texture Type III is developed to 88% cold reduction and there is a maximum R value at about 80% reduction. After 88% reduction Type IV textures are developed and result in a corresponding large reduction in R value. As Type IV textures are only developed under rolling conditions of severe friction Fig. 9.3.2. is representative of results from dry rolled material.

An extensive examination of annealed material exhibiting Type II texture was made to establish the cause of the reduction in R value after R_o max. Fig. 9.3.3. is the plot of R_o value versus cold reduction prior to the final anneal. $R_o$max in this material occurred at 80% cold reduction and therefore material cold rolled 75%, 80% and 85% and annealed was texturally examined. The mid-plane (110) pole figure for 80% cold rolled and annealed steel is shown in Fig. 9.3. 4a. To assist in the determination of this texture two inverse pole density measurements were made with the sheet normal direction and rolling direction as reference axes, Table 9.3.1. A suitable X-ray reflecting surface was obtained for rolling direction pole density measurements by the construction of a 'sandwich' from the steel sheet. Fig. 9.3.5. is a schematic representation of a three sheet sandwich where, for convenience, through thickness texture segregation in each sheet is displayed simply as a surface plane texture and different centre plane texture with a distinct boundary between the two. Measured texture intensities will thus be an average of the intensities expected from the two areas separately.

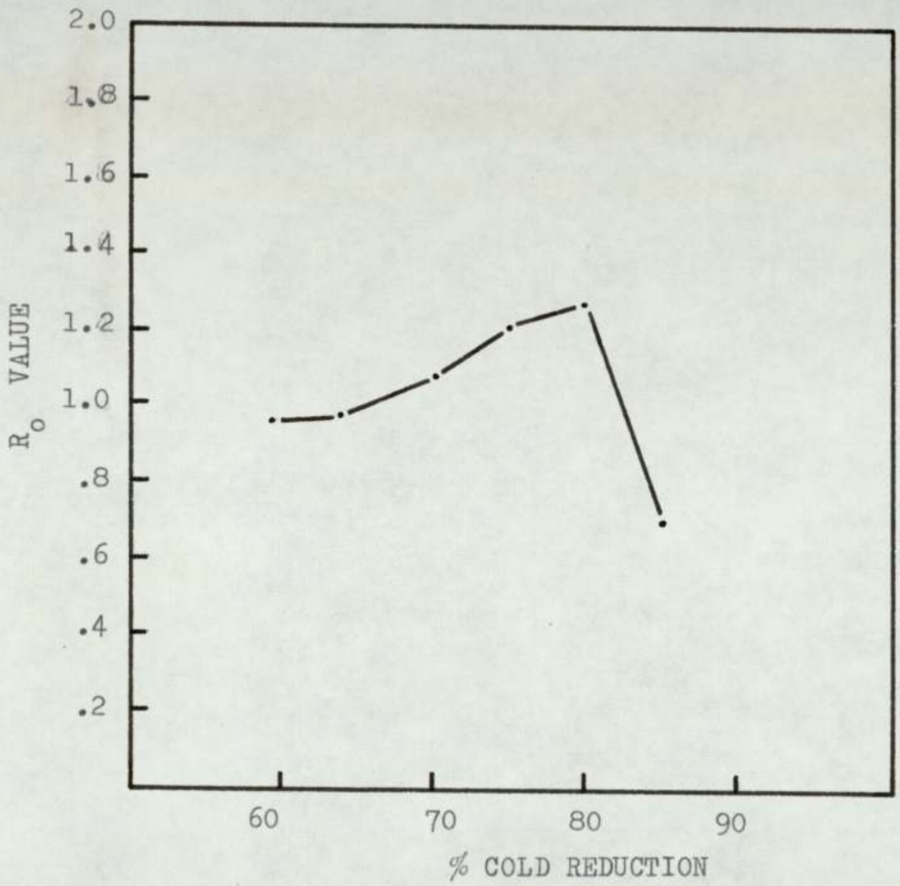

Fig. 9.3.3. R_o value plotted as a function of percentage cold reduction, prior to a standard anneal, for strip rolled to exhibit Type II texture segregation.

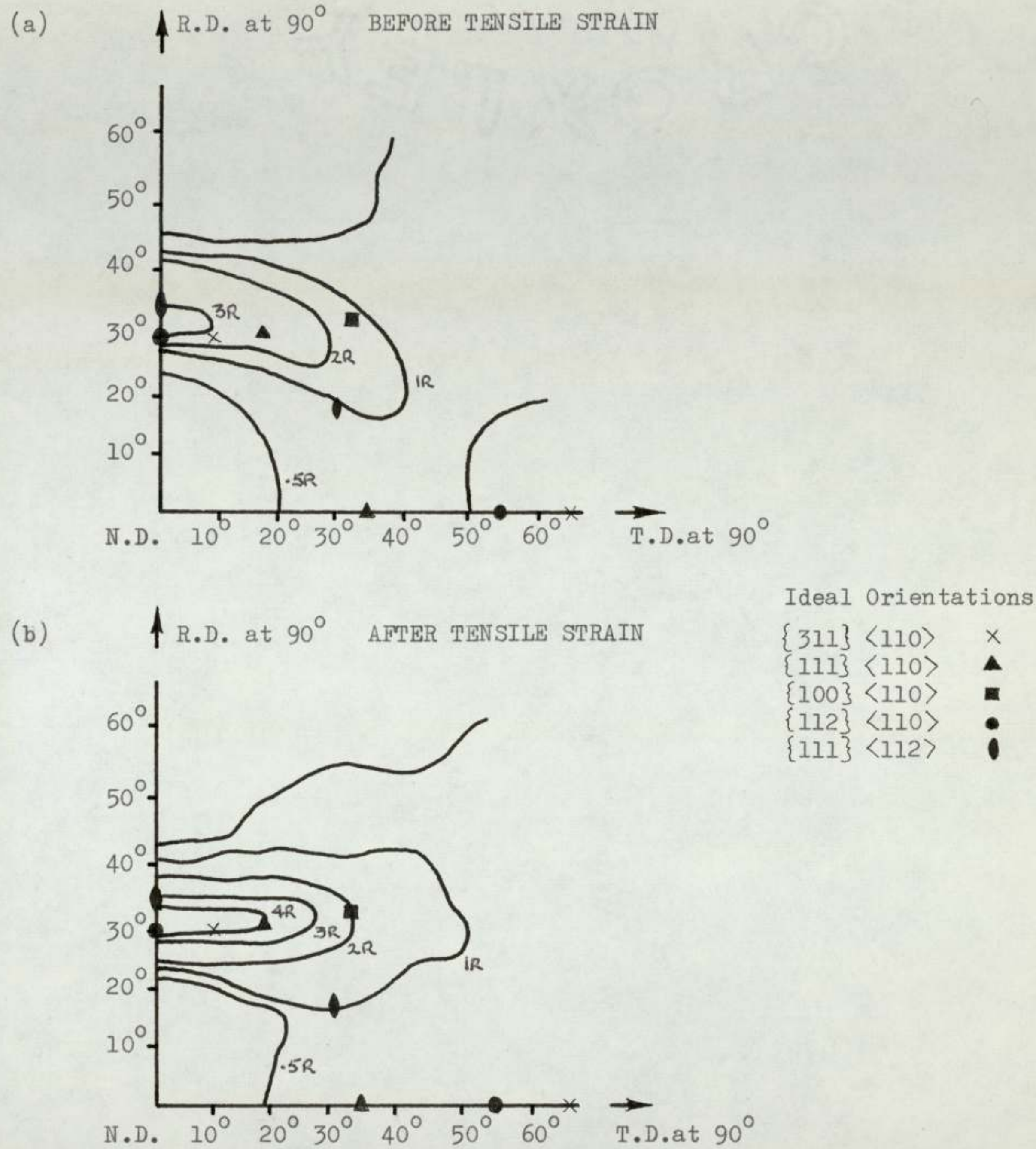

Fig. 9.3. 4. (110) pole figures at centre plane of steel cold rolled 80% with draughts of .125 mm. followed by (a) standard anneal (b) as (a) followed by 20% tensile strain.

Crystallographic Direction	Axis Density (X Random)	
	Sheet Normal	Rolling Direction
111	5.2	-
100	.75	-
110	-	3.0
112	1.3	1.2
332	1.5	-
210	-	1.5
310	-	1.3

Table 9.3.1. Sheet normal and rolling direction axis density for 80% cold rolled and annealed strip.

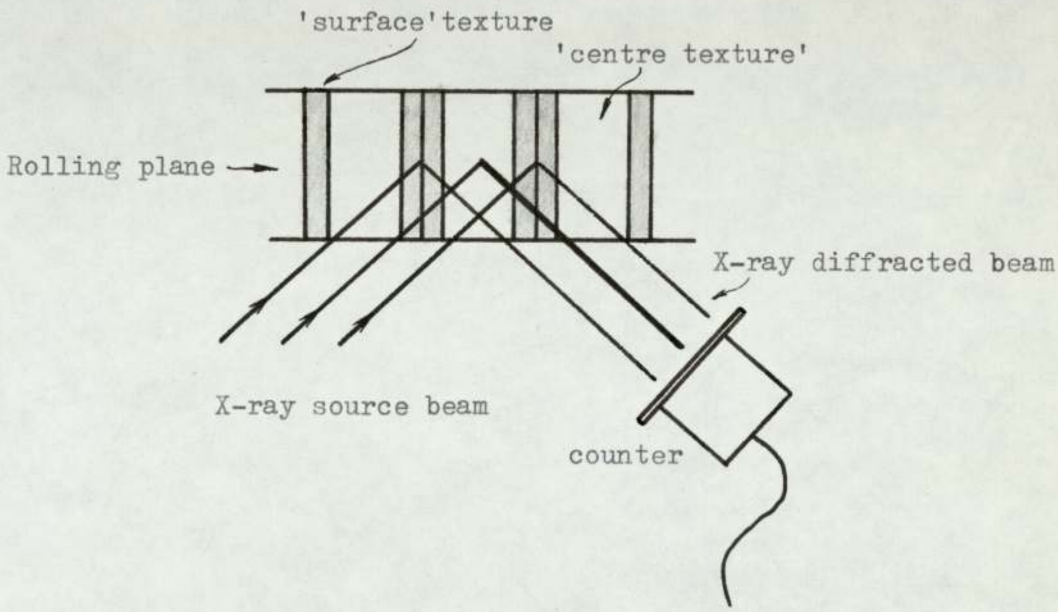

Fig. 9.3.5. Schematic representation of the arrangement of composite strip specimen relative to X-ray source and diffracted beams to enable an estimate of the intensity of crystallographic directions aligned parallel to the strip rolling direction. Note how through thickness, texture segregation leads to 'average intensities' being measured.

Through thickness texture segregation will, therefore, limit the precision of texture description when using such a sandwich specimen.

$\{111\}$ crystal planes are most predominantly aligned parallel to the rolling plane, Table 9.3.1., and $\{332\}$ and $\{211\}$ textures are next most intense. It is to be noted that $\{100\}$ texture is a minor texture component in annealed steel strip. The crystals are also aligned with $\langle 110 \rangle$ axes parallel to the rolling direction although crystals with $\langle 112 \rangle$, $\langle 210 \rangle$ and $\langle 310 \rangle$ directions parallel to the rolling direction are also present at above random intensity. The texture developed after 80% reduction followed by annealing can therefore be described as a partial fibre texture with $\langle 110 \rangle$ directions parallel to the rolling direction. Planes parallel to the plane of the sheet that belong to this fibre texture range from $\{001\}$ to $\{111\}$. $\{001\}$ texture is quite weak at approximately random intensity, whereas $\{112\}$ texture is quite strong, and $\{111\}$ texture the most intense at 5.2 random intensity. The (110) pole figure, Fig. 9.3. 4a. can be accounted for by assuming spread about this texture that is equivalent to rotation about the sheet normal such that $\langle 210 \rangle$ directions also become aligned parallel to the rolling direction. Superimposing the $\{111\}$ $\langle 112 \rangle$ orientation upon this orientation spread completes the description of the pole figure and accounts for the $\langle 112 \rangle$ rolling direction measured on the sandwich specimen.

Increasing the deformation to 85% reduction causes a sharpening of the preferred orientation by reduction in the spread about the sheet normal direction and an accompanying reduction in the component $\{111\}\langle 112\rangle$, Fig. 9.3. 6a, and Table 9.3.2. This is confirmed by the reduction in $\langle 210\rangle$ and $\langle 112\rangle$ rolling direction intensity and a corresponding increase in $\langle 110\rangle$ rolling direction intensity. The description of mid-plane texture for material cold rolled 80% and 85% and annealed are summarised in Table 9.3. 3.

Complete through thickness pole density plots were obtained for 75, 80 and 85% cold rolled and annealed material, Figs. 9.3. 7. and 9.3. 8. The measurements were made on material selected from adjacent sites to the areas of strip from which tensile test pieces were cut for the R value determinations. Further pole density measurements were made from specimens constructed from the actual tensile test pieces. These results are superimposed upon the results measured before tensile strain in Fig. 9.3. 7. and Fig. 9.3. 8. (110) mid-plane pole figures were determined for the material cold rolled 80% and 85% annealed and extended in tension. The results are illustrated in Figs. 9.3. 4b. and 9.3. 6b. so that direct comparison can be made with the pole figures constructed from material not subjected to tensile strain.

Tensile strain decreases the intensity of $\{111\}$ texture, increases the intensity of $\{100\}$ and $\{332\}$ texture, and leaves $\{411\}$ texture unchanged.

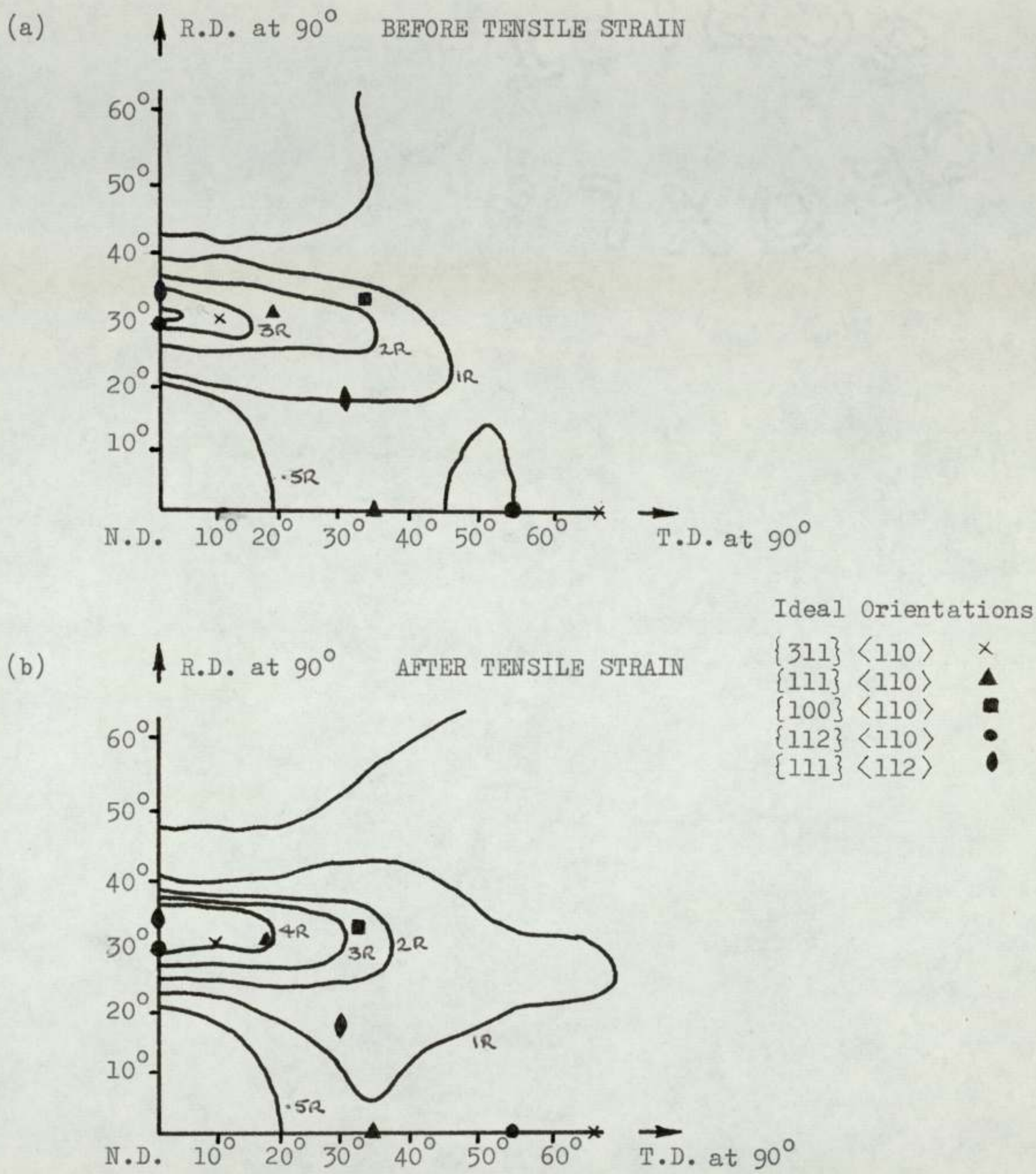

Fig. 9.3. 6. (110) pole figures at centre plane of steel cold rolled 85% followed by (a) standard anneal (b) as (a) with 20% tensile strain. Rolling draught .125 ins.

Crystallographic Direction	Axis Density (X Random)	
	Sheet Normal	Rolling Direction
111	5.1	-
100	.9	-
110	-	3.8
112	1.1	.8
332	1.2	-
210	-	1.1
310	-	1.1

Table 9.3.2. Sheet normal and rolling direction axis density for 85% cold rolled and annealed strip.

% Cold reduction	Description of texture
80%	$\langle 110 \rangle_{RD}$ with spread about strip normal so that $\langle 210 \rangle$ directions are also aligned parallel to RD + $\{111\}$ RP
85%	$\langle 110 \rangle_{RD}$

Table 9.3. 3. Summary of the mid-plane textures for 80% cold rolled and annealed and 85% cold rolled and annealed strip.

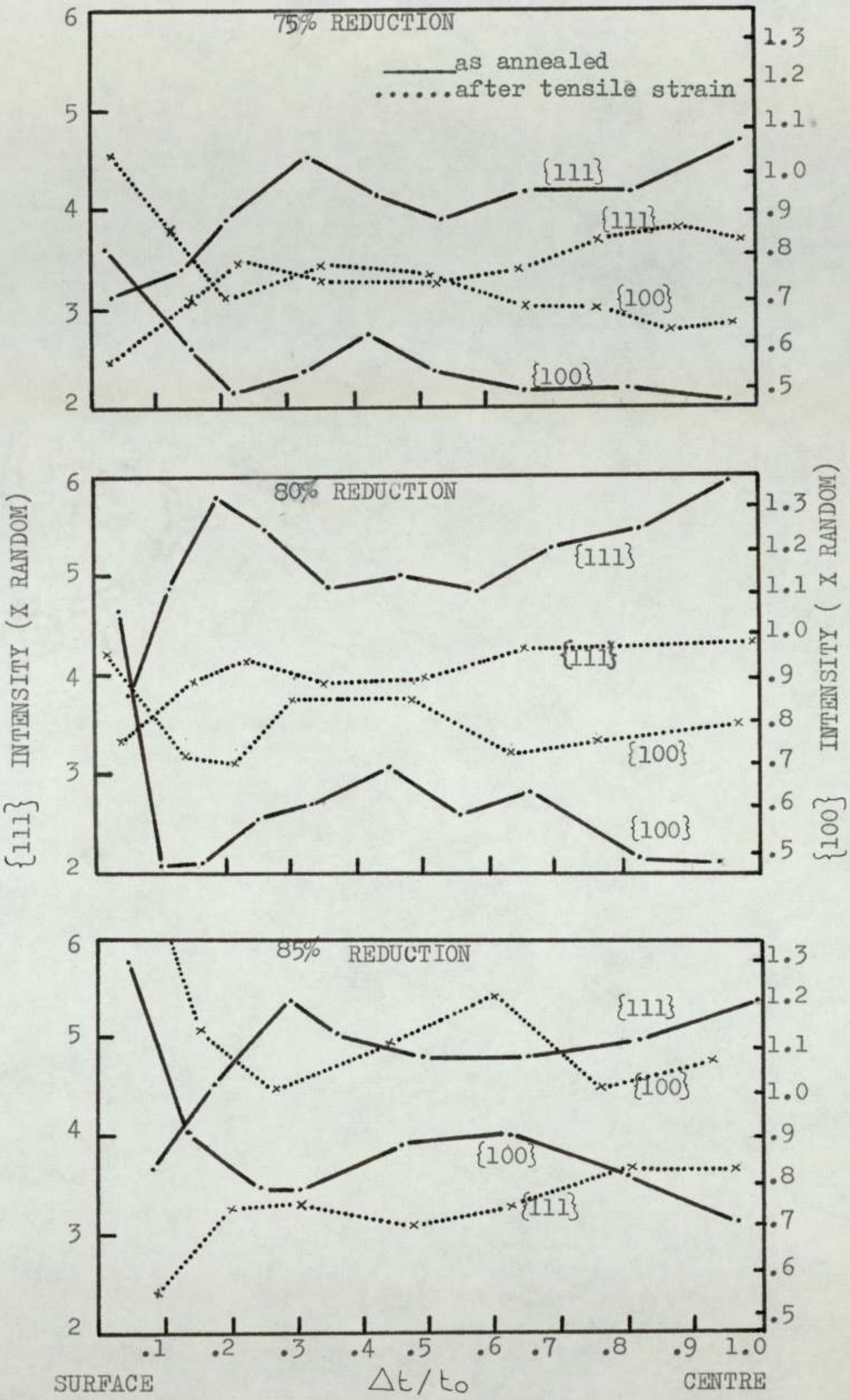

Fig. 9.3. 7. {111} and {100} pole density as a function of depth in the strip for 75, 80 and 85% cold rolled and annealed strip before and after tensile strain; strip rolled with draughts of .125 mm. and oil lubrication.

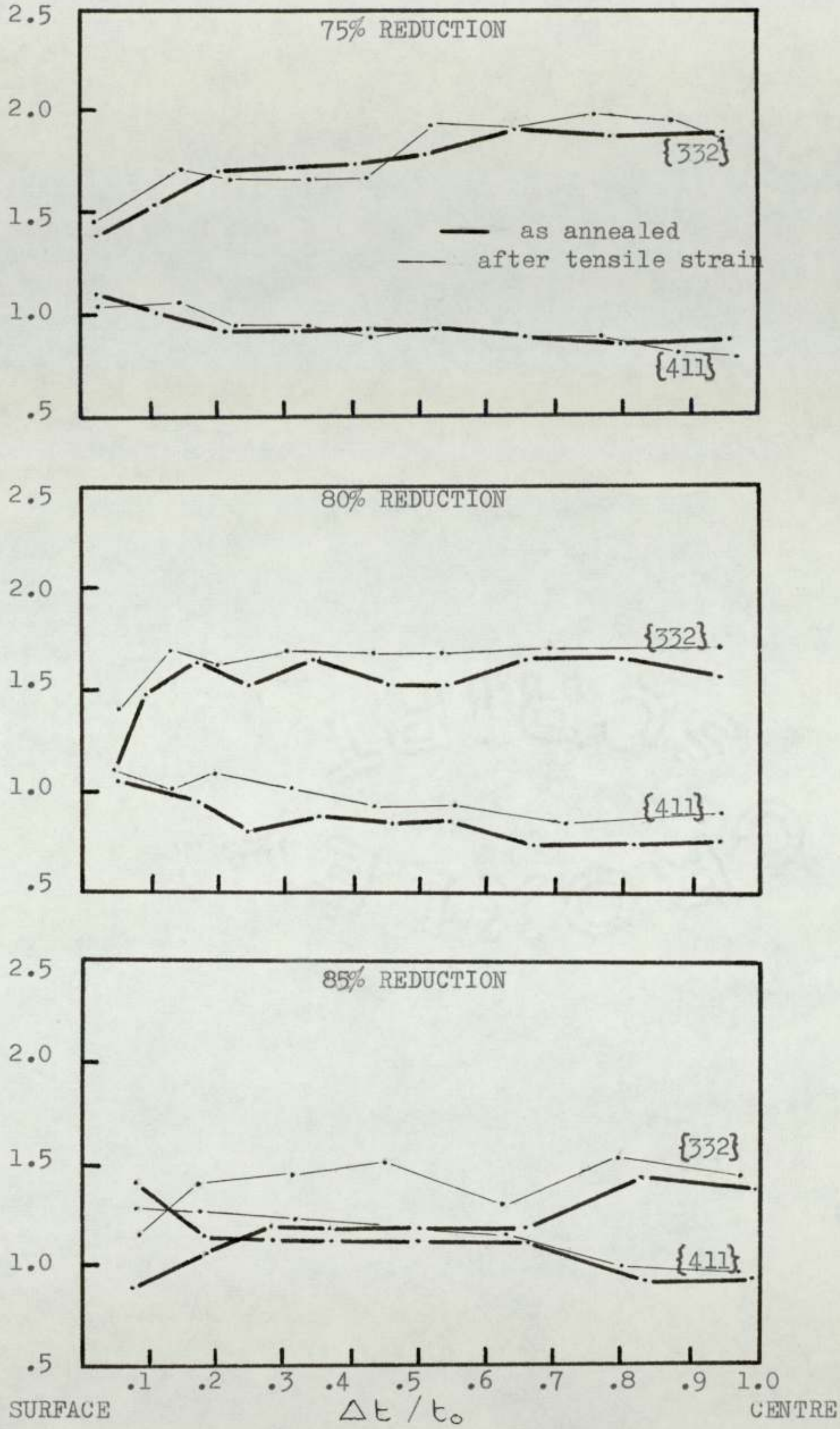

Fig. 9.3.8. {322} and {411} pole intensity as a function of depth in the strip for 75, 80 and 85% cold rolled and annealed strip before and after tensile strain; strip rolled with draughts of .125 mms. and oil lubrication.

The pole density diagrams can be summarised by calculation of the T ratio where $T = \frac{\{111\}_{average}}{\{100\}_{average}}$ and $\{100\}_{average}$ and $\{111\}_{average}$ are as previously defined. T values before and after tensile strain are tabulated in Table 9.3. 4. The magnitude of the change in T ratio after tensile strain is different for each of the three cold rolling reductions, being higher for 85% cold rolled and annealed strip than 80% cold rolled and annealed strip.

The difference in texture reorientation is also apparent in (110) pole figures after tensile strain when Fig. 9.3. 4b is compared with Fig. 9.3. 6b. The reorientation in the material cold rolled 80% and annealed can be considered as a combination of three crystal rotation mechanisms. These are schematically represented in the stereographic projection, Fig. 9.3. 9.

> Firstly (a) there is a sharpening of the recrystallisation texture previously described in Table 9.3. 3. and illustrated in Fig. 9.3. 4a., by reduction of the spread about the sheet normal resulting in a 'sharp' partial fibre texture $\langle 110\rangle_{RD}$.
>
> (b) This is accompanied by rotation away from the component $\{111\}\langle 112\rangle$.

Rotation (a) would increase the intensity of all $\{xyz\}$ planes in the $\langle 110\rangle_{RD}$ fibre texture including $\{111\}$ orientations. Conversely, rotation (b) will decrease the intensity of $\{111\}$ texture. The T ratio will therefore be maintained approximately at its pre-tensile strain level if rotations (a) and (b) occur simultaneously.

% cold reduction prior to anneal	T ratio = $\{111\}_{average}/\{100\}_{average}$	
	before tension	after tension
75	8.0	4.8
80	8.8	5.3
85	6.8	3.1

Table 9.3.4. T ratio before and after tensile strain for strip cold rolled 75, 80 and 85% and then annealed.

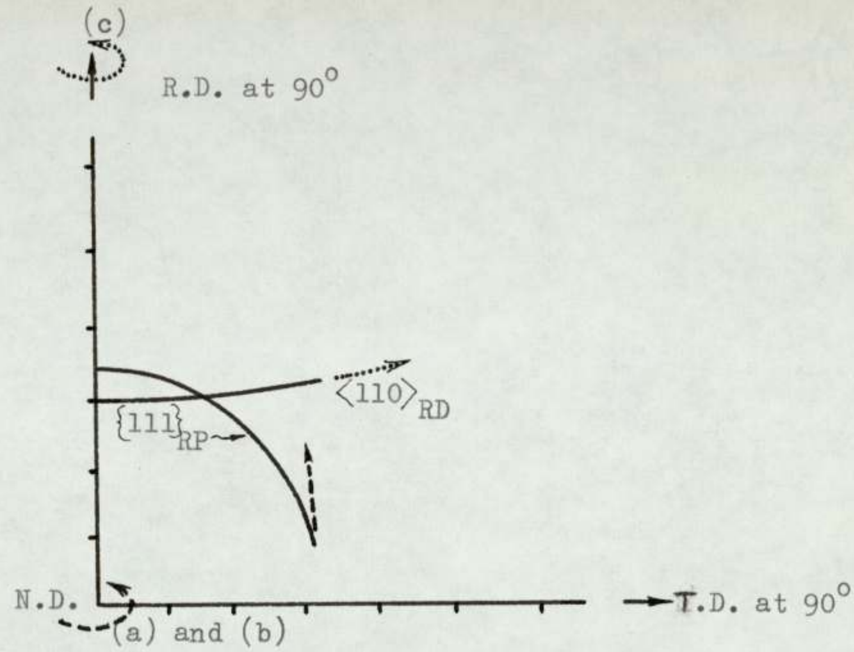

Fig. 9.3.9. Reorientation of (110) pole figure as a result of rotation of partial fibre textures $\langle 110 \rangle_{RD}$ and $\{111\}_{RP}$ accompanying tensile strain.

(c) At the same time as rotations (a) and (b) spread is occurring and can be represented by rotation about the $\langle 110 \rangle$ rolling direction.

Rotation (c) depletes the intensity of $\{111\}$ planes parallel to the plane of the sheet plane and increases the intensity of $\{100\}$ planes.

The reorientation in the material cold rolled 85% and annealed is achieved by crystal rotation of type (c) only, but the extent of the rotation is far more pronounced than in the material cold rolled 80% and annealed. (Compare Figs. 9.2. 4b and 9.2. 6b. with schematic representation of rotation (c) in Fig. 9.3. 9.). It is rational that type (c) rotation predominates in the 85% cold rolled and annealed material since the initial (a) type 'sharpening' of the $\langle 110 \rangle_{RD}$ fibre texture, as ascribed to the 80% cold rolled and annealed material, cannot take place. This is because the texture is already 'sharp' before tensile strain commences. Also rotation (b) away from the orientation $\{111\}\langle 112 \rangle$ cannot occur since the component is not significantly represented in the 85% cold rolled and annealed texture.

The net result is a greater reduction in T ratio after tensile strain for material cold rolled 85% and annealed, when rotation (c) is predominant, than for steel cold rolled 80% and annealed, when rotations (a), (b) and (c) occur simultaneously.

The texture change resulting from tensile strain is approximately equal throughout the strip thickness, i.e. the extent of crystal reorientation, if measured by the reduction in $\{111\}$ intensity, is the same at the free surface as the mid-plane.

Therefore texture changes that occur with progressive increments in tensile strain can, for any one particular prior processing condition, be usefully monitored in one sample. The surface of a standard 150 mm.(6 inch) tensile test specimen was etched with a solution of nitric acid to provide an area suitable for X-ray examination. Pole density measurements were made after successive 4% strain increments and $\{111\}$ texture intensity is plotted in Fig. 9.3. 10. The decrease in $\{111\}$ texture intensity is linearly related to tensile strain. Also the higher the initial intensity of $\{111\}$ texture the more rapid the decrease in intensity with tensile strain. This accounts for the difference in T ratio reduction, accompanying tensile strain, for material cold rolled 80% and 85% and annealed.

T ratios before and after tensile strain are in the correct magnitude sequence to account for the observed R_o values i.e. low ratio result in low R_o values and vice-versa, (compare Fig. 9.3. 3. with Table 9.3. 4.) R_o values were calculated for the three differently processed materials using measured textural data before and after tensile strain and are illustrated in Table 9.3. 5. The Fukuda[20] analysis of texture and associated R value was used for the calculations (See Table 9.3.5. for details). There is clearly a closer correlation between R_o value and texture after tensile strain than R_o value and texture before tensile strain.

9.4. Effect of intragranular precipitates upon R value.

A number of post anneal heat treatments were designed to produce a range of intragranular carbide dispersions. Cementite was precipitated from super-saturated solutions of ferrite at temperatures of 150, 200 and 300°C.

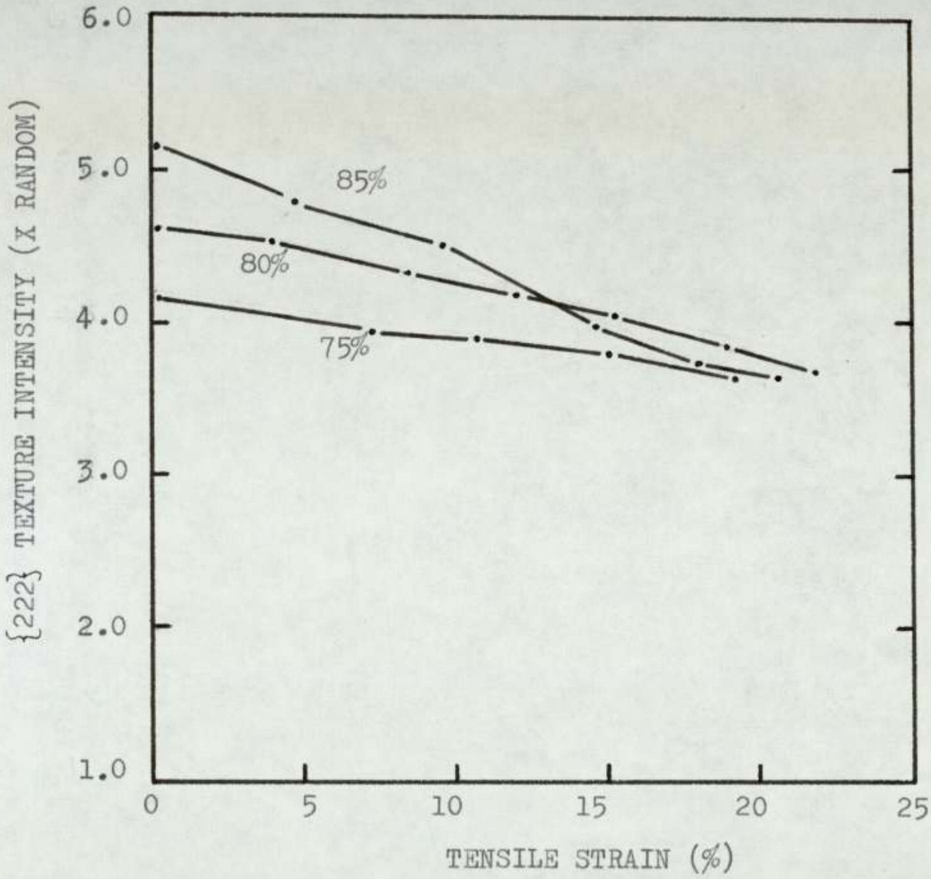

Fig. 9.3.10. Reduction in {222} surface texture intensity of annealed strip as a function of tensile strain; samples cold rolled 75, 80 and 85% to exhibit Type II texture segregation and then subjected to a standard annealing treatment.

% cold reduction prior to anneal	Calculated R_o value using data in Table 9.3.4.		Measured R_o value
	before tension	after tension	
75	1.7	1.35	1.2
80	1.8	1.5	1.25
85	1.6	1.0	.65

Table 9.3.5. R_o value, calculated from textural data obtained before and after tensile strain, compared with measured R_o values for strip cold rolled 75, 80 and 85% and then annealed.

R_o values were calculated in the following way {111} texture is predominantly a mixture of components {111} <110> and {111} <112>. Therefore, {111} texture can be said to result in an R_o value of 2.5[20]. {100} texture is predominantly composed of orientations {100} <110> , to which a predicted R_o value of 0 can be given. To give equal 'weight' to the individual components of the multicomponent texture R_o values were converted to D_o values prior to summation according to equation 2.3.2., D_o values were then reconverted to R_o values for tabulation.

Stereoscan photographs of the precipitates are shown in Fig. 9.4. 1. Fig. 9.4.2. illustrates the effect of cementite precipitates upon R_o value for material processed to exhibit Type II texture. The R_o value in the region of $R_o$max, which in this case occurred at 75% cold reduction, is increased when precipitates are present and the effect is greater the larger and more widely dispersed the precipitate, at least within the range studied. R_o values for Type III textures containing dispersed carbides are also improved, Fig. 9.4.3. It has also been noted in some experiments that the R_o value maximum is shifted to a higher percentage reduction, by as much as 10%, (40% true strain) when dispersed carbides are present.

Through thickness pole densities, after 20% tensile strain were determined for material corresponding to the R value measurements in Fig. 9.4.2. The results for the 75% cold rolled and annealed specimens are graphically illustrated in Fig. 9.4.4. The initial recrystallisation textures, for each of the four conditions considered, are obviously the same and Fig. 9.4.4. illustrates a through thickness texture which is typical of each case. However, the samples behave quite differently during tensile strain and is illustrated by the differences in crystal rotation associated with the strain. After strain, the through thickness texture of the normally processed material (with no overaging treatment) is subject to most crystal reorientation from the recrystallisation texture. The final intensity of $\{111\}$ texture is higher for aged specimens in the order 300^oC, 200^oC and 150^oC overaging treatments.

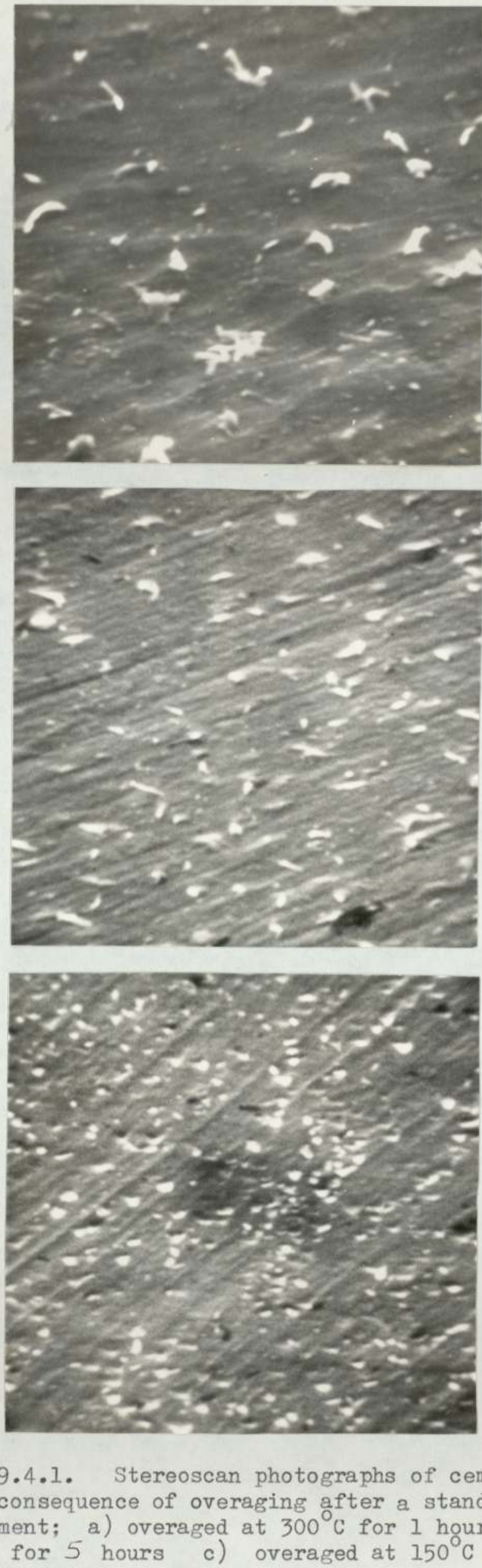

a)

Range of;

(i) Particle sizes

$.5\mu \rightarrow 1.\mu$

(ii) Interparticle spacing

$1.\mu \rightarrow 2.\mu$

b)

Range of;

(i) Particle sizes

$.25\mu \rightarrow .5\mu$

(ii) Interparticle spacing

$.25\mu \rightarrow 1.\mu$

c)

Range of;

(i) Particle sizes

$.1\mu \rightarrow .2\mu$

(ii) Interparticle spacing

$.1\mu \rightarrow .5\mu$

Fig. 9.4.1. Stereoscan photographs of cementite precipitated as a consequence of overaging after a standard annealing treatment; a) overaged at 300°C for 1 hour, b) overaged at 200°C for 5 hours c) overaged at 150°C for 25 hours.
Mag X 12500

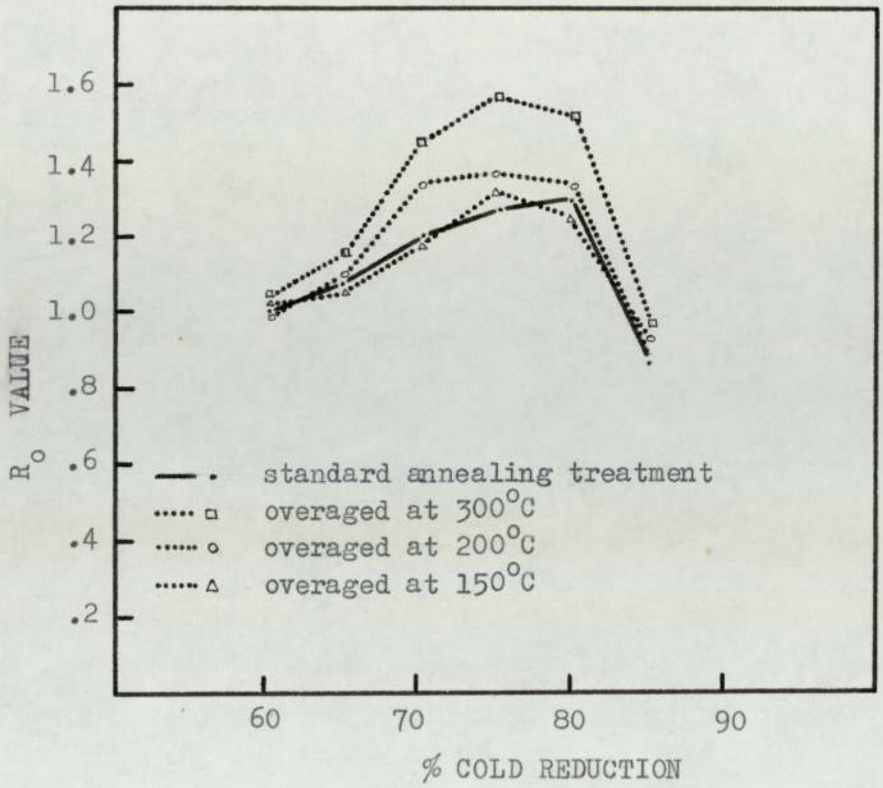

Fig. 9.4.2. The effect of overaging treatments, subsequent to a standard anneal, upon the R_o value of rimmed steel cold rolled to a range of reductions and to exhibit Type II texture segregation.

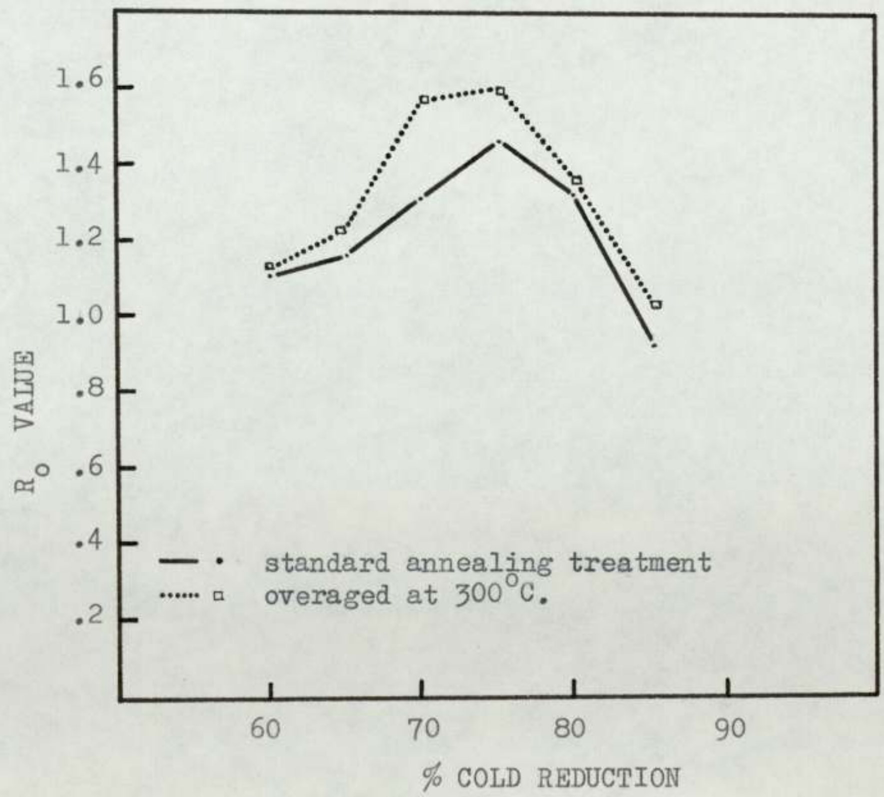

Fig. 9.4.3. The effect of a 300°C overaging treatment, subsequent to a standard anneal, upon the R_o value of rimmed steel cold rolled to a range of cold reductions and to exhibit Type III texture segregation.

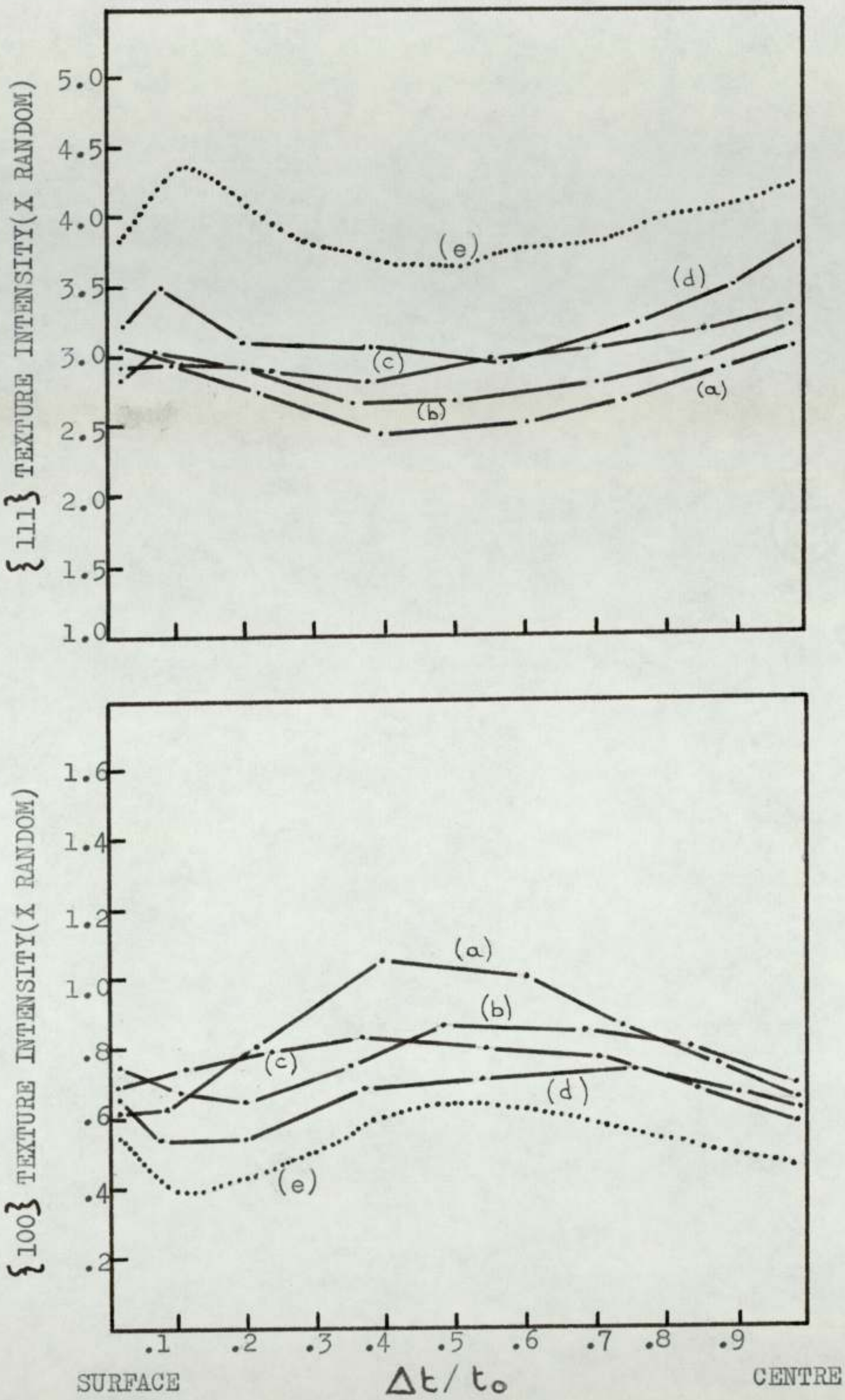

Fig. 9.4. 4. Through thickness {111} and {100} texture intensity after tensile strain for material cold rolled 75% and; a) annealed at 700°C,
b) as a)+ overage at 150°C,
c) as a)+ overage at 200°C,
d) as a)+ overage at 300°C,
e) texture typical of all four heat treated conditions <u>before</u> tensile strain.

Therefore the T ratio, which equals $\{111\}_{average}/\{100\}_{average}$, after tensile strain is lowest for the normally processed material and highest for the material undergoing the $300^{o}C$ overaging treatment, Table 9.4.1. The R value is also lower in the former than the latter case. Since a change in $\{111\}$ texture implies some through thickness shear it can be concluded that carbide precipitation inhibits through thickness shear and thus enhances R value.

(110) pole figures constructed after tensile strain revealed no discernable difference between the differently heat treated materials.

To test if precipitates have a corresponding effect upon $\bar{R}$ values, measurements were also made at 90^{o} and 45^{o} to the tension axis for $300^{o}C$ overaged material. The results, Fig. 9.4. 5., indicates a significant improvement in $\bar{R}$ value at reductions corresponding to $\bar{R}_{max}$, even though R_{45} is little affected.

Condition	Textural data after tension			R_o value
	{111} average	{100} average	T	
Standard anneal	2.72	.85	3.2	1.23
+ 150°C overage	2.90	.73	3.9	1.30
+ 200°C overage	3.06	.74	4.1	1.37
+ 300°C overage	3.34	.65	5.1	1.54

Table 9.4.1. T ratio and R_o value for annealed strip and also annealed and overaged strip; processing included cold rolling 75% to exhibit Type II texture segregation.

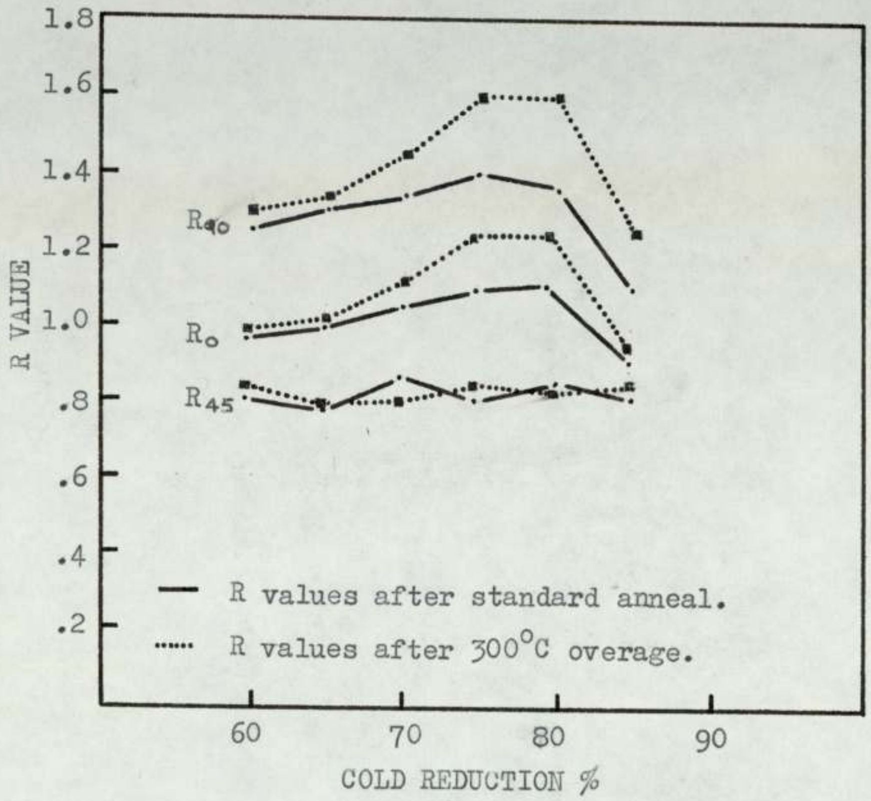

Fig. 9.4. 5. The effect of a 300°C overaging treatment subsequent to a standard anneal, upon R_0 R_{45} and R_{90} value of rimmed steel cold rolled to a range of cold reductions and to exhibit Type II texture segregation.

10. Discussion.

A preliminary textural study has been made of rimmed steel hot band, used as starting material in the present work. This was necessary since any texture resulting from commercial hot processing may influence texture development during subsequent cold rolling. The textures observed will be accounted for by applying a Kurdjumov-Sachs phase transformation to the f.c.c. pure metal textures likely to be present in the material at the hot rolling temperature of 965°C.

Four types of through thickness texture segregation have been observed in cold rolled strip and each significantly influences R value in the finished material. Each type will be discussed and an attempt made to account for the textural observations by examining the rolling conditions under which they were developed.

As R value, which is closely related to drawability, is measured after a finite strain during the tensile test, the crystal reorientation associated with tensile strain has been examined for a range of cold rolled and annealed specimens. These results will be discussed with a view to explaining the reduction in R value, of finished strip, after a critical cold reduction i.e. $R_o$max. It should, subsequently, be possible to account for the different total cold reductions at which $R_o$max occurs, depending upon the prevalent through thickness texture type. Analogies will be drawn between these results and the results obtained for the subsequent work upon the effect of inter-granular precipitates upon R value.

10.1. Hot rolled stock.

Hot rolling reductions of the order of 99% are typical during the production of rimmed steel sheet, and the possibility of texture development with its' consequent effect upon cold rolling textures cannot be overlooked.

Hot working is usually regarded as the working of a metal at a sufficiently high temperature that dynamic recrystallisation occurs. In practice, hot work refers to the rolling of steel between the extremes of temperature encountered in the strip industry, i.e. at temperatures between approximately 800°C and 1150°C. The temperature falls progressively throughout the hot rolling process and as rolling at the lower temperatures in the range have a more profound effect upon properties, it is usual to quote the temperature at the end of hot rolling, i.e. finishing temperature. The temperature range straddles the A_3 temperature and hot rolling textures can therefore be categorised into those that develop during rolling above or below this temperature.

The material used in the present experiments was rolled above the A_3 temperature when austenite is the stable phase. The through thickness pole density plots for the hot band material are illustrated in Fig.9.1. 2. A Kurdjumov-Sachs type phase transformation can be used in an analysis to account for the observed hot rolling texture segregation.

Low carbon steel at 965°C can be considered to deform as does a high stacking fault energy f.c.c. metal. Dynamic recrystallisation would inevitably occur but the hypothesis is that a weak f.c.c. pure metal texture develops exhibiting the segregation that has been observed in copper and aluminium rolled at room temperature under conditions of high friction[40].

The centre texture would then be expected to be a mixture of components $\{110\}\langle 112\rangle$ and $\{112\}\langle 111\rangle$ with the former predominating as only weak texture is envisaged. The surface texture will be a mixture of $\{100\}\langle 011\rangle$ and $\{111\}\langle 110\rangle$ orientations, the latter being most prominent when rolling under high friction conditions.

To these textures one can apply the Kurdjumov-Sachs transformation when $\{hkl\}$ planes of the parent austenite phase, γ, transform to $\{h+k, h-k, 2l\}$ planes of ferrite, α. Hence at the surface during the phase transformation:

$\{111\}_\gamma$ transforms to $\{101\}_\alpha$
$\{100\}_\gamma$ transforms to $\{110\}_\alpha$ and $\{001\}_\alpha$

$(201)_\gamma$ and $(101)_\gamma$ textures would be of low intensity in the austenite texture and therefore $(111)_\alpha$ and $(112)_\alpha$ ferrite textures are expected to be of low intensity.

At the sheet mid-plane during the phase transformation:

$\{110\}_\gamma$ transforms to $\{200\}_\alpha$ and $\{112\}_\alpha$
$\{112\}_\gamma$ transforms to $\{102\}_\alpha$ and $\{312\}_\alpha$

Furthermore, $(111)_\gamma$ and $(100)_\gamma$ austenite textures are of low intensity and therefore $\{110\}_\alpha$ will be a low intensity ferrite texture since $(111)_\gamma$ transforms to $(101)_\alpha$ and $(100)_\gamma$ transforms to $(110)_\alpha$.

The predictions of the final ferrite texture, suitably amended to allow for the original conditions of the hypothesis with regard to austenite texture components present, are listed in Table 10.1.1. The magnitude of the texture segregation is very low, ranging between .6 and 1.5 random, and therefore the descriptions 'high' and 'low' in Table 10.1.1. merely represent magnitude relative to each other.

Sheet Plane			
Surface		Centre	
high $\{110\}$	texture intensity	high $\{100\}$	texture intensity
medium $\{100\}$	"	high $\{112\}$	"
low $\{111\}$	"	medium $\{123\}$	"
low $\{112\}$	"	low $\{110\}$	"

Table 10.1. 1. A summary of predicted relative ferrite textures, at sheet mid-plane and surface plane, resulting from the phase transformation of austenite exhibiting weak texture segregation.

Low absolute texture intensity is to be expected, since dynamic recrystallisation prohibits the development of intense austenite texture. Texture intensity is also reduced further during the phase transformation, on cooling, because of the multiplicity of possible phase transformations[53].

The predicted through thickness ferrite texture is in close qualitative agreement with the measured results shown in Fig. 9.1. 2. although no explanation has, as yet, been offered for the texture discontinuity at $\Delta t/to$ of approximately .15. The 'rim' zone of the rimmed steel used in the present work also occupies about .15 of half the thickness of the strip. Consequently, it is difficult to determine if the texture discontinuity is associated with the rim zone, or is attributable to conditions at the roll-sheet interface during rolling. However, the latter is more likely, since a similar feature has been observed in cold rolled and annealed strip, Fig. 9.2.5. 3., and the depth to which it is present, in this case, is significantly variable. The presence of the texture discontinuity in the hot rolled stock is not the reason for the similar feature at the surface of material heavily cold rolled with draughts of .125 mms., although the reason for their appearance is probably related. This can be proven, since the discontinuity is lost during cold rolling to about 60% reduction, Fig. 9.2.5. 3., and only develops with further increased reduction.

The texture of steel hot rolled above the A_3 temperature has been described as $\{110\}\langle 110\rangle$ at the sheet mid-plane and $\{110\}\langle 100\rangle$ at the surface[47].

This description of mid-plane texture conflicts with the pole density data of Table 10.1.2. abstracted from the work of Thomson et al[45]. In this case the centre texture clearly cannot be described as {110}<110> as the intensity of {110} planes is of less than random intensity. The pole density results at the mid-plane of the hot band used in the present investigation, Table 10.1.3., are in very good agreement with the data in Table 10.1.2., except for the intensity of {111} texture. Both sets of results clearly show that the degree of texture segregation resulting from hot rolling above the A_3 temperature is small.

No texture segregation was evident in strip produced by cold rolling the hot band 40%. Thus hot rolling texture segregation can be disregarded in subsequent discussion as it does not contribute to texture segregation observed in heavily cold rolled strip.

10.2. The effect of draught and lubrication upon texture, and R value.

Four types of through thickness texture segregation have been observed in heavily cold rolled rimmed steel strip and have been classified as Types I, II, III and IV. Type I texture segregation was developed with very small draughts, i.e. .025 mm, and Type IV texture segregation with the heaviest draughts, i.e. 1.0 mm. The distinct characteristics of each type have been illustrated by particular reference to {111} and {100} pole density profiles and also (110) pole figures. Table 9.2.6.1. and Fig. 9.2.5.5. summarise the main features of the four types of texture, and the rolling conditions under which they were developed. Copies of the summary Table and Fig. are contained in the flap attached to the back cover of the thesis. These can be removed and referred to during discussion pertaining to texture segregation.

xyz pole	111	332	321	110	210	410	310	100	211
intensity X random	1.26	1.03	.89	.74	.61	.91	.99	1.38	1.19

Table 10.1.2. Mid-plane normal direction pole densities for hot rolled steel sheet(45).

xyz pole	111	332	321	110	210	410	310	100	211
intensity X random	.93	.98	.95	.68	.74	.90	.90	1.30	1.11

Table 10.1.3. Mid-plane normal direction pole densities for hot rolled rimmed steel sheet used in the present investigation.

The differences between the texture types are most pronounced at the free surface and reduce with depth to the mid-plane where they are all very similar. Consequently attention will be concentrated on the differences in surface texture in the succeeding discussion of the four texture types. The centre textures can be described as consisting of varying proportions of partial fibre textures $\langle 110 \rangle_{RD}$ and $\{111\}_{RP}$ depending upon the total rolling reduction considered.

Texture Type IV is a special case as the surface texture, Fig. 9.2.4. 2a., in no way resembles the normal rolling texture. Type IV texture will, therefore, be considered separately at a later stage. Within the three other texture segregations, i.e. Types I, II and III, it is proposed that there are two alternative characteristics to which all the textural observations can be attributed.

Firstly (a) there is texture heterogeneity which is primarily associated with differences in texture at the surface plane and mid-plane, but is characterised by a gradual transition from one to the other through the strip thickness. Type I texture, Fig. 9.2.5. 5., is typical of this case. (b) The second type of segregation is also associated with a distinct texture difference between strip surface plane and mid-plane. However, in this case, the transition zone from one to the other is limited to a small thickness element adjacent to the free surface. Type III texture segregation, Fig. 9.2.5. 5. is typical of this case. It will be demonstrated later that texture segregation Type II is a composite of texture segregations Type I and III.

There is considerable evidence to support the existence of the two distinctly separate types of texture segregation rather than the two cases simply being two variations of a single type. Type III segregation is more intense the heavier the draught and is reduced in intensity with increased friction, whereas Type I texture segregation is developed regardless of lubrication conditions and also of draught, provided it is kept below a maximum level. However, the difference between Type I and III texture segregation is best illustrated by superimposing the two random intensity contours of the respective surface plane (110) pole figures upon a mid-plane pole figure that is typical of both cases, Fig. 10.2. 1. Relative to the mid-plane, the two random intensity contour area for Type III texture segregation is reduced, whereas the Type I two random contour area is increased. For the surface plane this can be considered as equivalent to a reduction in $\{100\}\langle 110\rangle$ orientations in Type III texture, and an increase in $\{100\}\langle 110\rangle$ orientations for Type I texture, both relative to the common mid-plane texture. This in turn suggests a positive $\{100\}$ surface to centre texture gradient for the former case and a negative $\{100\}$ texture gradient for the latter, which is supported by the inverse pole density data of Fig. 9.2.5. 5.

The characteristics of texture segregation Types I and III are therefore sufficiently different to conclude that they are in fact developed as a result of different mechanisms.

Texture segregation Types I, II and III, as developed during cold rolling, are of more than academic interest, since the segregation is retained even after annealing, Figs. 9.2.5. 1. and 9.2.5. 2. (adjacent to page 52). The anisotropic properties of finished strip are therefore influenced by texture segregation as will be the deep drawability.

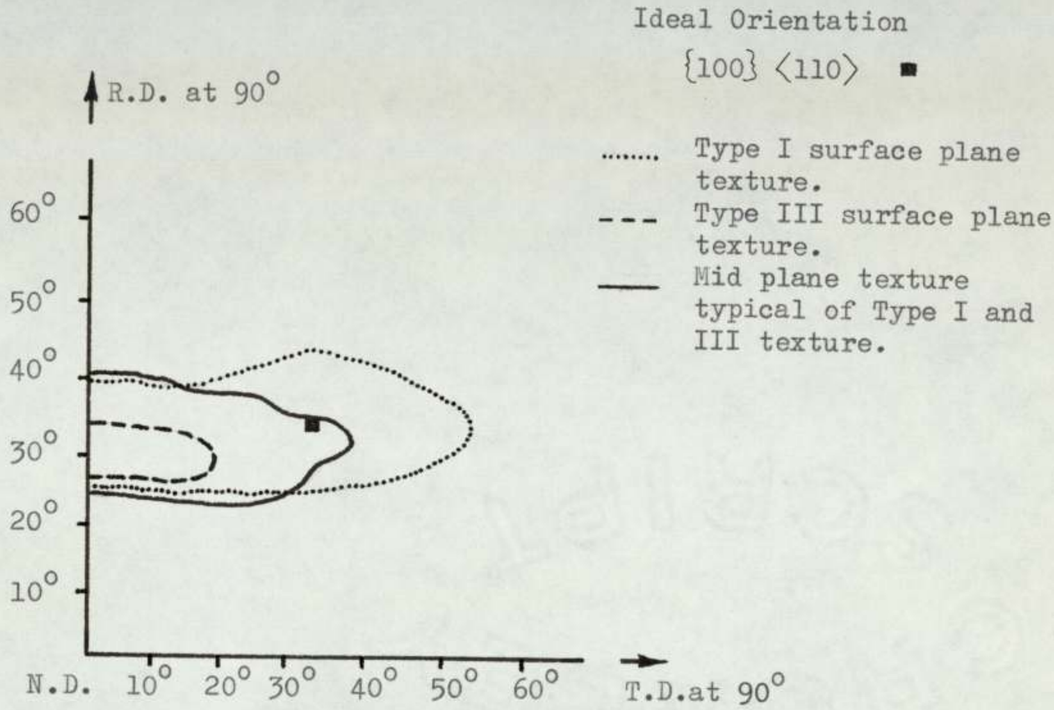

Fig. 10.2. 1. Typical mid plane (110) pole figure superimposed upon surface plane (110) pole figures for material processed to exhibit Type I and III textures. All three pole figures are for material cold rolled 80%. To enable simple comparison only the two random intensity contour is plotted.

Consequently the performance of industrially processed sheet, in deep drawing applications, will also depend upon which Type of texture is present.

A more detailed discussion of the effect of texture segregation upon R value is to be given in Section 10.3.

10.2.1. <u>The development of texture segregation Type I.</u>

Textures that develop during rolling are dependent upon the imposed stress system which in turn is controlled by the deforming mechanism. Since a gradual transition in texture from surface plane to mid-plane has been observed, and described as Type I texture segregation, the stress system imposed upon the rimmed steel during rolling must vary with depth in the strip. Moreover, the segregation is generally lamellar as plane strain rolling conditions still apply.

It is now possible to apply the Dillamore and Roberts[40] concepts for the development of texture heterogeniety in f.c.c. metals to account for texture segregation Type I in rimmed steel. They used slip line field theory for plane strain compression as a device to illustrate the relative orientation of maximum resolved shear stress axes in rolling and also the presence of the neutral point. Crane and Alexander, in discussion, were critical of this approach[41]. However, although the slip line field analogue was not entirely satisfactory, it was possible to make general observations that are applicable to rolling.

Solutions were presented for conditions of zero friction and sticking friction, Fig. 10.2.1. 1. The slip line field at the mid-plane is the same in both cases and would be the same for any conditions of friction.

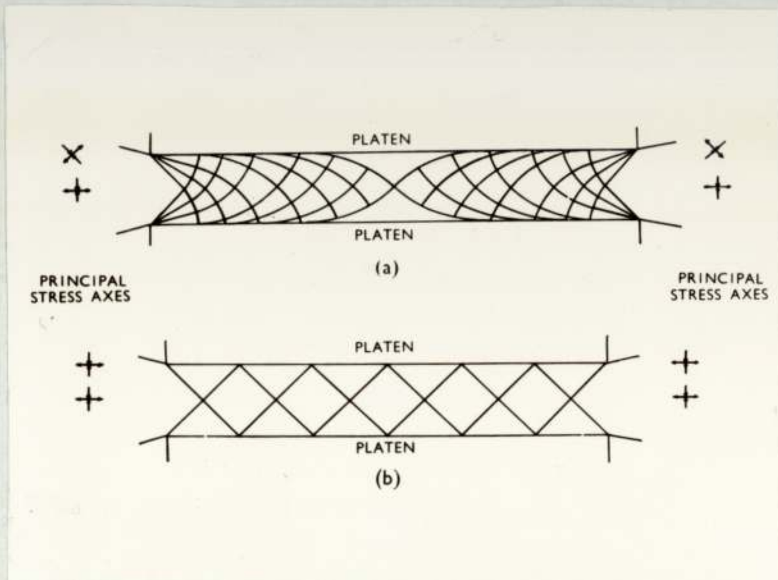

Fig. 10.2.1. 1. Slip line fields for :
(a) completely rough platens; strip thickness: platen breadth 1:6.6;
(b) zero friction; strip thickness: platen breadth 1:6.[40]
Note, for condition (a), the difference in stress axes either side of the neutral point for all planar thickness elements other than the mid-plane and surface plane.

Consequently the mid-plane texture is always developed under the same stress conditions, regardless of strip-roll interface friction conditions. Mid-plane rolling textures should, therefore, always be the same. This is as observed in the present work. Under both extreme conditions of friction the stress system at the surface is not altered on passing through the neutral point. For material between surface and centre, the stress system on the exit side of the neutral point is a mirror image of the stress system on the entry side, i.e. the plane normal to the rolling direction is a mirror image plane. However, as depicted by the principal stress axes in Fig. 10.2.1. 1a, the stress systems are not equal. This will also be the case from the extreme surface plane to planes adjacent to the mid-plane, for friction conditions intermediate between the two extremes. Thus, for intermediate friction conditions, an additional stability condition is imposed upon end orientations for all thickness elements relative to the mid-plane zone. This is that the texture must be stable under both orientations of the stress system.

Type I texture segregation was developed when rolling was performed under intermediate friction conditions. This corresponds to the plane strain compression slip line field analogue for intermediate friction conditions. Thus, at the surface plane during rolling, orientations developed on the entry side of the neutral point must present a mirror image plane normal to the rolling direction to be stable on passing through the exit side of the neutral point. That is, the end orientation must be stable under both orientations of the slip line field, which is only so if the $\{xyz\}$ plane of the orientation $\{uvw\}\langle xyz\rangle$ is a mirror image plane.

The mid-plane textures observed in the present work are described as consisting of orientations $\{111\}_{RP}$ and $\langle 110\rangle_{RD}$, Table 9.2.6. 1. All components of the $\langle 110\rangle_{RD}$ partial fibre texture present a mirror plane normal to the rolling direction, Fig. 10.2.1. 2a. and are, therefore, expected to be stable orientations through the strip thickness. However, no orientations of the $\{111\}_{RP}$ partial fibre texture, with the exception of the component $\{111\}\langle 110\rangle$ which is common to both partial fibre textures, have this mirror plane relationship, Fig.10.2.1.2b. Therefore, the $\{111\}_{RP}$ partial fibre texture, (except for the component $\{111\}\langle 110\rangle$), will not be stable at the surface plane. Consequently, the intensity of $\{111\}$ texture is expected to be reduced at the surface plane relative to the mid-plane. The $\{111\}$ texture will be replaced by orientations that display the requisite mirror plane relationship. In this case it is predominantly $\{100\}\langle 110\rangle$ texture.

The major component of the $\{111\}_{RP}$ partial fibre texture other than $\{111\}\langle 110\rangle$ is $\{111\}\langle 112\rangle$. Therefore texture segregation Type I could be described as being attributed to the presence of $\{111\}\langle 112\rangle$ texture at the mid-plane, with a gradual transition to its' total absence at the surface plane.

The above account of the reason for texture segregation is satisfactory for Type I textures, but makes no provision for the transition to Types II and III texture segregation when rolling draughts of .125 mm. and .500 mm. are used. To account for this change in texture type, a second condition needs to be invoked.

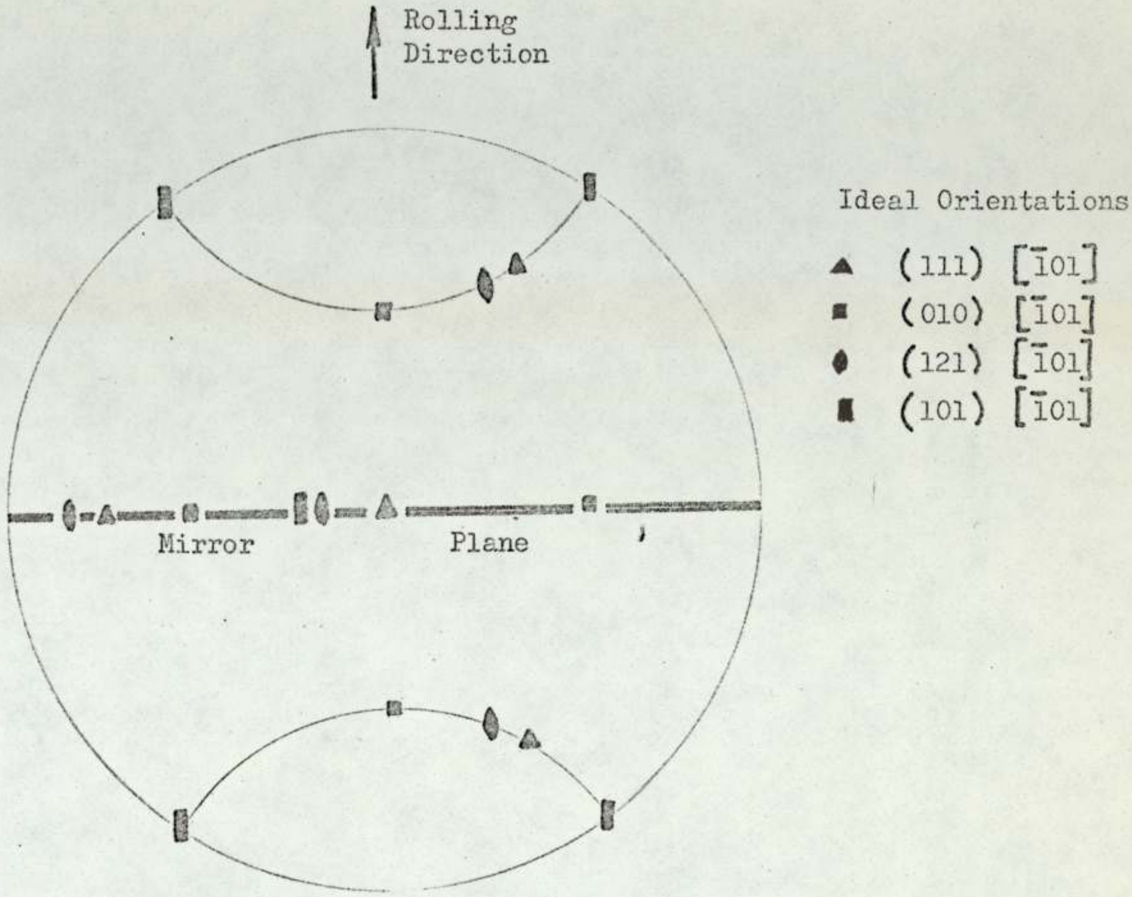

Fig. 10.2.1.1a. Stereographic projection showing locus of (111) poles for $\langle 110 \rangle_{RD}$ partial fibre rolling texture. Stable orientation must present a mirror image plane normal to the rolling direction. All components of the $\langle 110 \rangle_{RD}$ texture fulfil this condition.

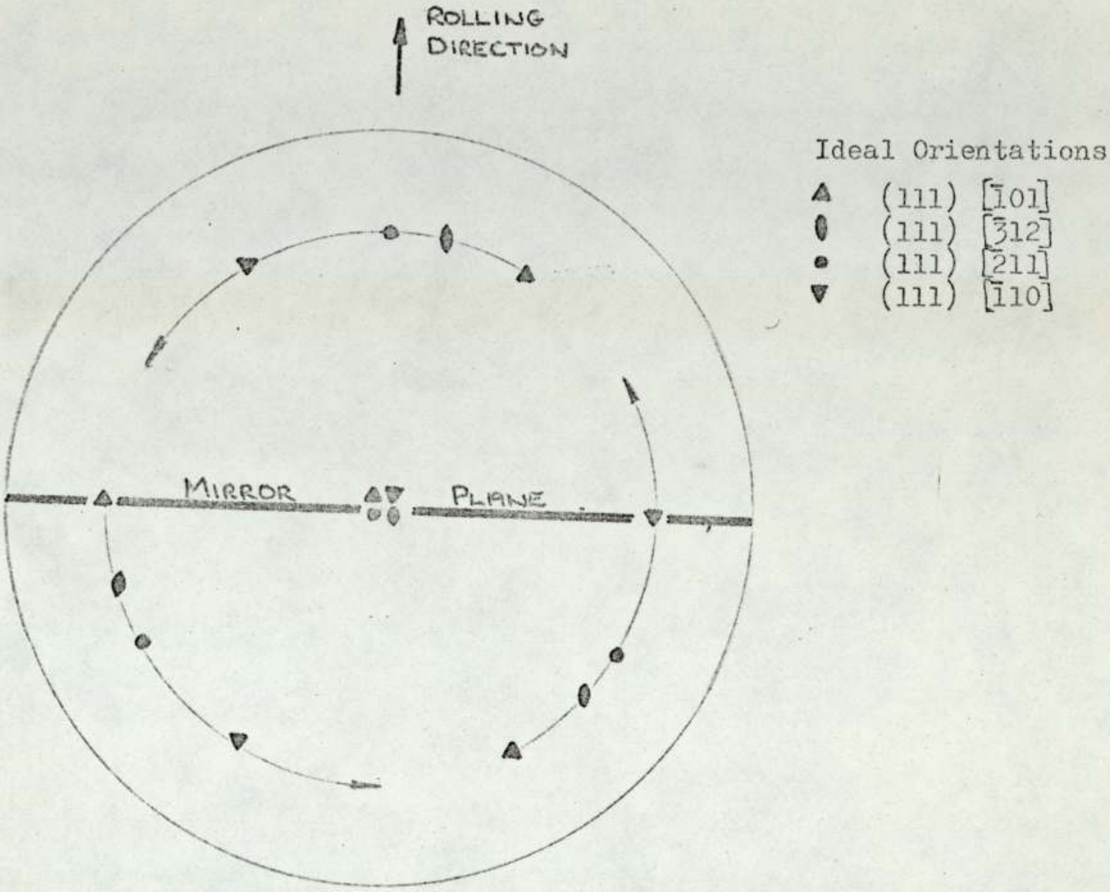

Fig. 10.2.1. 2b (111) projection showing locus of (111) poles for $\{111\}_{RP}$ partial fibre texture. Stable orientations must present a mirror image plane normal to the rolling direction. Only components of the type $\{111\}\langle 110\rangle$ fulfil this condition.

Obviously the mirror image stability condition cannot be applicable if the deformation conditions in the roll gap are such that very little deformation occurs on the exit side of the neutral point. It is also probable that the more equal the deformation on either side of the neutral point, at each rolling pass, the more significant will be the mirror image stability condition.

The amount of deformation on the exit side of the neutral point can be defined as[40]:

$$K = 50\text{-}100 \left[\frac{1}{\mu} \quad \frac{\Delta h}{2D}^{\frac{1}{2}} - \frac{1}{\mu^2} \cdot \frac{\Delta h}{4D} \right] \ldots\ldots\ldots \; 10.2.1.\ 1.$$

where K is the percentage deformation per pass occurring after the neutral point, μ is the coefficient of friction Δh is the draught, and D is the roll diameter. K values for the three rolling draughts used to develop Types I, II and III textures with a roll diameter of 150 mm. and coefficient of friction of .1 are shown in Table 10.2.1. 1. Deformation is most nearly equal either side of the neutral point for draughts of .025 mm. and most unequal for draughts of .500 mm. Therefore, Type I texture segregation is to be expected with 'light' draughts but not with 'heavy' draughts. This is precisely as observed in the present work.

10.2.2. The development of texture segregation Type III.

When rolling with large draughts (.500mm) the majority of the deformation at each pass occurs on the entry side of the neutral point, Table 10.2.1. 1. Therefore, the mirror plane condition for stable orientations does not apply and the texture will consequently be expected to be constant from surface plane to mid-plane, provided the friction conditions do not approach sticking friction.

Rolling draught mm.	% Deformation after neutral point, K. equ. 10.2.1.1.	Texture Type
.025	41	I
.125	32	II
.500	18	III

Table 10.2.1.1. K value calculated for three rolling draughts. Note that K as defined in equation 10.2.1.1. is constant for a given draught regardless of the strips initial thickness or percentage reduction. However, the absolute value of K increases progressively with increase in total percentage reduction when draught is maintained constant.

If sticking friction conditions were approached, an entirely new texture would be developed at the surface plane.

Type III textures are essentially homogeneous, which is as expected since rolling draughts of .500 mm. were used, except for the heterogeneity in the extreme surface planes. It has previously been stated that this heterogeneity results from an entirely different mechanism to that responsible for Type I texture segregation, since Type III texture is attributable to a reduction in texture intensity at the surface plane rather than a change in texture components, as is the case for Type I textures. At the present time, no explanation can be offered for the reduction in texture intensity at the surface plane for Type III textures. It has previously been attributed to the 'folding over of surface asperities'(37), but if this be so then it is difficult to appreciate why the 'effect' should be less pronounced with dry rolling. (Compare Type III texture of Fig.9.2.5.5. with Fig.9.2.3.3. The latter Fig. is adjacent to page 49).

10.2.3. <u>The development of texture segregation Type II.</u>

Texture segregation Type II, Fig. 9.2.5.5. and Table 9.2.6.1., can be divided into two parts. There is an initial thickness element which is characterised by a positive gradient in the $\{111\}$ texture profile and a corresponding negative gradient in $\{100\}$ texture versus $\Delta t/t_o$. This segregation is similar to that at the surface elements of Type III textures although the severity of the segregation is considerably reduced. Further evidence for this conclusion can be obtained from the similarity of the effect of lubrication upon the surface texture in both cases.

Dry rolling greatly reduces the texture segregation for Type III textures, Fig. 9.2.3. 3., and eliminates the initial peak in $\{111\}$ texture intensity for Type II textures, Fig. 9.2.2. 3.

The similarity between Type II textures, after $\Delta t/t_o$ of approximately .4, and Type I textures, is readily apparent from examination of Fig. 9.2.5.5. Therefore, although the satisfactory interpretation of texture heterogeneity is complicated by the relatively low intensity of segregation, Type II texture is clearly a composite of Type I and Type III texture.

Type II texture is comprised of a surface zone that resembles Type III surface texture segregation and a zone between $\Delta t/t_o$ equals .4 and the mid-plane that resembles Type I texture segregation. The thickness element in between these two zones is thus the transformation zone from one Type to the other.

The magnitude of texture segregation Type II reaches a maximum at 80% reduction and then decreases in intensity. This is illustrated in the plot of S, which is a parameter defining the intensity of texture segregation, as a function of total reduction, Fig. 9.2.5.4., page 52. The reduction in S after 80% reduction can be predominantly attributed to a reduction in the Type I component part of Type II texture segregation. Type I texture segregation is due to the segregation of $\{111\}_{RP}$ partial fibre texture (with the exception of component $\{111\}\langle 110\rangle$), and has been attributed to the fraction of deformation at each rolling pass, being approximately equal either side of the neutral point.

It has further been shown that this fraction is constant for a constant draught, equation 10.2.1. 1., other factors being equal, regardless of strip thickness. Consequently, texture segregation should continually increase in magnitude with increase in rolling reduction. The reason for this apparent anomaly can be found by examining the stable texture at the sheet mid-plane. Obviously $\{111\}_{RP}$ partial fibre texture must be present at the mid-plane before it can be segregated between mid-plane and surface plane. It is an important component of the mid-plane texture up to 80% cold reduction, Fig. 9.2.1. 3., page 45, but at higher reductions, Fig. 9.2.4. 2b., page 50, is a considerably less important component. Consequently, the magnitude of texture segregation Type II is reduced after 80% cold reduction.

Vandermeer and Ogles[37] observed texture segregation in rolled niobium strip. It was illustrated by reference to (110) pole figures. A graph of (110) pole intensity at angle ϕ, 33° from the sheet normal direction and 57° from the rolling direction, was plotted against $\Delta t / 2t_o$ Fig. 10.2.3. 1. The shape of this graph is similar to that for the $\{111\}$ through thickness texture contours in the present work for material exhibiting Type II textures, Fig. 9.2.5. 5. The peak intensity in the b.c.c. metal rolling texture at ϕ angles of 33° is, as already outlined in Section 9.2.1. the result of $\{111\}\langle 112\rangle$ texture and, to a lesser extent, $\{112\}\langle 110\rangle$ texture. Consequently, the plot of ϕ peak intensity versus $\Delta t / 2t_o$ can be considered as a $\{111\}\langle 112\rangle$ through thickness texture plot.

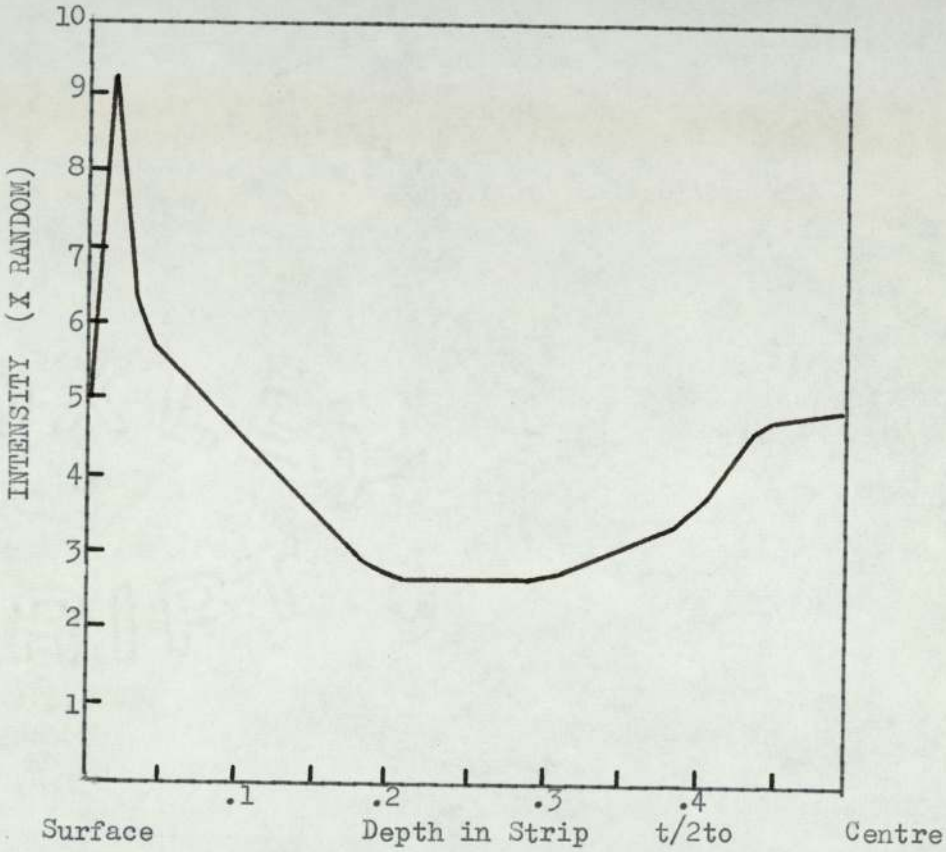

Fig. 10.2.3. 1. X-ray intensity at angle ϕ, 33° from the rolling plane normal along the N.D. to R.D. radius of (110) pole figures, versus strip depth for a niobium specimen cold rolled 70%. Strip depth is plotted as a function of half the original thickness i.e. t/2to [37].

Thus because of the similarity with the {111} through thickness profiles of the present work, Fig. 10.2.3. 1. is indicative of texture segregation Type II in niobium.

Vandermeer and Ogles observed the dependence of texture segregation Type II upon the geometry of deformation and also noted that it was reduced in intensity after a critical cold reduction. The segregation observed was related to $1/t_m$, as defined in equation 5.1. (page 27), which is a parameter defining the geometry of deformation. With $1/t_m$ values greater than 1.0, Type II segregation was considerably reduced in intensity. In the present work, as a constant draught was used, $1/t_m$ increases progressively with total reduction, Table 10.2.3. 1. Therefore, the reduction in segregation in rimmed steel could also be associated with a critical $1/t_m$ value although for steel it is approximately 3.0 and not 1.0 as with niobium. However, since Vandermeer and Ogles used small draughts, the significance of K value as hypothesised in the present work, is equally applicable to the results for niobium. Therefore, is it K value or $1/t_m$ value that is important in controlling the magnitude of texture segregation Type II? The evidence supports K value since using this analysis the textural observations can be completely accounted for, whereas although Type II segregation has been associated with $1/t_m$ [37], no satisfactory explanation was given.

The intensity of texture segregation observed in niobium[37] was far greater than in the present work with rimmed steel.

Thickness of strip mm.	1/tm equ.5.1	Total reduction %
4.750 4.65	.58	2
2.15	1.4	55
1.90	1.6	60
1.40	2.1	70
1.025	2.8	80
.475	5.5	90

Table 10.2.3. 1. 1/tm values[37] at selected passes during the cold rolling of rimmed steel; after the first pass, draught was maintained constant at .125 mm.

$$1/tm = R^{\frac{1}{2}} \frac{(ta - tb)^{\frac{1}{2}}}{(ta + tb)/2}$$

where l is the length in the rolling direction of the geometrical zone of deformation, tm is the average thickness of the zone, R is the radius of the work rolls, and ta and tb are the entry and exit thicknesses of the strip respectively.

However the rolled niobium strip was only 18.75 mm. wide and originally 10 mm. thick. Consequently conditions near to plane stress would apply over a significant area of the strip. Similar conditions apply at the extreme edges of wide strip. Therefore, to test if the intensity of texture segregation Type II is affected by strip width textural measurements were made across the full width of 150 mm. wide strip. The extent of segregation was found to be consistent across the full width except for the extreme edges. However, the intensity of segregation was reduced in this area, Fig. 9.2.2. 5. It is therefore concluded that the low intensity of texture segregation Type II for rimmed steel relative to niobium is not due to the use of wide strip in the former case. Since the segregation is related to the presence or absence of $\{111\}_{RP}$ texture it is possible that this texture is a stronger component of the niobium rolling texture than rimmed steel rolling texture.

10.2.4. <u>General comments on texture segregation Types I, II and III.</u>

The previous observations and discussion of texture segregation Types I, II and III are of interest with regard to the theories[2] presently devised to explain rolling texture formation in b.c.c. iron. It is evident from the present results that workers must make textural examinations at the same depth in rolled strip if similar rolling textures are to be consistently observed. For example, the texture component $\{100\}\langle 110\rangle$ is often quoted as being at the centre of the orientation spread of b.c.c. metal rolling textures. The present work however, clearly indicates that the presence of this orientation can be significantly affected by rolling draught and under certain conditions is strip depth dependent (compare Figs. 9.2.1. 3a. and 9.2.1. 3b.) A suitable plane that will yield consistent results regardless of rolling conditions is the strip mid-plane.

Previous workers have reported that partial fibre texture $\{111\}_{RP}$, becomes less pronounced in rolling textures after about 60% total reduction. The theory used in the present work to account for texture segregation leads to the conclusion that this fibre texture will not become absent at one critical total reduction, since rolling conditions will modify it, particularly at or close to the surface plane of the sheet. Thus the critical reduction will be at relatively low values for Type I rolling conditions, as $\{111\}_{RP}$ partial fibre texture is considered unstable in this case at all reductions, and higher values for Type III rolling conditions.

10.2.5. <u>The development of Texture segregation Type IV.</u>

The surface texture of Type IV segregation can be described as consisting of orientations $\{110\}\langle xyz\rangle$, where $\langle xyz\rangle$ ranges between $\langle 001\rangle$ and $\langle 111\rangle$ directions, Fig.9.2.4. 2a. It is therefore similar to the surface textures observed by Stickels[6] in iron, and Vandermeer and Ogles in niobium[37], and equivalent to reported shear textures[38,39]. Type IV surface texture has previously been described as a shear texture resulting from roll friction[6]. The need for high roll friction is confirmed in the present work as it was necessary to degrease and dust the rolls with magnesia before it was possible to develop the texture.

Vandermeer and Ogles related the presence of Type IV texture segregation to percentage reduction per pass and noted that a critical value was necessary. A draught of 1.0 mm. was used during the first pass, in the present work, although it was thereafter progressively reduced finally to about .25 mm. during the last pass, because of the limitations of the mill used. There was evidence of Type IV texture segregation when the reduction per pass reached 35% at 77% total reduction, but was not particularly marked until 88% total reduction, Table 9.2.4.1.

The results in Table 9.2.4.1.lead to two conclusions. Firstly, the incidence of Type IV texture segregation cannot be simply related to draught as even when rolling with constant draughts or, as in the present case, reducing draughts, heavy total reductions are necessary. Secondly, there is no simple relationship between Type IV texture segregation and percentage reduction per pass as an approximately constant percentage reduction per pass was used over the range of total reductions. Consequently, the Vandermeer and Ogles criterion for the development of Type IV texture in niobium is not so simply applicable to rimmed steel. Evidently total rolling reduction is also an important condition to be considered. For rimmed steel and the mill used in the present work, the critical rolling reduction to be exceeded was 88%.

Increasing total reduction, even with a constant reduction per pass, increases the roll pressure necessary to achieve the next roll pass because of work hardening. Thus friction forces at the roll-strip interface will increase proportionately, and Type IV texture segregation is more likely developed.

If Type IV surface texture is a result of simple shear then the shear strength of the metal has, of necessity, to be exceeded during rolling. The shear strength of metals, will, like other properties, differ. Consequently, critical rolling conditions will differ from metal to metal. From this point of view, as the surface of strip is being mainly considered, rimmed steel and aluminium killed steels can be considered as different metals since the outer skin of the former is practically pure iron, as the majority of the solute elements are concentrated in the 'core' zone. There is therefore little to be gained by comparing the critical rolling condition established by other workers with the present results, as results are not only likely to differ from metal to metal, but also from mill to mill. However, it can be said that 'heavy' draughts, 'heavy' reductions per pass, high total reductions and high friction conditions are necessary to establish Type IV texture segregation.

Like Type I, II and III texture segregation, the development of Type IV texture segregation is of considerable technological significance, from the point of view of drawability, since this segregation is also retained after annealing, although of reduced intensity. The segregation leads to material with very low R values. It is, nevertheless, impossible to determine in the laboratory if this could be a problem in commercially processed strip, since the rolling conditions needed to develop Type IV texture are so critical. Therefore, strip processed on individual industrial mills would have to be examined and each case assessed separately.

10.3. The effect of total rolling reduction upon texture and R value.

The results of the present investigation confirm those of earlier workers, reviewed in Section 6, in that it has been established that R_{max} can be related to a maximum value in the texture ratio $\{111\} / \{100\}$. However, in the present work an average through thickness $\{111\} / \{100\}$ ratio, i.e. T ratio, was used to avoid the difficulty arising from materials exhibiting texture segregation. The critical reduction corresponding to R_{max} is now shown to be variable and dependent upon the type of texture segregation generated during cold rolling, Fig. 9.3.1. It is the primary objective, within this part of the thesis, to present an explanation for this phenomenon based, primarily, on the analyses of pole figure data. Furthermore, due regard will be given to the effect of tensile strain upon textured strip. This is important since R value is measured in the uniaxial tensile test.

Two important mid-plane textural observations have been noted in material exhibiting Type II texture segregation. Firstly, annealing texture changes progressively from $\{111\}_{RP} + \langle 110\rangle_{RD}$ components to the single $\langle 110\rangle_{RD}$ component with increasing rolling reduction prior to the annealing treatment. Furthermore, R_{omax} coincides with a reduction at which there is a distinct change from $\{111\}_{RP} + \langle 110\rangle_{RD}$

texture to $\langle 110 \rangle_{RD}$ texture, Fig. 10.3.1a.

Secondly, the behaviour of strip to tensile strain, as manifest by crystal reorientation, is markedly influenced according to which of these textures is present and also the 'sharpness' of the texture. This is illustrated by reference to (110) mid-plane pole figures before and after tensile strain, Fig. 9.3.4. and Fig. 9.3.6. The effect is further characterised by a greater reduction in T ratio, $\{111\}/\{100\}$, with tensile strain, for materials exhibiting $\langle 110 \rangle_{RD}$ texture as compared to materials exhibiting $\{111\}_{RP} + \langle 110 \rangle_{RD}$ texture.

During tensile strain of randomly oriented b.c.c. metals, $\langle 110 \rangle$ crystallographic directions tend to align parallel to the tension axis[54]. The planes of the $\langle 110 \rangle$ zone axis align randomly with respect to any reference plane. Thus, using the plane of the strip as a reference plane, the T ratio will tend to a value of 1.5. This value is achieved by dividing the ratio of $\{111\}$ planes to $\{100\}$ planes in the $\langle 110 \rangle$ zone axis by the ratio of their multiplicity factors.

i.e. for a texture with $\langle 110 \rangle$ directions parallel to the tension axis:

ratio of $\{111\}$ planes to $\{100\}$ planes = 2:1

and ratio of $\{111\}$ to $\{100\}$ multiplicity factors = 4:3

Therefore T ratio = $(2/1) \div (4/3) = 1.5$

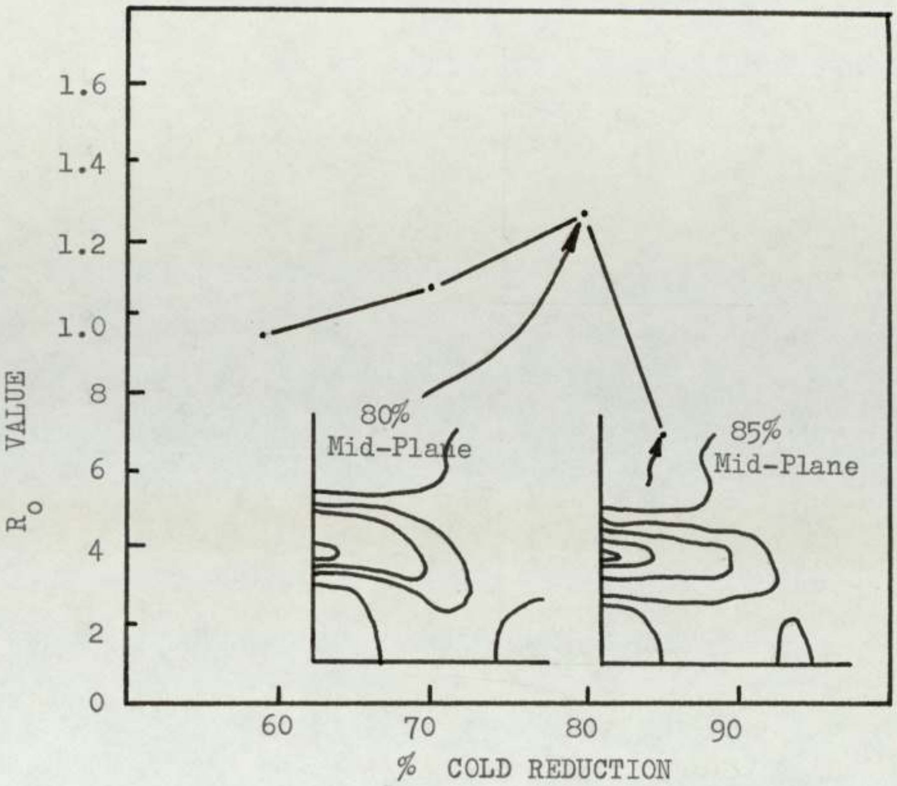

Fig. 10.3.1.a. R_o value versus % cold reduction for material exhibiting Type II texture segregation. Superimposed upon the graph are (110) mid-plane pole figures for 80 and 85% cold rolled and annealed strip. This diagram is a composite of Figs. 9.3.3., 9.3.4a and 9.3.6a.

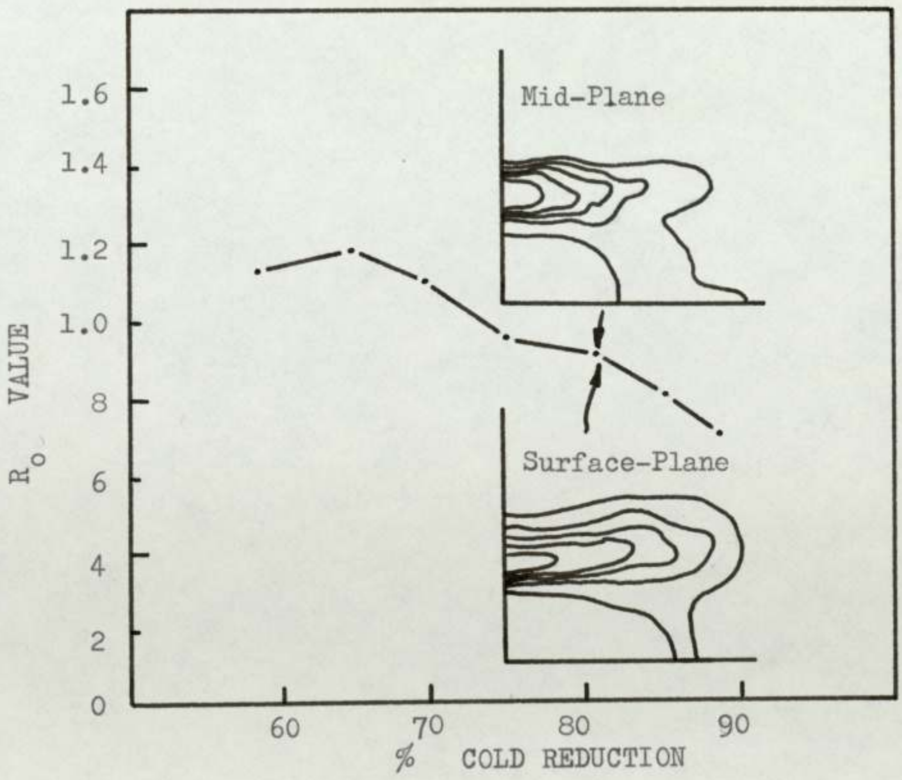

Fig. 10.3.1b. R_o value versus % cold reduction for material exhibiting Type I texture segregation. Superimposed upon the graph are (110) mid-plane and surface plane pole figures for 80% cold rolled strip. This diagram is a composite of part of Fig. 9.3.1. and Fig. 9.2.1.3.

This value of 1.5 is significantly less than is encountered in annealed unstrained strip. Consequently it is to be expected that T ratio will decrease with tensile strain. However, it is not so evident why materials with $\langle 110 \rangle_{RD}$ texture lead to a greater reduction in T ratio than do materials with $\{111\}_{RP}$ texture. As $\langle 111 \rangle$ slip directions are symmetrically disposed about the tension axis $\langle 110 \rangle_{RD}$ texture should be stable. Nevertheless, it has been experimentally observed that although the $\langle 110 \rangle$ tension axis is maintained and even intensified, the planes of the $\langle 110 \rangle$ zone axis are not stable. During tensile strain $\{111\}$ planes are decreased in intensity and $\{100\}$ planes increased in intensity.

It has been shown[18] that R value can be computed for b.c.c.iron using the relationship :

$$R = \cos\Theta \;/\; \cos\phi$$

where Θ is the angle between the operative slip direction and strip width direction and ϕ is the angle between the operative slip direction and strip thickness direction, Fig. 10.3.2.

This gives R_o values for $\{111\}_{RP}$ and $\langle 110 \rangle_{RD}$ texture components as illustrated in Fig. 10.3.3. $\{111\}_{RP}$ texture clearly will result in high R_o values irrespective of the predominant orientations of the $\{111\}_{RP}$ texture. For $\langle 110 \rangle_{RD}$ texture R_o varies between zero and infinity dependent upon the components present. However, the most prominent orientations are between $\{001\}$ and $\{111\}$. Furthermore, during tensile strain, the ratio of $\{001\}$ orientations to $\{111\}$ orientations is increased.

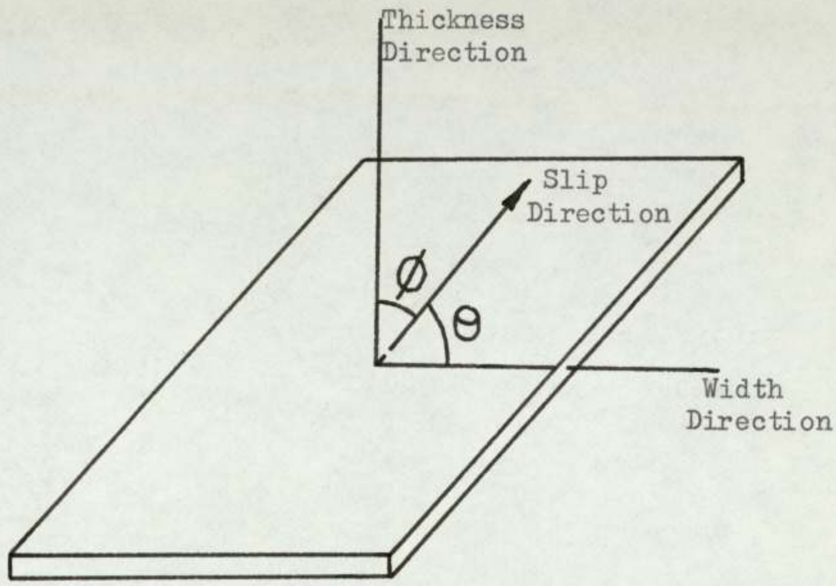

Fig. 10.3.2. Section of tensile test piece showing angular relationship between operative ⟨111⟩ slip direction and strip thickness and width direction.

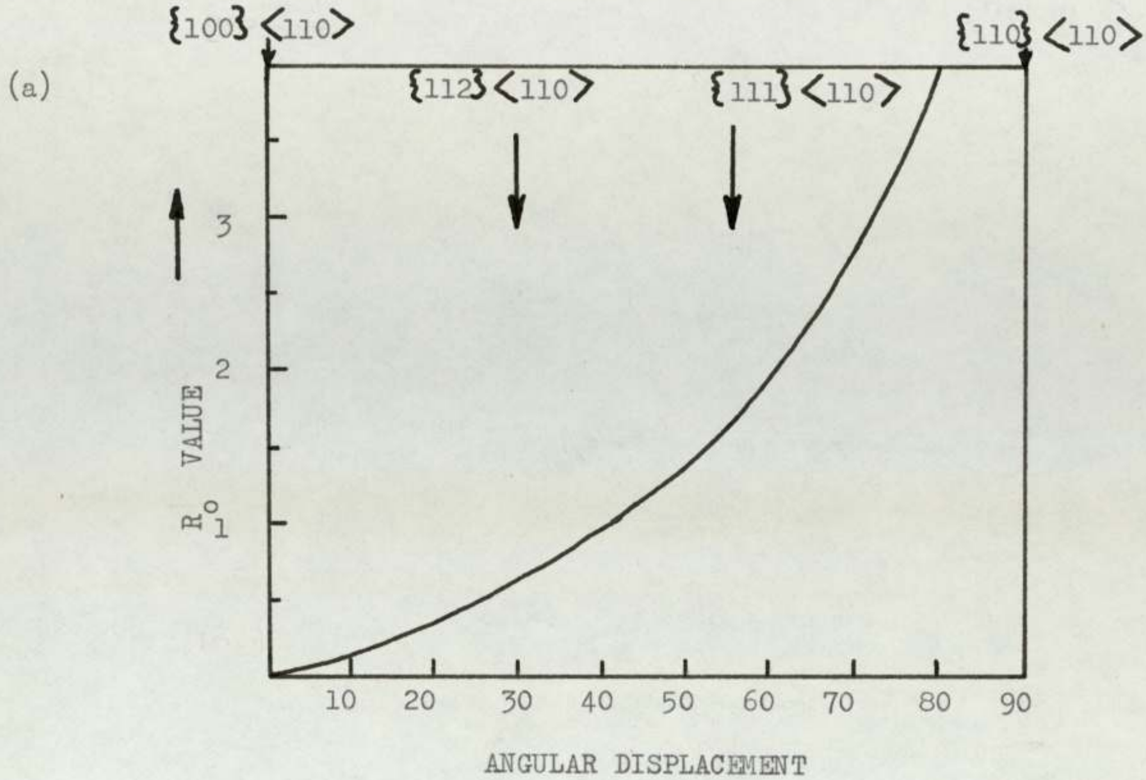

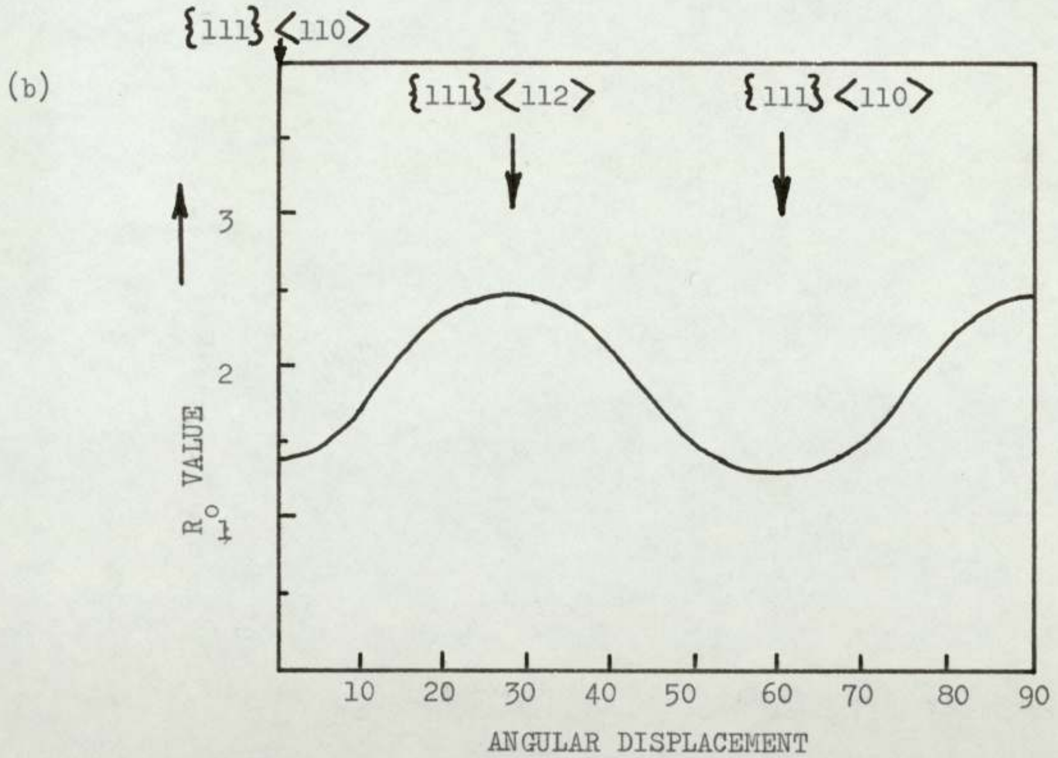

Fig. 10.3.3. Variation in calculated R_o value for angular displacement; (a) about <110> axis of {100} <110> texture (b) about <111> axis of {111} <110> texture.

Consequently low R_o values will result for materials exhibiting $\langle 110 \rangle_{RD}$ texture or a predominance of $\langle 110 \rangle_{RD}$ texture. Thus, R_{omax} can be explained on the basis that R increases with increase in proportion of the $\{111\}_{RP}$ texture and decreases with increase in proportion of the $\langle 110 \rangle_{RD}$ texture. Since the $\langle 110 \rangle_{RD}$ texture becomes predominant at high reductions, then R value increases to a maximum at a reduction when the increase due to $\{111\}_{RP}$ texture development is in balance with the decrease due to $\langle 110 \rangle_{RD}$ texture development.

The importance of the development of $\{111\}_{RP}$ and $\langle 110 \rangle_{RD}$ annealing texture and subsequent effect upon R value can now be used to account for the different reductions at which R_{omax} occurs for materials exhibiting either Types I, II or III texture segregation, Fig. 9.3.1. As previously indicated, texture segregation is primarily the result of different textures being produced, during rolling, at strip mid-plane and surface plane. Fig. 10.3.1a. illustrates the progressive variation in R_o value with cold reduction and the (110) mid-plane pole figures for 80 and 85% reductions corresponding to R_{omax} and 5% greater than R_{omax} respectively. The equivalent surface plane pole figures would be very similar since Type II textures are being considered. Fig. 10.3.1b. illustrates, for material exhibiting Type I textures, the progressive variation in R_o value and the (110) mid-plane and surface plane pole figures for 80% cold reductions only.

It is important to note that in this case, cold rolling textures are illustrated, whereas in Fig. 10.3.1a. cold rolled and annealed textures are illustrated. However, it has previously been indicated that, apart from differences in texture intensity, rolling and annealing textures are very similar, Fig. 9.2.5.1. The surface plane pole figure for 80% cold rolled material exhibiting Type I texture segregation is comparable with the mid-plane pole figure for 85% cold rolled material exhibiting Type II texture. Both pole figures were described in previous sections (Sections 9.2.1. and 9.3.) as being mainly comprised of $\langle 110 \rangle_{RD}$ orientations. Consequently, it is the presence of this orientation in the surface planes that lead to relatively low R values for material exhibiting Type I textures. Thus, the textures of particular importance, from the point of view of R value, are $\{111\}_{RP}$ and $\langle 110 \rangle_{RD}$ at the mid-plane and also the progressive development of $\langle 110 \rangle_{RD}$ texture at the surface plane. Since surface plane $\langle 110 \rangle_{RD}$ texture develops at lower reduction than mid-plane $\langle 110 \rangle_{RD}$ texture for Type I textures relative to Type II textures R_{omax} occurs at correspondingly lower reductions.

Type II segregation is a composite of Types I and III, and therefore, material exhibiting Type III texture segregation is expected to result in R_{omax} after higher percentage cold reductions, than material exhibiting Type II textures.

Since it is commercially desirable to 'delay' the onset of R_{max}, rolling conditions that lead to Type III, rather than Type I texture segregation, are desirable. In the commercial production of rimmed steel strip or sheet, the cold rolling reduction is selected to result in a specific range of properties. For example, a cold rolling reduction of 70% will ultimately lead to satisfactory grain size and R value. To reduce production costs the rolling is completed in a minimum number of passes. A typical plant would, therefore, include a three tandem mill. Consequently, the rolling is performed with heavy draughts. Work rolls of 500 mm. are common which, in conjunction with lubrication and 'moderate' draughts of .5 mm., will lead to K values (see equation 10.2.1. 1.) of the order of 5%. Type III textures are therefore likely to be developed during the commercial production of rimmed steel sheet.
Thus, from the point of view of drawability, the best rolling conditions are probably currently being used in commercial plants.

10.4. <u>The effect of intragranular precipitates upon R value.</u>

In the preceding section, the reduction in R value after a critical cold reduction was attributed to a change in the relative proportions of $\{111\}_{RP}$ and $\langle 110\rangle_{RD}$ partial fibre textures, Fig. 10.3.3. The cold reduction at which the 'inferior' texture $\langle 110\rangle_{RD}$ became predominant, was dependent upon cold rolling conditions prior to the final anneal. Since R value begins to reduce with cold reduction at a critical reduction, the change over point is precisely determinable.

To test if non crystallographic features could influence the critical cold reduction at which R_{omax} occurs, an experiment was undertaken to examine the effect of intragranular precipitates upon R value.

The three important observations associated with precipitate interaction upon R_o value are :

(i) The improvement in R_o value by precipitates is limited to the cold reductions close to those at which R_{omax} occurs, Fig. 9.4.2. The mechanism by which R_o value is improved is therefore probably connected with the mechanism causing the reduction in R_o value after R_{omax}.

(ii) Increasing the size and dispersion of precipitates results in further R value improvement, at least within the range studied.

(iii) The T ratio, was reduced less, during tensile strain for the overaged material than for the material having undergone the standard anneal, Table 9.4.1.

As there was no perceptible difference between(110) pole figures for the strained materials, an explanation for the precipitate effect is deduced from the inverse pole density data. $\{111\}_{RP}$ partial fibre texture leads to small reductions in T ratio with tensile strain and $\langle 110 \rangle_{RD}$ partial fibre texture to large changes in T ratio. Small reductions in T ratio after tensile strain are associated with low R values and vice-versa. The effect of precipitates upon crystal reorientation can thus be considered as equivalent to prohibiting the detrimental rotation associated with the $\langle 110 \rangle_{RD}$ component of the recrystallisation texture.

Thus precipitates are only effective when $\langle 110 \rangle_{RD}$ texture is significantly represented in the recrystallisation texture, i.e. after cold reductions greater than about 70%. Furthermore, results would indicate that the precipitates cannot influence $\langle 110 \rangle_{RD}$ texture if it is the only significant texture component present, i.e. after cold reductions greater than about 80%.

Leisner et al[49] have reported upon the effect of alumina particles upon wi~~ø~~re drawing textures. With particle sizes of .05μ $\{100\}$ textures were developed, whereas with particle sizes between 1μ and 25μ $\{111\}$ + $\{100\}$ textures were produced. They also noted that with large volume fractions (10 volume percent) of the larger particles, a random texture was developed, i.e. the random orientation of crystals present before drawing was maintained. In this work large precipitates of cementite, of 1μ size, tend to modify deformation during tensile strain also, so that there is a greater tendency to maintain the crystal orientation in existence before tensile strain. However, the phenomenon is only evident under the special circumstances as outlined above.

Adams and Bevan[55] questioned the possibility of replacing batch annealing by the continuous annealing of deep drawing quality rimmed steel because of the potential cost reductions. They foresaw two problems that would need to be overcome. Firstly, a long soaking period was necessary to obtain optimum finished grain sizes and secondly, a very slow cooling rate to obtain satisfactory aging characteristics. It is not the object of this work to review such possibilities, but an overaging treatment of 300°C for one hour was proposed as an effective means of overcoming the latter problem[56].

This is, of course, equivalent to one of the overaging treatments used in the present work. Consequently, such a heat treatment if incorporated into a future continuous annealing cycle would give the significant bonus of an improved R value.

11. Summary and Conclusions.

(i) The intensity of texture segregation in rimmed steel hot rolled at 965°C and coiled at 683°C is relatively low but can be accounted for by an analysis applying a Kurdjumov-Sachs type transformation to an f.c.c. pure metal texture exhibiting segregation.

(ii) Four types of through thickness texture segregation have been observed in cold rolled rimmed steel. They have been categorised according to the rolling draughts used. Type I textures were developed with draughts of less than .025 mm., Type II textures with draughts of .125 mm., Type III textures with draughts of .500 mm., and Type IV textures with draughts of greater than .500 mm. Generally, the major characteristic of all four types of segregation is a significant through thickness $\{111\}$ and $\{100\}$ texture variation.

The normal rolling texture[2] was observed at the strip mid-plane in each case and has been described as $\langle 110 \rangle_{RD}$ + $\{111\}_{RP}$ partial fibre textures, although the relative proportion of the two components depend upon the total reduction considered. Texture segregation is associated with deviation from this rolling texture through the strip.

(a) The presence or absence of partial fibre texture $\{111\}_{RP}$, at planes other than the sheet mid-plane, has been shown to be dependent upon the position of the neutral point during the rolling process. The texture is absent for the very light draughts, when deformation on either side of the neutral point is approximately equal, resulting in texture segregation Type I and present for heavy draughts (.500 mm.) resulting in essentially homogeneous textures of Type III.

The intensity of texture segregation Type I is reduced after 80% cold reduction. This is due to the coincident reduction in relative intensity of $\{111\}_{RP}$ texture at the strip mid-plane.

(b) There is also segregation which is present at the extreme surface planes only. This is associated with a general reduction in texture intensity at the surface planes relative to the mid-plane, rather than a change in textural components. The effect is most pronounced with heavy lubricated draughts and is present in Type III textures, but absent in Type I textures.

(c) Type II texture segregation is a composite of Type I and III textures. The intensity of texture segregation Type II is reduced after 80% cold reduction. This is due to the coincident reduction in the relative intensity of the $\{111\}_{RP}$ component of the $\{111\}_{RP} + \langle 110\rangle_{RD}$ partial fibre texture at the strip mid-plane. The intensity of segregation is reduced at the extreme edges of rolled strip and has been attributed to the deviation from plane strain conditions at the edges of strip during rolling.

(d) Type IV texture segregation results from a low intensity shear type texture in the strip surface planes. This texture is described as consisting of orientations $\{110\}\langle xyz\rangle$ where $\langle xyz\rangle$ ranges between $\langle 001\rangle$ and $\langle 111\rangle$ directions. There is a gradual transition through the strip thickness from the surface shear texture to the normal rolling texture at the mid-plane.

The segregation is produced by rolling with MgO dusted rolls and the heaviest draughts and is attributed to high frictional forces at the roll strip interface.

Type IV segregation is the same as previously observed in iron[6] and niobium[37]. A critical percentage reduction per pass, as previously observed, is necessary before Type IV texture is developed, but it has also been shown that a high total reduction is also required. For the two high 150 mm. rolling mill used in the present work, the critical total reduction was 88%.

(iii) The texture segregation observed after cold rolling, for Types I, II, III and IV textures, is retained after annealing, although the magnitude of the texture components are generally altered. The T ratio, i.e. $\{111\}_{average} / \{100\}_{average}$ is considerably increased in each case but the inter-relationship between T_I, T_{II}, T_{III} and T_{IV} is maintained. Consequently, even after annealing $T_{IV} < T_I < T_{II} < T_{III}$. Since T ratio can be directly related to R value the texture segregation associated with rolling under various draughts and lubrication conditions, are therefore of technological significance, particularly from the point of view of deep drawability. Thus, to obtain rimmed steel strip with maximum drawability, for a predetermined total cold reduction, rolling should be performed with heavy draughts and oil lubrication.

(iv) The recrystallisation texture of rimmed steel strip has been described as $\{111\}_{RP} + \langle 110 \rangle_{RD}$. The relative proportions of the two components depend upon total rolling reduction and rolling draught.

Textural measurements have revealed significant crystal reorientation during tensile strain for all specimens examined, irrespective of its processing conditions. There is a general reduction in T ratio but the magnitude of the reduction is dependent upon the texture present before tensile extension. Analysis of the reorientation, using (110) pole figures, showed that $\{111\}_{RP}$ partial fibre texture, which is associated with small reductions in T ratio, promotes high R_o values, whereas $\langle 110\rangle_{RD}$ partial fibre texture, which leads to large reductions in T ratio, promote relatively low R_o values. The reduction in R_o value after R_{omax} is thus associated with a balance in $\{111\}_{RP}$ and $\langle 110\rangle_{RD}$ components of the recrystallisation texture.

(v) R_{omax} occurs at successively lower rolling reductions, prior to a standard anneal, for materials processed to develop texture segregation in the sequence Type I < Type II < Type III. This has been attributed to the interference of the $\{111\}_{RP} : \langle 110\rangle_{RD}$ balance by texture segregation, i.e. $\langle 110\rangle_{RD}$ texture is dominant after relatively low reductions for material exhibiting Type I texture segregation and after relatively high total reductions for material exhibiting Type III texture segregation.

(vi) The R_o value for strip rolled to reductions corresponding to the reductions associated with R_{omax} are improved if intragranular cementite, 1μ in size, is precipitated in the material as a result of a $300^{\circ}C$ overaging treatment. R value is similarly improved.

The improvement in R_o value has been examined by observing the difference in crystal reorientation accompanying tensile strain for overaged and normally processed specimens. The reduction in T ratio associated with tensile extension is reduced in the former case. Thus, from the point of view of R value and drawability, the overaged steel behaves as would a material exhibiting a 'superior' texture.

An overaging treatment of 300°C for one hour is an effective means of overcoming the aging problems inherent in continuously annealed strip or sheet. Consequently, if continuously annealed drawing quality rimmed steel became a viable proposition in the future, such a heat treatment would result in the significant bonus of improved $\bar{R}$ and R values.

References.

1. R.L. Whiteley, D.E. Wise and D.J. Blickwede, Sheet Metal Industries, 1961 May 349.

2. I.L. Dillamore and W.T. Roberts, Metallurgical Reviews 1965 10 271.

3. G. Wasserman and J. Grewen, Texturen Metallischer Werkstoffe Springer, Berlin 1962.

4. H. Hu, R.S. Cline and S.R. Goodman, Recrystallisation Grain Growth and Textures, H. Margolin Ed., A.S.M. Metals Park, Ohio 1966 p.295.

5. C.S. Barrett and T.B. Massalski. Structure of Metals 3rd Ed., McGraw Hill, New York, 1966.

6. C.A. Stickels, Trans. Met.Soc. A.I.M.E. 1967 239 1857.

7. R. Whiteley and D. Wise 4th Mech. Working Conf. A.I.M.E. Chicago. Jan. 1962.

8. D.V. Wilson. Metals and Materials. 1969 3 175.

9. W.F. Hosford and W.A. Backofen, Strength and Plasticity of Textured Metals. Proc. 9th Sagamore Conf. 1962. Syracuse N.Y. Syracuse University Press.

10. R. Hill Proc. Roy. Soc. 1949 198 428.

11. D.V. Wilson. J. Inst.Metals 1965/6 94 84.

12. B.D. Cullity 'Elements of X-ray Diffraction' 1956 Reading, Mass. (Addison-Wesley).

13. A. Taylor, 'X-ray Metallography' 1961 New York, London (John Wiley)

14. G.B. Harris, Phil. Mag. 1952 43 113.

15. M.H. Mueller, W.P. Chernock, and P.A. Beck, Trans.Met.Soc. A.I.M.E. 1958 212 39

16. L.K. Jetter, G.J. McHargne and R.O. Williams, J.Appl. Physics 1956 27 368.

17. R.S. Burns and R.H. Heyer. Sheet Metal Industries 1958 35 261

18. J.A. Elias, R.H. Heyer and J.H. Smith. Trans.A.I.M.E. 1962 224 678

19. S. Nagashima, H. Takechi and H. Kato, Textures in Research and Practice, Proc. Clausthal-Zellerfeld Symposium. Oct. 2 - 5 1968.

20. M. Fukuda. Trans. Jap. I.S.I. 1968 8 68.

21. G.I. Taylor, J. Inst. Metals 1938 62 307.

22. J. Dudley-Evans. Sheet Metal Industries. 1970 May 421.

23. W. Jolley, J.I.S.I. 1967 205 321

24. E.A. Calnan and C.J.B. Clews, Phil.Mag. 1950 41 1085

25. I.L. Dillamore and W.T. Roberts. Acta. Met. 1964 12 281

26. L.R. Underwood. The Rolling of Metals. Chapman and Hall Ltd., London 1958.

27. H. Hu, in Recovery and Recrystallisation of Metals, Interscience, New York, 1963 p. 311.

28. J.F.W. Bishop. J. Mechanics Physics Solids 1954 3 130.

29. T. Ll. Richards, J. Applied Materials Research 1963 July 156.

30. W.C. Leslie, Trans. Met. Soc. A.I.M.E. 1961 221 753.

31. P.N. Richards and N.K. Ormay. Trans. Met. Soc. A.I.M.E. 1969 245 715.

32. J. Bennewitz Arch Eisenhuettenw, 1962 33 393.

33. R.A. Vandermeer and J.C. Ogles. Trans. Met.Soc. A.I.M.E. 1968 242 1317.

34. H. Takechi, H. Kato, and S. Nagashima. Trans.Met.Soc. A.I.M.E. 1968 242 56

35. H.Hu, and R.S. Cline, Trans.Met.Soc. A.I.M.E. 1962 224 784.

36. J.F. Held, Trans.Met.Soc. A.I.M.E. 1967 239 573.

37. R.A. Vandermeer and J.C. Ogles. Trans.Met.Soc. A.I.M.E. 1969 245 1511.

38. R.O. Williams. Trans. Met.Soc. A.I.M.E. 1962 224 129.

39. W.A. Backofen and B.B. Hundy, Trans.Met.Soc. A.I.M.E. 1953 197 61.

40. I.L. Dillamore and W.T. Roberts. J.Inst. Metals 1963 - 4 92 193.

41. F.A.A. Crane and J.M. Alexander. J. Inst. Metals 1963 - 4 92 382.

42. N.K. Chen and R. Maddin. Trans. Met.Soc. A.I.M.E. 1953 197 300.

43. C.S. Barrett and L.H. Levenson. Trans. A.I.M.E. 1941 145 281

44. M. Atkinson, P.G. Brooks, A.O'Connor and T.G. Phillips, Sheet Metal Ind. 1963 40 57.

45. T.R. Thomson and J.M. Baker. J. Aust. I.M. 1969 14 84.

46. W.T. Roberts. Contribution to Inst.of Metals meeting Edinburgh 1969

47. P.N. Richards J.I.S.I. 1969 207 1333.

48. M.J. Dickson. Sheet Metal Industries 1968 Dec. 873.

49. Ch. Leisner and G. Wasserman, Textures in Research and Practice Proc. Clausthal-Zellerfeld Symposium Oct. 2 - 5 1968 p. 357.

50. I.L. Dillamore and S.F.H. Fletcher, Recrystallisation Grain Growth and Textures. Seminar of the American Society for Metals. Oct. 16 and 17, 1965.

51. G. Jegaden, J. Voinchet and R. Rocquet. Sheet Metal Industries 1968 Nov. 789.

52. H.H. Ascough, Proc. International Symposium on the Annealing of Low Carbon Steel, Cleveland, Ohio, 1957 Oct. 9.

53. M. Gensamer and P.A. Vukmanic. Trans.Met. Soc. A.I.M.E. 1937 125 507.

54. G.Y. Chin, Textures in Research and Practice. Proc. Clausthal-Zellerfeld Symposium Oct. 2 - 5 1968 p.51.

55. M.A. Adams and J.R. Bevan, I.S.I. Spec.Report No.95 p. 135.

56. R.F. Dewsnap, I.S.I. Spec. Report No.79 1963 112.

Acknowledgements.

The author would like to express his appreciation to Dr. T. Ll. Richards for the encouragement and advice received over the last three and a half years. Thanks are also due to Mrs. A. Hellewell and Mrs. J. Pinkney for the help received during the preparation of this thesis.